

Performance Studies on Portland-Limestone Cement in Sulfate Environments

by

Md Manjur A Elahi

A thesis submitted to the Graduate Division
in partial fulfillment of the requirements for the degree of

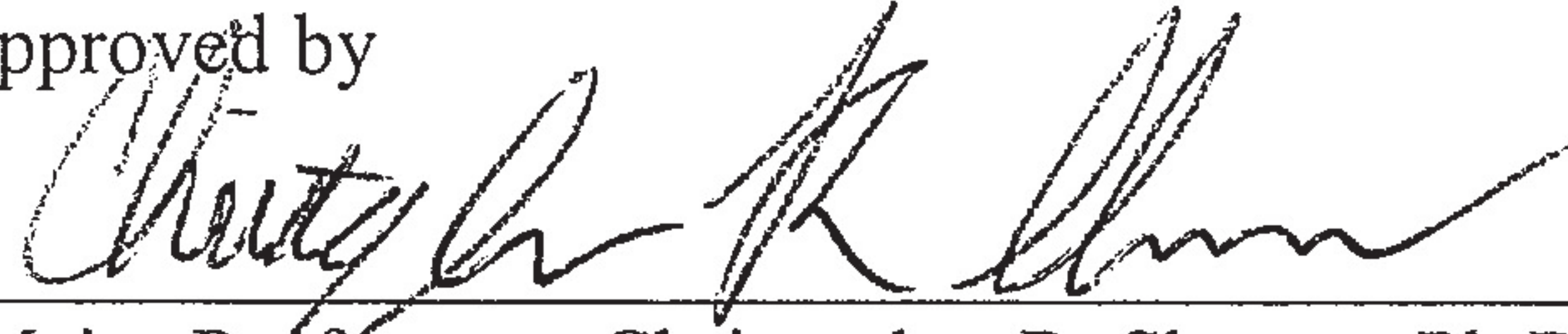
Master of Science in Civil & Environmental Engineering

South Dakota School of Mines and Technology

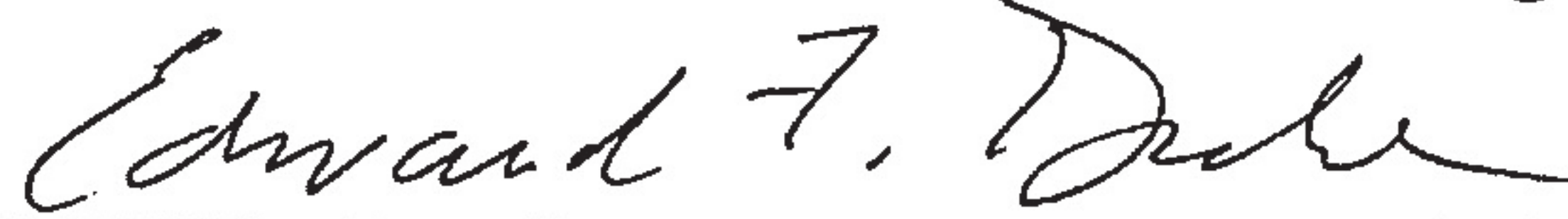
Rapid City, South Dakota

Date Defended: July 6, 2018

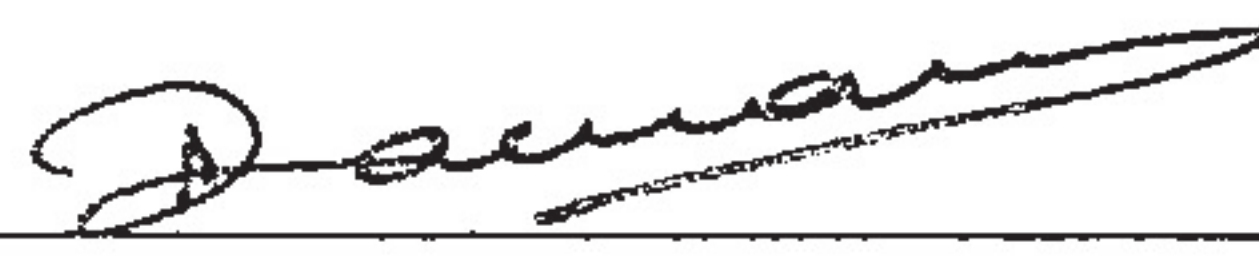
Approved by


Major Professor – Christopher R. Shearer, Ph.D.,
Department of Civil and Environmental Engineering

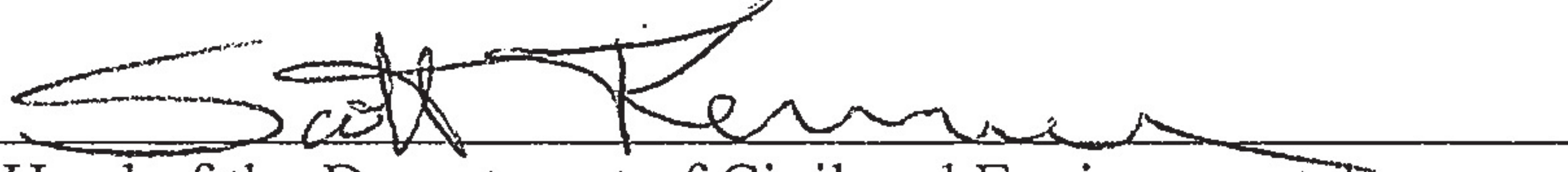
7/9/2018
Date


Graduate Division Representative – Edward F. Duke, Ph.D.,
Department of Geology and Geological Engineering

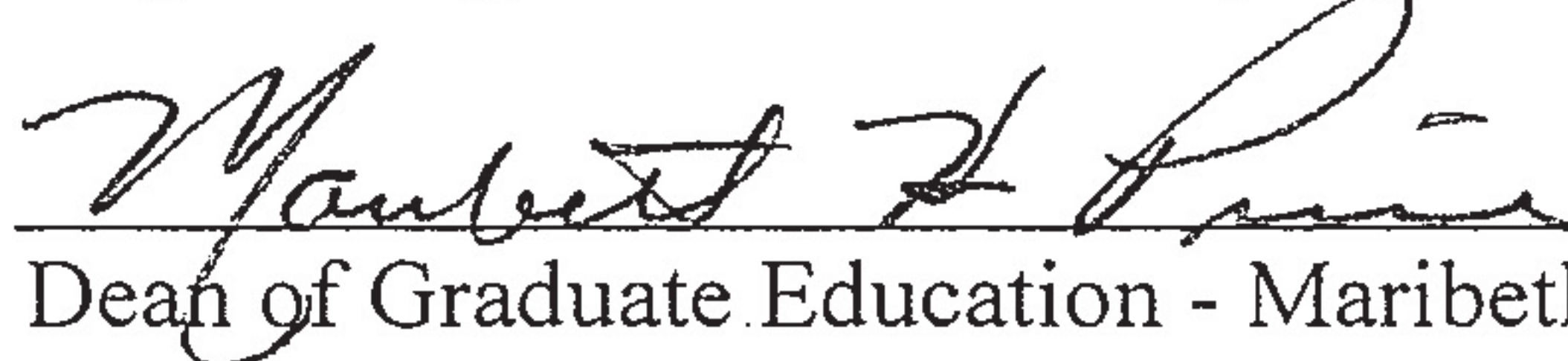
7/10/2018
Date


Committee Member – Venkata R. Gadhamshetty, Ph.D.,
Department of Civil and Environmental Engineering

7/9/18.
Date


Head of the Department of Civil and Environmental
Engineering – Scott J. Kenner, Ph.D.

7/10/2018
Date


Dean of Graduate Education - Maribeth H. Price, Ph.D.

18 July 2018
Date

ProQuest Number: 13850813

All rights reserved

INFORMATION TO ALL USERS

The quality of this reproduction is dependent upon the quality of the copy submitted.

In the unlikely event that the author did not send a complete manuscript and there are missing pages, these will be noted. Also, if material had to be removed, a note will indicate the deletion.



ProQuest 13850813

Published by ProQuest LLC (2019). Copyright of the Dissertation is held by the Author.

All rights reserved.

This work is protected against unauthorized copying under Title 17, United States Code
Microform Edition © ProQuest LLC.

ProQuest LLC.
789 East Eisenhower Parkway
P.O. Box 1346
Ann Arbor, MI 48106 – 1346

Abstract

Sulfate attack can occur in concrete due to external sulfate ions reacting with hydrated cement paste. The sulfate attack resistance of portland-limestone cements (PLCs) has been questioned due to their high limestone content, which has the potential to initiate a rare type of sulfate attack that forms thaumasite. This research evaluates the performance of portland-limestone cements in sulfate prone environments by investigating changes in the physical, chemical, and mechanical properties of specimens. Mortar and paste specimens prepared by replacing Type I/II and Type V cement with 4.4, 10, 14.6 and 20 percent of calcitic and dolomitic limestone powders and fly ash are examined for their sulfate resistance. An accelerated cube test for measuring strength loss due to sulfate attack was developed using 33,800 ppm sodium and magnesium sulfate solutions at 5°C and 23°C. Results from this testing are compared to ASTM C1012 expansion measurements. The physical and chemical transformation in paste specimens are analyzed using visual observation, mass loss measurements, and X-ray diffraction.

All mixtures prematurely exceeded the ASTM C1157 12-month expansion limit. Results revealed higher expansion of Type I/II cement with increased calcitic limestone contents, especially in sodium sulfate solution. Type V cement showed greater sulfate resistance in both expansion and strength measurements compared to Type I/II, and the addition of calcitic limestone to Type V cement decreased its expansion. Increased calcitic limestone contents did not significantly impact strength loss for either cement. The addition of a small dosage (4.1% by mass) of dolomitic limestone improved sulfate resistance by exhibiting less strength loss in magnesium sulfate and lower expansion in both solutions in part due to ettringite stabilization. The incorporation of Class F fly ash with 14.6% PLCs showed higher sulfate resistance than other mixtures. Higher expansion (up to 80%) at 180 days and greater strength loss (up to 62%) at 120 days was observed in sodium sulfate compared to magnesium sulfate. Higher strength loss (up to 62%) was observed at 5°C compared to 23°C for most mixes in both solutions, especially for magnesium sulfate exposure. More surface deterioration, including extensive cracking at the corners and along the edges, bulging on the surfaces, and spalling was found in the paste samples at 5°C. Samples with higher limestone contents, in general, showed greater deterioration. At 5°C, thaumasite was detected in all samples in addition to gypsum and ettringite.

Acknowledgements

I would like to take this opportunity to thank all the people who have helped me throughout my life. I would like to express my sincere gratitude to my supervisor Dr. Christopher R. Shearer for his motivation, supervision, and assistance all along my research work. I thank him for giving me the opportunity to work on this project. His experience and guidance helped me to better investigate the project whenever I faced difficulties. I would also like to thank Dr. Edward F. Duke and Dr. Venkata R. Gadhamshetty for their insightful comments on the experiments. I am grateful to them for their valuable time and guidance to improve my thesis.

I also thank Dr. Jon J. Keller and Dr. Willian M. Cross for allowing me to use the materials grinding laboratory in the Materials Engineering department. I am grateful to the lab technician in the Civil Engineering department, Mr. Forest Cooper, who helped me in designing and fabricating tools for my experiments. I would also like to thank the lab technicians of GCC Dacotah for helping on experiments and for supplying materials.

I convey my sincere and special thanks to my dear parents who have served me since the beginning of my life in this world. I am grateful to my mom and dad for their dedication and sacrifice that landed me here in the United States. Moreover, if it was not for the effort of my mother, I would not have been in this position now. I also want to say a big thanks to all of my friends and well-wishers.

Table of Contents

Abstract.....	i
Acknowledgements.....	ii
Table of Contents.....	iii
List of Tables.....	iv
List of Figures.....	vi
Acronyms.....	ix
1. Introduction	1
1.1 Overview of portland-limestone cement usage.....	1
1.2 Sulfate attack on portland-limestone cement	2
1.3 Significance of the study	3
2. Literature Review	5
2.1 External sulfate attack	5
2.1.1 Ettringite formation	5
2.1.2 Gypsum formation.....	6
2.1.3 Thaumasite sulfate attack	7
2.2 Testing and Measurement of Sulfate Attack	16
2.2.1 Testing and measurement of conventional sulfate attack.....	16
2.2.2 Testing and measurement of thaumasite sulfate attack	18
2.3 Factors affecting TSA	21
2.3.1 Source of sulfate ions	21
2.3.2 Source of carbonates.....	22
2.3.3 Alumina content in cement.....	22
2.3.4 Temperature.....	23
2.3.5 Moisture.....	23
2.3.6 pH value.....	23
2.4 Prevention of sulfate attack	24
2.4.1 Water content.....	24
2.4.2 Cement and aggregate content.....	25
2.4.3 C ₃ A content.....	25
2.4.4 Use of SCMs.....	26

3. Experimental program	27
3.1 Materials.....	27
3.2 Preparation of limestone powder.....	28
3.3 Mixture design.....	30
3.4 Mixing, casting, and measurement procedures	33
3.4.1 Mortar bar expansion measurement	33
3.4.2 Strength measurement, mass loss, and visual rating of pastes	36
3.4.3 X-ray diffraction testing on pastes.....	39
4. Results and Discussion	40
4.1 Expansion of mortar bars	40
4.1.1 Influence of limestone percentage	40
4.1.2 Influence of limestone type and composition.....	44
4.1.3 Influence of fly ash.....	49
4.2 Mg and Na expansion trend	51
4.3 Visual appearance of mortar specimens.....	55
4.4 Change in compressive strength of paste specimens	58
4.4.1 Influence of limestone percentage	58
4.4.2 Influence of limestone type and composition.....	64
4.4.3 Influence of fly ash.....	68
4.4.4 Influence of pH.....	71
4.5 Visual inspection of paste specimens.....	72
4.6 Mass loss of paste specimens	76
4.7 Mineralogical changes measured by X-ray diffraction	78
4.7.1 X-ray diffraction results in Na ₂ SO ₄ solution	78
4.7.2 X-ray diffraction results in MgSO ₄ solution.....	84
5. Conclusion.....	90
Bibliography	92
Appendix: A.....	108
Appendix: B.....	112
Vita	118

List of Tables

Table 1: Details and results of most important experimental research on PLCs and sulfate attack.....	12
Table 2: Different sulfate severity class in soil and groundwater.....	17
Table 3: Requirement to protect against damage to concrete by external sulfate attack ..	18
Table 4: Chemical composition and physical data for the cements and fly ash	28
Table 5: Mineralogical composition of limestone powder	29
Table 6: Mix design for mortar bars expansion test exposed to sulfate solution at 23°C.	32
Table 7: Mix design for paste cubes exposed to sulfate solution at 23°C and 5°C.....	33
Table 8: Visual rating used to classify surface damage	73
Table 9: Visual inspection of paste specimens placed in sulfate solutions at 120 days ...	75

List of Figures

Figure 1: Simplified schematic for the direct and indirect routes of TSA.....	11
Figure 2: Particle size distribution of limestone powder	30
Figure 3: Expansion of different dosages of PLC mortars placed in 5% sodium sulfate solution.....	40
Figure 4: Expansion of different dosages of PLC mortars placed in 4.23% magnesium sulfate solution	41
Figure 5: Expansion of different dosages of PLC mortars placed in 5% sodium sulfate solution.....	46
Figure 6: Expansion of different dosages of PLC mortars placed in 4.23% magnesium sulfate solution	47
Figure 7: Expansion of different dosages of PLC mortars placed in 5% sodium sulfate solution.....	48
Figure 8: Expansion trend of different PLCs (calclitic limestone) in sulfate solutions at 180 days	52
Figure 9: Time required for different PLCs to exceed the average expansion of 0.1% in sulfate solutions	54
Figure 10: Images of mortar samples exposed to Na ₂ SO ₄ (a and b) and MgSO ₄ (c and d) for 7 months	57
Figure 11: Compressive strength of paste cubes (calclitic limestone only) placed in sulfate solutions, 11(a) Na at 23°C, 11(b) Mg at 23°C, 11(c) Na at 5°C, and 11(d) Mg (bars show 1 standard deviation) at 5°C.....	61

Figure 12: Percent reduction of compressive strength of paste (calcitic limestone only) cubes placed in sulfate solutions, 12(a) Na at 23°C, 12(b) Mg at 23°C, 12(c) Na at 5°C, and 12(d) Mg at 5°C	62
Figure 13: Compressive strength of paste (calcitic and dolomitic limestone) cubes placed in sulfate solutions, 13(a) Na at 23°C, 13(b) Mg at 23°C, 13(c) Na at 5°C, and 13(d) Mg (bars show 1 standard deviation) at 5°C	66
Figure 14: Percent reduction of compressive strength of paste (calcitic limestone only) cubes placed in sulfate solutions, 14(a) Na at 23°C, 14(b) Mg at 23°C, 14(c) Na at 5°C, and 14(d) Mg at 5°C	67
Figure 15: Compressive strength of Type V cement replaced PLC paste cubes placed in sodium sulfate solutions, 15(a) Na at 23°C and 15(b) Na at 5°C	70
Figure 16: Percent reduction of compressive strength of Type V cement replaced PLC paste cubes placed in sodium sulfate solutions, 16(a) Na at 23°C and 16(b) Na at 5°C	70
Figure 17: Compressive strength (a) and percent reduction of strength (b) of different PLCs placed in sodium sulfate solution at 5°C at pH= 7.2	72
Figure 18: Visual appearance of paste specimens after 120 days of sodium and magnesium sulfate exposure at 23°C and 5°C	74
Figure 19: Mass loss of paste specimens placed in sodium sulfate solution at 5°C	77
Figure 20: Mass loss of paste specimens placed in magnesium sulfate solution at 5°C ..	77
Figure 21: XRD patterns of paste samples exposed to sodium sulfate solution at 5°C for 28 days	79
Figure 22: XRD patterns of paste samples exposed to sodium sulfate solution at 5°C for 120 days	80

Figure 23: XRD patterns of paste samples exposed to sodium sulfate solution at 5°C for 28 days	81
Figure 24: XRD patterns of paste samples exposed to sodium sulfate solution at 5°C for 120 days	82
Figure 25: XRD patterns of paste samples exposed to magnesium sulfate solution at 5°C for 28 days.....	85
Figure 26: XRD patterns of paste samples exposed to magnesium sulfate solution at 5°C for 120 days.....	86
Figure 27: XRD patterns of paste samples exposed to magnesium sulfate solution at 5°C for 28 day	88
Figure 28: XRD patterns of paste samples exposed to magnesium sulfate solution at 5°C for 120 days.....	89

Acronyms

AFt	Ettringite
AFm	Monosulfoaluminates
C	Calcitic Limestone
CH	Calcium Hydroxide
CSA	Canadian Standard Association
CSH	Calcium Silicate Hydrate
D	Dolomitic Limestone
EN	European Standard
GGBFS	Ground Granular Blast Furnace Slag
NRCS	National Resources Conservation Service
PC	Portland Cement
PLC	Portland Limestone Cement
QXRD	Quantitative X-Ray Diffraction
SCM	Supplementary Cementitious Materials
TF	Thaumasite Formation
TEG	Thaumasite Expert Group
TSA	Thaumasite Sulfate Attack
USDA	United States Department of Agriculture
VR	Visual Rating

1. Introduction

1.1 Overview of portland-limestone cement usage

During the last few decades, portland-limestone cement (PLC) has been widely used in the cement industry to accomplish the goal of reducing the use of raw materials (e.g., calcium carbonate, silica, alumina, and iron ore), saving fuel energy, and curtailing CO₂ emissions. Portland cement clinker is manufactured through an energy-intensive process which produces a considerable amount of greenhouse gases, particularly CO₂ that annually contributes more than 5% of global anthropogenic CO₂ discharge [1]. CO₂ release is primarily a result of decalcination of the limestone during clinkering in addition to the fuel consumption needed to generate the high temperatures necessary to form clinker. The reduction of portland cement clinker will substantially cut back the environmental impacts associated with concrete by reducing carbon emissions. To reduce the environmental impact of cement, most cement plants have produced blended cements, containing supplementary cementitious materials like slag, silica fume, and fly ash. Cement that is partially replaced with uncalcined limestone requires comparatively less clinker to produce an equivalent amount of cement, and therefore less energy is consumed, and CO₂ emissions and other greenhouse gases are reduced. PLCs have been formally adopted by many specifications around the world.

The majority of the portland cement specifications permit adding up to 5% limestone (by mass) in portland cement mixtures. Above this allowable limit, PLCs are classified depending on the proportion of limestone added to the parent cement. The European

Standard (EN 197-1-2011) has designated 5% limestone as a minor additional component. It also identifies four types of PLC containing 6 – 20% limestone (types II/A-L and II/A-LL) and 21-35 % limestone (types II/B-L and II/B-LL) respectively [2]. Canadian Standards Association (CSA) CSA 3001 has allowed the inclusion of 5-15% limestone whereas China and Russia both have permitted up to 10% of limestone as a filler material in PLCs. In the U.S., the ASTM C 150M – 17 [3] standard currently permits up to 5% limestone content as a filler material. On the other hand, ASTM C595M - 17 [4] (hydraulic cement) classifies cement based on its performance requirement which allows up to 15% limestone replacement. This specification classified limestone cement as Type IL (Portland-Limestone Cement) which is considered a binary blended cement (a blend of ordinary portland cement and limestone filler).

1.2 Sulfate attack on portland-limestone cement

One important concern with the use of PLCs is the potential development of sulfate attack due to the presence of limestone. Research has shown that the amount of limestone in PLCs can have an impact on the sulfate attack of cementitious materials, particularly through the formation of thaumasite. Sulfate attack in concrete and mortar is the chemical reaction that can either be caused by internal or external sulfate sources. Internal sulfate attack occurs where the source of sulfate-rich aggregates or higher amounts of gypsum in the cement may result in such an attack. One common internal sulfate attack issue is delayed ettringite formation (DEF). External sulfate attack is caused when sulfates ingress into concrete from a sulfate-rich environment like soil, seawater, decaying organic matter, and industrial effluent [5]. These external sulfate ions react with the components of cement paste resulting

in concrete deterioration over time where significant microstructural changes weaken the cement paste binder. Some important factors that increase influence permeability of concrete includes w/cm, properties of cement and aggregates, absorption and homogeneity of concrete, curing, maturity of concrete and use of admixtures. Sulfate attack in concrete can manifest in the form of expansion and cracking, which increases the permeability of concrete and thus accelerates the aggressive penetration of deleterious ions (including chloride ions) into the concrete. Sulfate attack can also cause the concrete to become mushy and lose its strength.

In this study, cement mortars and pastes specimens will be made of 4.4%, 10%, 14.6% and 20% limestone filler used to replace control Type I/II and Type V cements. These percentages were selected to evaluate the degree of sulfate attack at varying limestone replacement levels in different sulfate environments. The mortar and paste specimens will be immersed in sodium and magnesium sulfate solutions having a concentration of 5% (w/w) in room (23°C) and cold temperature (5°C). The mortar specimens will be tested for expansion for at least a period of 12 months. The paste specimens will be tested for mass and strength loss, and changes in appearance. Selected specimens will be tested to identify the mineralogical formation of different products formed in the hardened matrix due to sulfate ingress using X-ray diffraction (XRD).

1.3 Significance of the study

Numerous studies have already been conducted on sulfate attack on PLCs with a variety of cementitious materials in different sulfate environments. The majority of the research

conducted on sulfate attack either used Type I/II cement to make PLCs or mixed PLCs with different SCMs [6-8]. In most studies, calcitic limestone (CaCO_3) was used to produce/replace the PLCs for the research conducted thus far because of the purity and availability of the limestone. Further, calcitic limestone is more desirable to use for cement clinker manufacturing. Another common research aspect is the use of sodium sulfate as the primary sulfate exposure specified in ASTM C1012 [9]. Larger samples including cement mortars (2 in cube samples) and concrete cylinders (4-in \times 8-in) were primarily used for strength testing in sulfate environments [10].

Based on the literature search on the materials and test methods used to study sulfate attack in PLCs, some new or much less studied research directions are included in this study. The new aspects added in this research are:

1. The use of limestone to replace high sulfate resistant Type V cement.
2. Incorporation of dolomitic limestone as a cement replacing material.
3. The use of MgSO_4 solution (same sulfate concentration as Na_2SO_4) to compare the effect of sulfate attack in different exposures.
4. The use of 0.5 - in cube specimens for strength testing following a modified accelerated test method [11] at 5°C .

2. Literature Review

2.1 External sulfate attack

Generally, external sulfate attack is classified into two categories: (1) classical sulfate attack and (2) thaumasite sulfate attack. There are mainly two types of classical form of sulfate attack: (1) ettringite formation and (2) gypsum formation. Thaumasite type of sulfate attack is considered as the most deleterious form of sulfate attack that can completely destroy the concrete matrix and turned it into a non-cementitious material.

2.1.1 Ettringite formation

Ettringite is the mineral name of calcium sulfoaluminate ($3\text{CaO} \cdot \text{Al}_2\text{O}_3 \cdot \text{CaSO}_4 \cdot 32\text{H}_2\text{O}$), which is a hydration product of portland cement. It has a needle-like morphology and contributes to stiffening of the mixture at early ages. If it is formed at later ages in the system, it can lead to significant damages to the concrete.

Alumina phases in portland cement clinker, tricalcium aluminate (C_3A) and tetra calcium aluminoferrite (C_4AF), are susceptible to this form of sulfate attack. In the presence of calcium hydroxide (CH) and water (H), monosulfate hydrate ($\text{C}_3\text{A} \cdot \text{C}\bar{\text{S}} \cdot \text{H}_{18}$) and calcium aluminate hydrate ($\text{C}_3\text{A} \cdot \text{CH} \cdot \text{H}_{18}$) react with sulfate ($\bar{\text{S}}$) to produce ettringite in the following reactions shown in cement chemistry notation¹ [12].



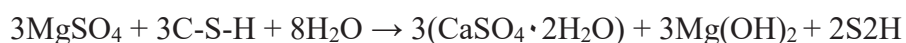
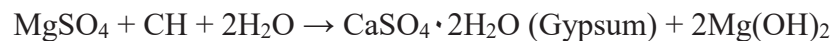
¹C=CaO, CH=Ca(OH)₂, M=MgO, H=H₂O, S=SiO₂, A=Al₂O₃, F=Fe₂O₃, C̃=CO₂, S̄=SO₃



The formation of a limited amount of ettringite may be acceptable; however, excessive amounts of this mineral may cause expansion and cracking of the hardened cement paste. Even though the expansion mechanism due to ettringite formation is still not fully known, two particular mechanisms have been widely published: (1) the topochemical reaction mechanism and (2) the swelling mechanism [13]. In the topochemical reaction mechanism, the reaction between C_3A and the sulfate and calcium ions in the concrete pore fluid is topochemical (i.e., in solid state) [14]. According to swelling theory poorly crystalline ettringite leads to expansion by adsorption of water [12].

2.1.2 Gypsum formation

The formation of gypsum takes place when the hydration product calcium hydroxide (CH) reacts with sodium (Na^+), magnesium (Mg^{2+}), or potassium (K^+) sulfates in the presence of water. Gypsum formation occurs due to cation exchange reaction between sulfates and CH. Calcium silicate hydrate (C-S-H) is also prone to conversion into gypsum by external sulfate attack in the presence of magnesium sulfate, which additionally forms brucite ($Mg(OH)_2$). These reactions are as described as follows [12].



In the gypsum formation process, the pH of the system is initially reduced and there is a significant loss in stiffness and strength in concrete. As the damage from the strength and loss of adhesion progresses, the concrete is eventually transformed into a non-cohesive mass. The exact process and nature of disintegration caused by gypsum, however, is not completely understood. Gypsum is primarily observed close to the surface in concrete that is deteriorated by sulfate, especially in cracks and voids [15, 16].

Likely the formation of gypsum does not lead to significant expansion of the samples [17-19] although some research has shown that with the right conditions gypsum formation can lead to some expansion and cracking [20]. The precise measurement of mechanical damage due to gypsum formation is difficult because it sometimes masked by the formation of ettringite during sulfate attack [15]. The ASTM C1012 [21] test does not really capture the damage from gypsum, because it only measures expansion. Therefore, compressive strength testing is a better tool to assess this form of sulfate attack.

2.1.3 Thaumasite sulfate attack

Thaumasite ($C_3S\bar{S}\check{C}H_{15}$) is a type of mineral that has a complex hexagonal crystal structure of sulfate salt and is usually found in metamorphic rocks and limestone [22]. During thaumasite sulfate attack in concrete, calcium-silicate-sulfate-carbonate hydrates ($CaSiO_3 \cdot CaCO_3 \cdot CaSO_4 \cdot 15H_2O$) form in the cement paste by reaction of calcium-silicate-hydrates (C-S-H) with sulfates in the presence of carbonate ions (all three must be available for the reaction to occur). Carbonate ions from limestone in PLCs could potentially lead to greater thaumasite formation. The formation of thaumasite usually takes

place in very wet environments and its rate of formation is higher at low temperatures. The type and concentration of sulfates, water-cement ratio, cement type, and type and dosage of limestone additive in cement, carbonate sources, curing methods, relative humidity, the proportion of supplementary cementitious materials (SCMs) are important controlling factors for thaumasite formation [23].

Thaumasite sulfate attack (TSA) was first recognized in portland cement concrete sewer pipes, cement grout, and in the base of pavements by Erlin and Stark in 1965 [24]. Thaumasite again attracted noticeable consideration in 1998 when it was discovered in some motorway bridge foundations in the United Kingdom (UK) [25]. The transformation of C-S-H into thaumasite transforms concrete into a non-cohesive mass and can completely damage its binding and load bearing capacities over time.

The formation of thaumasite is not always catastrophic. A recent report from the Thaumasite Expert Group (TEG) distinguishes two mechanisms in which thaumasite can precipitate as a reaction product within cementitious materials. These are (1) thaumasite formation (TF), and (2) thaumasite form of sulfate attack (TSA). TF refers to scenarios where thaumasite can be found in preexisting voids and cracks without necessarily affecting the integrity of the host concrete or mortar. On the other hand, TSA can lead to the complete disintegration of a concrete or mortar due to the transformation of calcium silicate hydrates (C-S-H) in the hydrated portland cement paste to thaumasite. During TSA, the damaged cement paste loosely holds aggregates due to its loss of binding capacity. Visible cracks filled with thaumasite and white haloes around the aggregates is another differentiating feature [26]. In case of buried concrete structures, TSA starts the attack at

the surface and progresses inwards which causes gradual disintegration of the C-S-H matrix.

2.1.3.1 Mechanisms of thaumasite formation

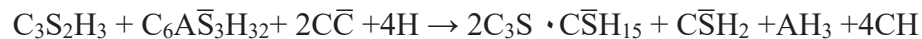
Generally, TSA favorably occurs at temperatures $\leq 15^\circ\text{C}$ in the presence of calcium silicate, sulfate, and carbonate ions [25]. However, TSA has also been reported in cement-based materials at higher temperatures [26, 27]. There are two possible routes for thaumasite formation: (1) the direct route and (2) the indirect route. The schematic diagram (Figure 1) shows the mechanisms of the two possible routes [28]. In the direct route, thaumasite is formed through the reaction of C-S-H with carbonate ions (potentially from limestone) in the presence of moisture and sulfate ions, according to following equation [29].



According to this hypothesis, initially, hydration products including ettringite, C-S-H gel, and CH are formed. Once a significant amount of C_3A is reacted, the external sulfate ions react with Ca^{2+} ions and additional CH decomposed into the pore solution, and gypsum crystallization starts. As more gypsum is produced due to the continuous removal of CH, hydroxyl (OH^-) ions in the system will eventually be depleted and as a result instability and decalcification of C-S-H will occur. In sodium sulfate (Na_2SO_4) solution, the disintegration of C-S-H is attributed to be the source of silica available in the pore solution that reacts with the carbonate and sulfate ions to form thaumasite. However, when magnesium ions are present (MgSO_4), the reaction mechanism is different. In this case, the overall reaction to form thaumasite has been outlined as follows [30].



In the indirect route, ettringite acts as a predecessor for thaumasite formation [31]. Ettringite formation takes place in the presence of moisture carrying sulfate ions, and ettringite reacts with C-S-H and carbonates transforming into thaumasite according to the following reaction.



2.1.3.2 Field and laboratory case studies of TSA

TSA has been found in many countries around the world including the UK, Germany, Norway, China, and South Korea [32-38]. The majority of the TSA resulted in softening and cracking of the concrete. For most cases, the limestone aggregate was the primary source of carbonates needed for the TSA formation. However, in Germany PLC may have contributed to the formation of TSA where researchers [34] found wet mush and scaling in a train tunnel potentially caused by portland-limestone cement and limestone aggregates, and the presence of magnesium in the groundwater. In North America, TSA has also been identified in structural and non-structural concrete primarily in Canada also due to carbonated aggregates [39, 40].

Some recent important laboratory studies conducted using PLCs and associated with classical and thaumasite type of sulfate attack are presented in Table 1.

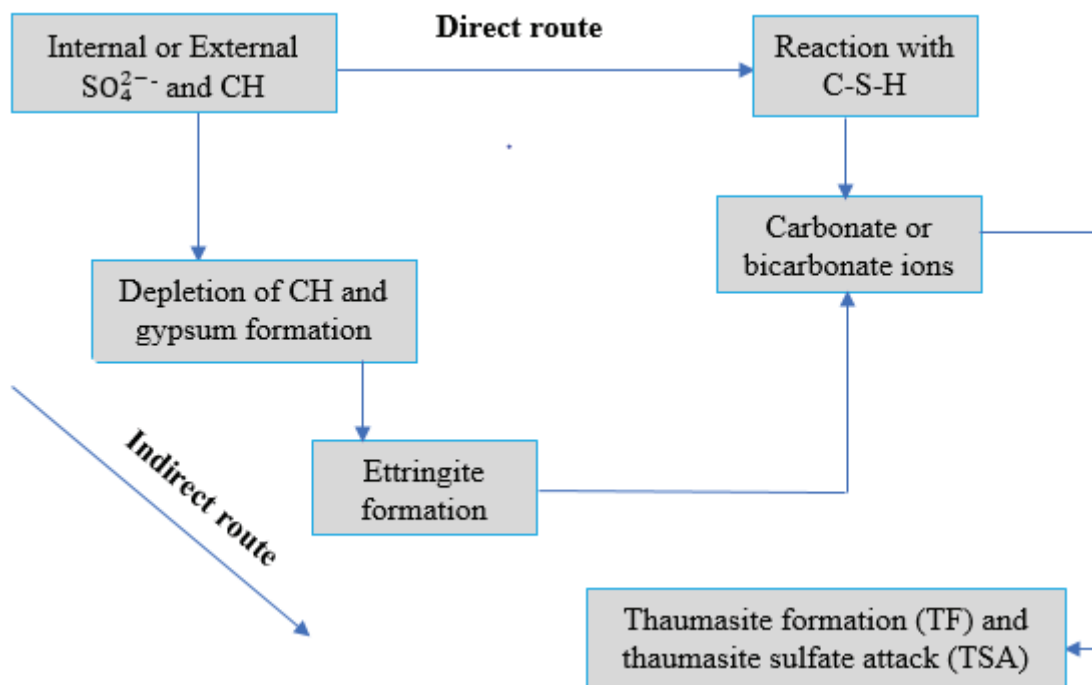


Figure 1: Simplified schematic for the direct and indirect routes of TSA

Table 1: Details and results of most important experimental research on PLCs and sulfate attack

Specimen size (mm)	Material	Time (month)	% limestone	% C ₃ A	Water/binder	Temp. °C	Compounds ²					Rating	Main Conclusion
							E	T	G	B	P		
25 × 25 × 159	M	11	0	11	0.70	20						3	LF improves sulfate resistance of mortars to a limited time. But, it did not produce a sulfate resisting mortar [41].
			10		0.78						3		
			20		0.88						3		
			30		1.00						3		
25 × 25 × 294	M	12	5	10.4	0.51	23						3	LF has no influence on sulfate resistance, except when diluting the C ₃ A content [42].
			5	9.0	0.51						3		
			3	8.0	0.50						2		

² E – Ettringite, G – Gypsum, T – Thaumastite, B – Brucite, P – Portlandite

25 × 25 × 294	M	12	0	0.0	0.49	20	E		G		P	0	Penetration of attack, CH depletion and gypsum are deeper when LF content increases [43].
			10		0.54				G		P	2	
			20		0.61				G		P	3	
			0	1.0	0.49		E		G		P	0	
			10		0.54				G		P	0	
			20		0.61				G		P	1	
25 × 25 × 294	M	36	0	2.0	0.49	20			G		n	1	For 0 and 12% LF, expansion was lower than failure criteria. For 18% LF, it failed after 6 months [8].
			12		0.55		E		G		n	1	
			18		0.59		E		G		n	2	
40× 40 × 160	M	36	0	12	0.60	8	E	T			P	3	Thaumasite formation can be avoided when appropriate pozzolana was used [44].
			15		0.71		E	T			P	2	
			12		0.68		E	T			P	2	

100× 100 × 100	C	24	0	13.1	0.60	20	No component reported					4	Sulfate performance of concrete was dependent on C ₃ A content of the cement. Addition of 5% and 25% LF produced no consistent effect; it sometimes improved, but others, it worsened [45].
			5		0.63							4	
			25		0.80							4	
			0	8.5	0.60							1	
			5		0.63							1	
			25		0.80							1	
20 × 20 × 15	M	24	20	13	0.75	5	E		G			4	Faster rate of deterioration when increased C ₃ A content. For the same C ₃ A content the attack depended on LF [46].
			20	10	0.75		E	T	G		4		
			20	9	0.75		E	T			-		
			25	5	0.80			T			-		
			35	0	0.92		E	T	G		0		
30 × 40 × 50	P	12	0	6.7	0.40	5						1	Metakaolin (10%) or low Al ₂ O ₃ blast furnace slag (50%) improves the sulfate resistance of PLC with 15% LF [47].
			15		0.47			T	G	B		3	
			30		0.57							4	

40 × 40 × 160	M	12	10	8.1	0.44	5					0	0	Damage was mitigated using a sulfate resistance portland cement (SRPC) and completely eliminated when this cement was blended with fly ash [48].		
			10	0.0	0.44										
		60	10	8.1	0.44		E	T	n	n				3	
			10	0.0	0.44		E	T	n	n				1	
40 × 40 × 160	P	7	0	12.4	0.40	5	E		G		0	0	No significant difference on sulfate resistance performance of PC and PLC exposed to wet – dry cycles [49].		
			15		0.47		E							P	0
			30		0.57		E	T						P	1
40 × 40 × 160	M	12	0	12.0	0.6	5	E	T	G		4	3	Common cement and SPRC mortars showed signs of deterioration after 4 and 6 months, respectively. Resistance to TSA was improved by the addition of silica fume (8%) or GGBFS (60%) [50].		
			0	4.0			E	T							

2.2 Testing and Measurement of Sulfate Attack

There is an ASTM standard test method for the measurement of expansion due to ettringite sulfate attack. However, there is no standard test method for the damage due to the thaumasite type of sulfate attack. Mass loss, strength loss and visual appearance change documentations are some of the common techniques followed to evaluate thaumasite sulfate attack. The testing and measurement of different forms of sulfate attack are discussed in detail in the following sections.

2.2.1 Testing and measurement of conventional sulfate attack

In the US, the resistance of cement-based materials to sulfate attack is generally evaluated by ASTM C1012 (expansion of mortar prism). In ASTM C1012, mortar specimens 25 × 25 × 11.25 mm are immersed into 5% (50 g/L) sodium sulfate solution at a temperature of $23 \pm 2^\circ \text{C}$ without controlling the pH. This test is performed for at least 12 months and expansion is measured at certain intervals (1, 2, 3, 4, 8, 13 weeks and 4, 6, 9, 12 months) time. This test method has been recommended for blended cements and cement-based materials incorporating supplementary cementitious materials (SCMs). For concrete in the field, ACI 201.2R: Guide to Durable Concrete has categorized different classes (Table 2 and 3) of sulfate exposure based on the concentration of the external sulfates sources. According to this guide, for any type of portland blended cements, the limit for expansion is set at 0.10% after 18 months in exposure class S3 (more than 10,000 ppm). For reinforced concrete exposed to different sulfate environments (class S0, S1, S2, and S4),

the required maximum w/c ratio for the mixture and minimum compressive strength of concrete materials are also specified by ACI 318.

Table 2: Different sulfate severity class in soil and groundwater

Severity of potential exposure	Water – soluble sulfate (SO_4) in soil, % by mass	Water – soluble sulfate (SO_4) in soil, ppm	Sulfates (SO_4) in water, ppm	w/c m by mass , max	Min. comp. strength, psi
Class S0	$SO_4^{2-} < 0.10$	1000	$SO_4^{2-} < 150$	N/A	2500
Class S1	$0.10 \leq SO_4^{2-} < 0.20$	$1000 \leq SO_4^{2-} < 2000$	$150 \leq SO_4^{2-} < 1500$	0.50	4000
Class S2	$0.20 \leq SO_4^{2-} \leq 2.0$	$2000 \leq SO_4^{2-} \leq 20,000$	$1500 \leq SO_4^{2-} \leq 10,000$	0.45	4500
Class S3	$SO_4^{2-} > 2.0$	$SO_4^{2-} > 20,000$	$SO_4^{2-} > 10,000$	0.45	4500

Table 3: Requirement to protect against damage to concrete by external sulfate attack

Severity of potential exposure	Cementitious material		
	ASTM C150	ASTM C595	ASTM C1157
Class S0	No type restriction	No type restriction	No type restriction
Class S1	II	Type IP, IS, or IT with (MS) designation	MS
Class S2	V	Type IP, IS, or IT with (HS) designation	HS
Class S3	V plus pozzolan or slag cement	Type IP, IS, or IT with (HS) designation plus pozzolan or slag cement	HS plus pozzolan or slag cement

The current ASTM test method for evaluating the sulfate resistance of cement-based materials has been criticized because it neglects important factors including temperature, humidity, pH level, and the type of sulfate solutions which usually control the field performance of concrete structures [51]. Therefore, modified versions of the sulfate attack test have been reported in the literature for measuring the effect of temperature and humidity variations [52], pH level [53], type of cation and solution concentrations [45].

2.2.2 Testing and measurement of thaumasite sulfate attack

As discussed earlier, TSA has been reported to occur preferentially at low temperatures. Standard methods for the measurement of deterioration due to TSA have not been adopted. Therefore, to study the resistance of cementitious materials to TSA, studies [30, 54] have

used a modified version of ASTM C1012 in which temperature was kept constant at 5°C. Canadian Standards Association (CSA) A3000 introduced a standard test method for TSA (CSA A3004 – 08, procedure B) in its 2010 amendment, which is identical to ASTM C1012 (CSA A3004 – 08, procedure A) except that the temperature was changed to 5°C. In procedure A, the expansion of mortar bars was limited to 0.1% and 0.05% for moderate and high sulfate resistant cement, respectively, for a period of 6 months. However, in CSA A3004 – 08 (procedure B), the expansion limit (0.1%) is set at 18 months instead of 6 months and the standard recommended running period for the test is 24 months.

However, a recent study conducted by the Portland Cement Association (PCA) has revealed that the modification of ASTM C1012 to CSA A3004 – 08 (procedure B at 5°C) is not a representative test method for measuring damage due to TSA [55]. This research was conducted on sulfate resistance testing on mortars (laboratory) and concrete (both laboratory and under simulated field condition) period of 5 years. Different types of cement-based materials including portland cement (PC) with and without SCMs, portland limestone cement (PLC) having 5 to 15% limestone content with SMCs (e.g., fly ash, slag, metakaolin, and silica fume), and Type II and Type V were investigated. The modified version (at 5°C) of ASTM C1012 test results indicated that non-sulfate resistant mixtures are initially affected by ettringite-based sulfate attack and thaumasite is only observed after significant damage from conventional sulfate attack. This research also reported that the low-temperature mortar bar test does not reliably predict the performance of concrete made with PC – SCMs or PLC – SCMs blends. This is likely due to the fact that the pastes are not mature enough at testing, which results in excessive damages unrelated to the sulfate

attack. This new study recommends that the standard ASTM C1012 test method at 23°C be used to test PLCs (ASTM C595 Type IL and IT cements) with and without SCMs for sulfate attack resistance, not modified to 5°C. However, thaumasite does not cause expansion, which is the type of damage measured by ASTM C1012, so additional testing is also warranted.

Most investigations of TSA have included a description of the visual appearance of specimens. Several techniques for this purpose include visual rating, photographic records, and measuring the proportion of surface or edges of specimens damaged. At the initial stage, sulfate attack products accumulated in the concrete pores which does not manifest any visible deterioration. The damage typically starts from the corner and is followed by extensive cracking along the edges leading to spalling and disintegration on the surface of the specimens.

Finally, the reduction of compressive strength is also measured as a compliment to the ASTM C1012 test when assessing TSA formation. Kurtis et al. [11] developed an accelerated test for sulfate resistance of portland cements by assessing compressive strength. In this test method, paste (0.5 × 0.5 × 0.5 inch) cubes are immersed in 4% Na₂SO₄ solution and the pH is controlled at 7.2 to better simulate field conditions (whereas the CH leaching in the C1012 test tends to increase pH in the solution). A modified version of this test set at a temperature of 5°C will be used for this research. Besides compressive strength measurement, the mass of paste cube specimens will be recorded over the selected testing periods and mass loss (by percent of the initial mass) will be calculated at any given testing age.

2.3 Factors affecting TSA

Thaumasite only forms in portland cement concrete if certain conditions are satisfied. The formation of thaumasite TSA mainly depends on factors including the presence of sulfate, the presence of carbonate, the amount of tricalcium aluminate in the cement, moisture content, temperature, and the pH of the sulfate exposures. Further, the transport properties (primarily the permeability) of concrete also plays a significant role regarding the migration process of sulfate ions into concrete. Research showed that TSA requires advance formation of classical sulfate attack products (ettringite, gypsum, and depletion of CH) along with the availability of calcium carbonate to occur [25]. However, these factors (minus the carbonate source) also affect the formation of conventional sulfate attack (ettringite and gypsum formation). These factors are described in more detail as follows.

2.3.1 Source of sulfate ions

Sulfate ions either provided inside the concrete or ingressed from the exterior must be present for thaumasite formation to occur. The internal sources are mainly from sulfates provided by the cement and aggregates. Additionally, there is a possibility of sulfate generation from the sulfide oxidation of aggregates (i.e., iron sulfide (pyrite) which can be oxidized to form a sulfate pore solution in the presence of oxygen and moisture [29]. Most common sulfates in the field that may result in TSA are associated with sodium, magnesium, potassium, and calcium in soils or groundwater. Among them, magnesium sulfate has shown to produce the most damaging effects on the hardened cement paste made with PLCs especially compared to sodium sulfate [31].

2.3.2 Source of carbonates

Availability of carbonate ions is an integral part of TSA [56]. If carbonates are available in the cementitious matrix with sufficient moisture and a prevailing low temperature, thaumasite can easily form and further lead to TSA. In a case study, mortar specimens were made with cement containing either 20% limestone or 20% quartz as filler material and investigated in the same experimental exposure. The test results revealed a large amount of thaumasite in limestone cement and only a negligible amount of ettringite in quartz cement [57]. The test results indicated that limestone was the probable source of carbonate ions which were deemed to be responsible for TSA. Additionally, carbonate aggregates have been found to cause TSA [58]. Moreover, de-dolomitization (a partial/complete transformation of dolomite to calcite on the scale of individual crystals) of dolomitic aggregate may also release carbonates [59].

2.3.3 Alumina content in cement

The sulfate resistance of cement-based materials usually decreases as the C_3A content is increased. This compound can react with external SO_4^{2-} to form ettringite (AF_t phase). Furthermore, monosulfoaluminates (AF_m phases) in hardened cement paste formed from C_3A can also react with sulfates resulting sulfate attack. Similarly, AF_t and AF_m phases may also be formed due to the hydration of C_4AF compound, where aluminum is exchanged for iron [60]. C_4AF reacts more slowly in sulfate exposures; however, the mechanism for sulfate attack is anticipated to be the same as for the C_3A phase [61].

2.3.4 Temperature

The favorable temperature for thaumasite formation ranges from 5-15°C. The rate of thaumasite formation is governed by the exposure temperature and it usually increases with decreased temperature. This is due to insolubility of thaumasite, the stability of Si(OH)₆ groups, solubility of CO₂, and extent of portlandite solubility at these temperatures [26]. However, thaumasite can also form at a higher temperature because it can be stable at 20-25°C.

2.3.5 Moisture

Thaumasite formation requires water to be present at the reaction site. Water transport in cement-based materials is determined by matrix porosity and the connectivity of the pore system. These components are closely related to w/cm and the development of cement hydration in addition to the environment in which the concrete is located.

2.3.6 pH value

The pH of the concrete and the environment has a significant impact in the aggressiveness of the sulfate attack [7]. Classical sulfate attack is more aggressive at low pH because it can decalcify the concrete (and the C-S-H) which is very deleterious. Zhou et al. [62] studied the role of pH regarding TSA in OPC, PLC, and SRPC both in acidic and alkaline media which reported that the acidic media does not promote thaumasite formation. Additionally, it was found that the combination of higher sulfate concentration and alkalinity can escalate the kinetics of TSA on cement-based materials. Based on laboratory

and field experiments some other researchers concluded that thaumasite does not form in cementitious materials at pH level below 10.5 [63] and can be disintegrated and transformed into popcorn calcite if the pH level falls below 10.5 [32].

2.4 Prevention of sulfate attack

Certain strategies can be used to prevent classical and thaumasite sulfate attack. Building Research Establishment (BRE) Special Digest 1 [64] for concrete in aggressive ground highlights some key factors including type of cement, w/cm, and supplementary cementitious materials (SCMs) that can increase the resistance of cement-based materials to sulfate attack (including TSA). This guideline emphasized using low cement contents, SCMs, low w/cm, and dense (well-compacted) concrete will prevent the ingress of ions in concrete. Moreover, state of the art research shows that preventing conventional sulfate attack (expansion due to ettringite formation) can also prevent thaumasite formation.

2.4.1 Water content

The w/cm ratio is the leading parameter in concrete mixture design which controls the penetration of moisture and deleterious ions into the concrete matrix. To improve the durability of concrete against any type of chemical attack including TSA, low w/cm ratio (less than 0.45) is recommended. The overall fineness of cement increases (as limestone used to replace portland cement must have higher fineness) when limestone powder is added into the parent cement. This makes the mixture more workable and increases the strength of concrete at early age. A lower w/cm minimizes the internal transport of ions

including Ca^{2+} , CO_3^{2-} , SO_4^{2-} and water [65]. To improve the resistance of cementitious materials against any type of sulfate attack (including TSA), low w/cm (typically less than 0.45) is recommended to lower the ingress and movements of attacking ions and moisture, which ultimately accelerates chemical reactions with the hardened cement paste [29]. Low w/cm helps to produce concrete with less porosity, and finer and disconnected pore structure which reduces its susceptibility to TSA. W/cm ratio is one of the fundamental mixture design parameters of cement-based materials which control its resistance to the ingress of moisture and aggressive sulfate ions because it changes the pore structure.

2.4.2 Cement and aggregate content

Several research studies conducted on TSA have shown that the reduction of cement or aggregate containing limestone can lower the formation of TSA [62, 66]. To mitigate sulfate deterioration, the European Standard (EN 206 -1) imposes limitations on minimum cement content (300 – 360 kg/m³). The minimum cement content is prescribed to enhance the physical resistance (lower permeability) of concrete susceptible to sulfate attack; however, it is conceivable that this will decrease the volume of paste sensitive to sulfate attack reactions, which may affect the chemical resistance of concrete.

2.4.3 C₃A content

It is generally believed that there is a correlation between alumina content and TF. The reduction of aluminate content in cement-based materials might be an effective way to mitigate ettringite formation and eventual TSA. However, in some cases, it has been

reported that the use of sulfate-resistant cement (Type V) having less than 5% C_3A may not control damage due to sulfate attack [67]. To improve the sulfate resistance lower C_3A cement is available in the market. ASTM C150 Type I/II cement (moderate sulfate resistance) has less than 8% C_3A , and Type V cement (high sulfate resistance) has less than 5% C_3A . However, lowering C_3A does not guarantee that sulfate attack will not occur, so SCMs should also be used.

2.4.4 Use of SCMs

The use of SCMs including ground granular blast furnace slag (GGBS), fly ash, and silica fume has been proven to mitigate TSA in concrete [68]. The amount of SCMs required to control the expansion due to external sulfate attack depends on the composition of both the portland cement and SCMs, as well as the exposure conditions [6]. Canadian Standard Association CSA 3001 recommends using 25% Class F fly ash or 40% slag for binary blends and 5% silica fume + 25% slag or 5% silica fume + 20% Class F fly ash for ternary blends. However, a recent study [69] showed that 8% silica fume, 40% slag or 20% metakaolin perform better in thaumasite sulfate resistance. This research also recommended 40% slag + 20% Class F fly ash or 35% slag + 15% Class F fly ash for ternary blend PLCs in high sulfate environments.

3. Experimental program

3.1 Materials

In this study, the sulfate resistance of portland limestone cements (PLCs) in pastes and mortars placed in sodium sulfate and magnesium sulfate solutions were used for expansion testing and pastes were used for strength, visual rating, and mass loss, respectively. The results of PLCs mortar and pastes were compared to the performance of Type I/II and Type V cement [70]. The Type I/II portland cement contains 4.4% calcitic limestone (by mass) interground with the clinker during the manufacturing process while the Type V cement does not contain any added limestone. PLCs were lab-produced by adding powdered limestone rock to these cements. Both calcitic limestone (the same rock used in Type I/II cement) and dolomitic limestone rock were used. Class F fly ash was also added as a supplementary cementitious material (SCM) in this research. In this study, standard graded sand [71] was used making mortar specimens for all mixes. The chemical composition and physical characteristics of cement and filler materials are presented in Table 4.

Table 4: Chemical composition and physical data for the cements and fly ash

	Type I/II	Type V	Class F fly ash
<i>Chemical composition (wt. %)</i>			
SiO ₂ , %	19.8	21.8	52.2
Al ₂ O ₃ , %	4.7	4.4	15.9
Fe ₂ O ₃ , %	3.1	3.9	5.7
CaO, %	64.8	64.7	13.0
MgO, %	1.1	1.2	4.4
SO ₃ , %	3.1	2.2	0.6
Na ₂ O, %	0.12	0.13	2.5
K ₂ O, %	0.64	0.67	2.4
CO ₂ , %	1.8	1.3	-
LOI, %	2.7	1.2	0.1
<i>Mineralogical compound (wt. %)</i>			
C ₃ S, %	64.2	59.5	-
C ₂ S, %	10.9	20	-
C ₃ A, %	4.3	4.0	-
C ₄ AF, %	12.1	13.3	-
Equivalent alkalis, %	0.54	0.57	1.5
<i>Physical characteristics</i>			
Blaine fineness (m ² /kg)	429	408	-
Residue 45 μm sieve (%)	3.9	4.7	21.0
Specific gravity	3.13	3.15	2.53

3.2 Preparation of limestone powder

To manufacture the limestone powder, calcitic and dolomitic limestone rocks were kept in water for 24 hours and then washed to remove any residue. The rocks were then dried in an oven at 23°C for 24 hours to remove the moisture. A Denver 2HP in laboratory scale Jaw Crusher and pulverizer were used to break the limestone rock into small pieces. The

pulverized limestone was then placed into a ball mill system. Using a wet grinding process, 300 g of pulverized limestone and 1 liter of water was used with a complete set of steel balls (approximately 8 kg) and ground for 20 minutes with a speed of 100 rpm. This wet mixture was then oven dried at 35°C for 8 hours. In a dry grinding process, 100 g of limestone was ground using the same equipment for 15 minutes at 150 rpm. Afterward, the limestone powder was sieved using a #325 sieve (45 μm) and analyzed by Sympatec Mytos system with dry-dispersion and laser diffraction measurement. The particle size distribution results revealed that a higher amount of finer limestone powder was produced in the dry grinding process. The particle size distribution of the limestone powders is shown in Figure 2. The mineralogical composition of the limestone powders as measured by QXRD is presented in Table 5.

Table 5: Mineralogical composition of limestone powder

Limestone type	Weight %							
	Quartz (%)	Pyrite (%)	Illite (%)	Kaolinite (%)	Albite (%)	Dolomite (%)	Calcite (%)	Fineness (m^2/kg)
Calcitic	1.7	0.01	0.3	1.2	0.0	0.4	96.4	778
Dolomitic	8.0	0.26	0.6	0.4	0.7	81.0	9.0	657

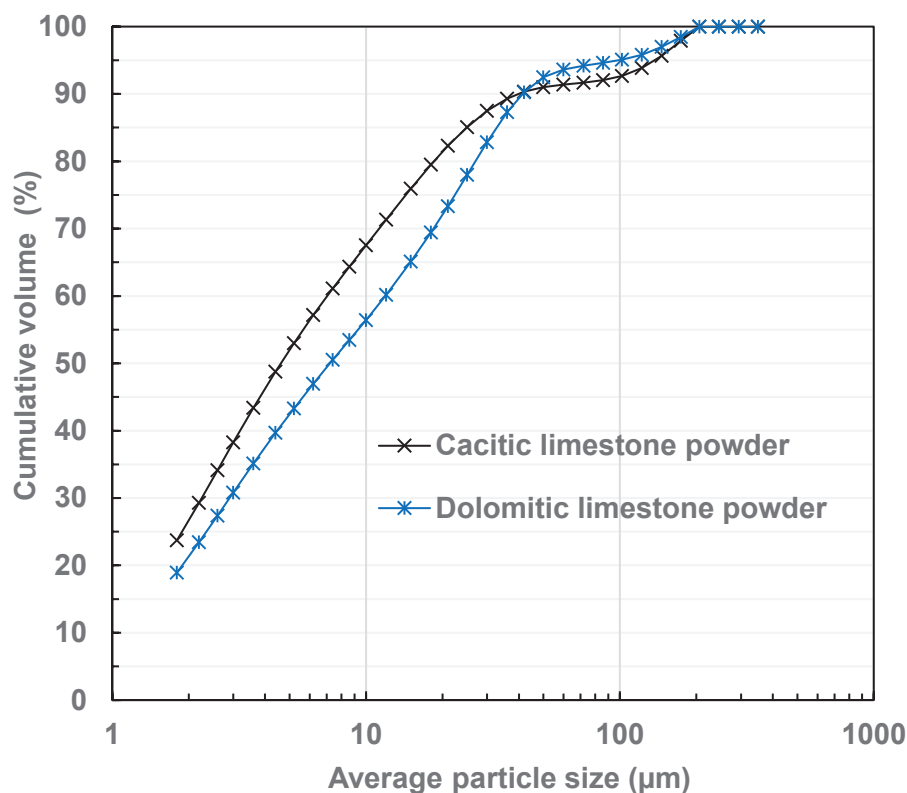


Figure 2: Particle size distribution of limestone powder

3.3 Mixture design

The details of the mixture design for the PLC mortars and pastes is shown in Table 6 and 7, respectively. The Type I/II cement itself contains 4.4% calcitic limestone powder. The cement was replaced by 5.6%; 10.2%; and 15.6% calcitic limestone powder to make 10%, 14.6%, and 20% PLCs, respectively. To note that, there is some level of potential error with the exact quantity of limestone in each mixture since it is calculated instead of measured. To evaluate the effect of adding fly ash, 20% (by mass) Class F fly ash was used to replace the 14.6% PLCs. Similarly, high sulfate resistant Type V cement was replaced

by 14.6% limestone powder (combinations of calcite and dolomite) and 20% (by mass) Class F fly ash.

Based on QXRD test results, the percentage of CaCO_3 in Type I/II cement, calcitic limestone powder, and dolomitic limestone powder was found to be 91%, 96.4%, and 9.0%, respectively. According to the standard specification for blended hydraulic cements, the limestone used to manufacture PLCs shall have a CaCO_3 content of at least 70% by mass [72]. To meet this requirement in some blended mixes the percentage of calcitic and dolomitic powder have been adjusted when added to the Type I/II and Type V cements. The percentage of dolomitic limestone powder to reach at least 70% of CaCO_3 content was calculated for the mixtures M-I-10.5C-4.1D and M-V-10.5C-4.1D (refer to Table 6 and 7). A sample calculation can be found in Appendix A.

The mixture designs are denoted using the generic placeholders “X-Y-##Z-F”, where the designator “X” represents mortar (M) or paste (P), “Y” designates the base cement type (Type I/II or Type V), “XX” represents the percentage of limestone in the cement, “Z” indicates the type of limestone (i.e., calcitic, C, or dolomitic, D), and F indicated the use of 20% fly ash. Additionally, Na and Mg represent submersion of the specimens in either sodium or magnesium sulfate solutions.

Table 6: Mix design for mortar bars expansion test exposed to sulfate solution at 23°C

Designation	Mixture proportion by mass					Sulfate solution types
	% control cement	% calcitic powder	% dolomitic powder	% F fly ash	w/cm	
M-I-4.4C	95.6	4.4	-	-	0.485	Na, Mg
M-I-10C	90	10	-	-	0.485	Na, Mg
M-I-14.6C	85.4	14.6	-	-	0.485	Na, Mg
M-I-10.5C-4.1D	85.4	10.5	4.1	-	0.485	Na, Mg
M-I-20C	80	20	-	-	0.485	Na, Mg
M-I-14.6C-20	65.4	14.6	-	20	0.485	Na, Mg
M-I-10.5C-4.1D-20	65.4	10.5	4.1	20	0.485	Na
M-V-0C	100	-	-	-	0.485	Na, Mg
M-V-14.6C	85.4	14.6	-	-	0.485	Na, Mg
M-V-10.5C-4.1D	85.4	10.5	4.1	-	0.485	Na
M-V-14.6D	85.4	-	14.6	-	0.485	Na
M-V-14.6C-20	65.4	14.6	-	20	0.485	Na

The details of mixture designs for the paste specimens is presented in Table 7. The pH of the solution was controlled for some of the mixtures, which is denoted by a “(pH)”: next to Na (refer to Table 7).

Table 7: Mix design for paste cubes exposed to sulfate solution at 23°C and 5°C

Designation	Mixture proportion by mass					Sulfate solution types
	% control cement	% calcitic powder	% dolomitic powder	% F Fly ash	w/cm	
P-I-4.4C	95.6	4.4	-	-	0.485	Na(pH), Mg
P-I-10C	90	10	-	-	0.485	Na, Mg
P-I-14.6C	85.4	14.6	-	-	0.485	Na(pH), Mg
P-I-10.5C-4.1D	85.4	10.5	4.1	-	0.485	Na(pH), Mg
P-I-20C	80	20	-	-	0.485	Na, Mg
P-I-14.6C-20	65.4	14.6	-	20	0.485	Na(pH), Mg
P-I-10.5C-4.1D-20	65.4	10.5	4.1	20	0.485	Na(pH)
P-V-0C	100	-	-	-	0.485	Na(pH), Mg
P-V-14.6C	85.4	14.6	-	-	0.485	Na(pH), Mg
P-V-10.5C-4.1D	85.4	10.5	4.1	-	0.485	Na
P-V-14.6D	85.4	-	14.6	-	0.485	Na
P-V-14.6C-20	65.4	14.6	-	20	0.485	Na(pH)

3.4 Mixing, casting, and measurement procedures

3.4.1 Mortar bar expansion measurement

The procedure outlined in ASTM C1012 [9] was followed to investigate the expansion of mortar specimens exposed to external sulfate. Following this standard, each mixture was proportioned as one part cement and 2.75 parts standard graded sand, and a water-to-cementitious materials ratio of 0.485. Before preparing the mortar mixtures, the filler materials and control cements were mixed properly as per the mixture design presented in

Table 6. The limestone powders, fly ash, and original cement was weighed as per the mixture design and mixed in an ASTM compliant mixer (Hobart H – 3844) for 5 minutes. The mortar mixtures were prepared according to ASTM C305 [73] and ASTM C109 [10]. Each mix consisted of 9 -2 inch × 2 inch × 2 inch mortar cubes and 6 -1 inch × 1 inch × 11.25 inch mortar bars. A thin coat of release agent (form oil) was applied to the interior surfaces of the standard cube and prism molds. Once the mortar was prepared it was cast into the metal cube and prisms molds. Hand tamping of the mortar was performed according to ASTM C109 with a 0.5 inch × 0.8 inch × 6 inch non-absorbent oak wood. Immediately after placement, the molds were covered by a plastic plate and placed over a riser in a closed container filled to 0.5 inches below the bottom of the molds with preheated water (35°C). Afterward, the container was covered by a lid and stored in an oven at 35°C for 24 hours.

After 24 hours of initial curing, all bars and cubes, except two cubes, were demolded and submerged in saturated Ca(OH)_2 at 23°C. The 24-hour compressive strength of the two cubes was tested, and subsequently, the compressive strength measurements were monitored daily until the average strength of mortar cubes reached 2850 psi. Once the mortar cubes in a batch gained the specified strength, the initial length of the mortar bars was measured with a digital length comparator according to ASTM C490 [74]. Next, 6 mortars bars were submerged in sodium or magnesium sulfate solution with a SO_4^{2-} concentration of 33800 mg/L and stored at 23°C. 50 g and 43.36 g of anhydrous sodium and magnesium sulfate respectively were diluted in deionized water to prepare the sulfate solutions. See Appendix A for sulfate concentration calculations.

In this study, local materials from South Dakota, USA, were used to make the PLCs for sulfate attack testing. Roughly 1,300 sulfate concentrations in South Dakota soils were studied to determine the appropriate solution composition for experimental sulfate attack testing. The ionic concentrations of saturated pastes were provided by measurements conducted by the Natural Resources Conservation Service (NRCS) under the United States Department of Agriculture (USDA). In addition to measuring sulfate concentrations, the sodium and magnesium concentrations associated with sulfate ions were measured for all test samples. Note that the soil samples analyzed in the study are not completely representative for South Dakota due to the limited sampling. Results showed that more than 50% of the counties shown have an average sulfate concentration between 2,000 mg/L to 20,000 mg/L which indicates a severe exposure class (S2) [75]. Many of the counties have both magnesium and sodium cations associated with sulfates. This is the reason magnesium sulfate solutions were also considered for the sulfate attack testing for this study. The details of the sulfate concentration associated with sodium and magnesium can be found in Appendix B.

750 ml of sulfate solution for each mortar bar was used and the initial pH of the sulfate solution fell in a range of 6.0 to 8.0 as specified in the standard. Afterward, the length of the mortar bars was measured at 1, 2, 3, 4, 8, 13, and 15 weeks after immersion in the sulfate solution. The length of mortar bars was measured every month after 15 weeks. The sulfate solution was refreshed after 4, 8, and 13 weeks, and after 6 and 9 months. No attempt was made to alter the pH of the sulfate solutions during the experiment.

3.4.2 Strength measurement, mass loss, and visual rating of pastes

Although the ASTM C1012 standard measures the expansion of mortar samples related to the ettringite form of sulfate attack, there is no standard procedure to measure the gypsum (or thaumasite) formation ($\text{CaSO}_4 \cdot 2\text{H}_2\text{O}$) during sulfate attack. Gypsum formation can take place due to the reaction between calcium hydroxide and external sulfate ions. The accelerated test methods adopted by some researchers use the loss in strength as an indication of sulfate resistance [11, 76].

In this study, a modification of the accelerated test method developed by Kurtis et al. has been followed to evaluate sulfate deterioration which measures the compressive strength reduction of paste specimens [11]. In this experiment, the compressive strength change over time of 0.5 inch \times 0.5 inch \times 0.5-inch paste specimens were tested. Steel molds were fabricated to cast the specimens. A standard mixing procedure (ASTM C305) for paste was followed for making the paste samples using a $w/cm = 0.485$ (same as for ASTM C1012) for all mixtures referred to Table 7. After molding, the specimens were covered to avoid shrinkage and kept at 23°C for 24 hours. After demolding, the paste cubes were submerged in water and kept in an oven at 50°C for 6 more days to accelerate their maturity. For each mixture, 100 cubes were made (specimens with imperfections were rejected).

Once the initial curing was finished, dimensions of the cubes were measured using a slide caliper. The size of the cubes generally varied from 0.50 inch to 0.52 inch. Afterward, the 7-day compressive strength of 12 cubes for each mixture was determined. This strength is

referred to the initial strength of the paste specimens. The loading rate for the compressive strength test was 10 lb/sec.

Because of the small sample size, there was a considerable variability in strength results. The surface of the cubes placed below the center of the upper bearing block of compression machine was not identified for all cubes in a batch. Moreover, all cubes were not equally smooth, which can affect the strength results. A statistical approach outlined in ASTM C109 was followed to identify the outliers.

In this method, the average strength was calculated from 12 cubes tested at each age and the standard deviation was computed thereafter using the following equation.

$$SD_b = \sqrt{\left(\frac{\sum(X-X_b)^2}{N_b-1}\right)}$$

Where,

SD_b = standard deviation of a single batch

X_b = average of test values in single batch

N_b = number of cubes per batch

Then, maximum normal deviation (MND) was calculated using the Excel function

“=norminv (1-0.25/ N_b , 0, SD_b)”

The normal range used to find out the outliers was as follows:

Maximum = (X_b + MND)

Minimum = $(X_b - MND)$

Outlier = any test value falling outside the calculated normal range.

In each testing age, 20 cubes were selected for mass loss measurements and visual appearance ratings, and 12 cubes were selected for strength testing. The mass of paste specimens was measured at every testing period for all mixtures placed in sodium and magnesium sulfate at both temperatures. The initial mass (7 -day after elevated curing) was measured after placing the paste cubes into the sulfate solutions for 24 hours. Soft facial tissue paper was used to soak out the water from the surfaces of the cubes before weighing. All specimens were placed in a large bin of sodium and magnesium sulfate solutions placed at 23°C and 5±1°C.

For select mixtures (refer to the mixtures presented in Table 7) the effect of a constant pH of the sulfate solution to mimic field conditions, the pH sodium sulfate solution was measured. For these samples, the pH of the sodium sulfate solution was maintained at 7.2 using a pH meter and a dosing pump (Milwaukee MC720). The dosing pump added aliquots of 0.1N H₂SO₄ from a flask (placed outside of the refrigerator) until the pH of the sulfate solution reached 7.2. The concentration of sodium and magnesium sulfate solution was kept constant at 33800 ppm. The initial mass of the paste cubes was determined after 24 hours of immersion in sulfate solutions. For this test, the excess water on the surface of samples was removed using paper towels and then the samples were weighed. The mass loss, visual inspection, and compressive strength were measured at 14, 28, 56, 91, and 120 days after the immersion of samples in sulfate environments.

3.4.3 X-ray diffraction testing on pastes

The paste specimens tested for strength at 28 days and 120 days placed in sodium and magnesium sulfate solutions at 23°C and 5°C were saved to perform a microstructural investigation using X-Ray diffraction (XRD). As sulfate attack is more severe at low temperatures, XRD was performed only on the specimens placed at 5°C. The broken cubes were ground into powder using a mortar and pestle and then sieved through a #200 sieve. The hydration was stopped using isopropanol alcohol and all samples were stored in a sealed bottle until testing to avoid carbonation.

4. Results and Discussion

4.1 Expansion of mortar bars

4.1.1 Influence of limestone percentage

The expansion results of the prismatic mortar specimens incorporating an increasing percentage of calcitic limestone (4.4% – 20%) powder submerged in sodium sulfate and magnesium sulfate solutions are presented in Figure 3 and Figure 4, respectively.

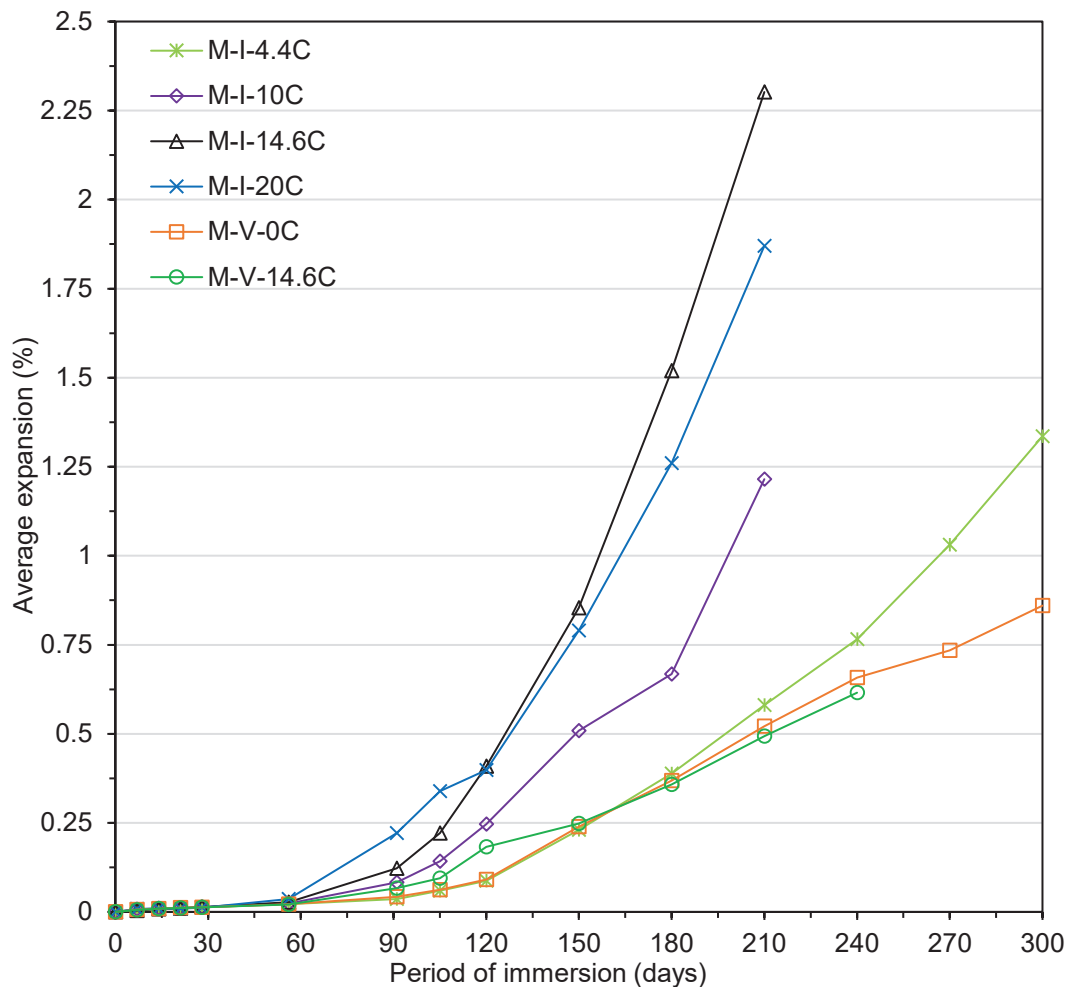


Figure 3: Expansion of different dosages of PLC mortars placed in 5% sodium sulfate solution

All mixtures experienced a similar trend of expansion at early ages in both sulfate solutions. Previous research has shown that mortar bars in this test expand slowly at the beginning and can have significantly increased expansion after 28 days of sulfate exposure [77]. After 91 days in solution, all mortar bars showed a gradual expansion trend. The expansion trend observed in magnesium sulfate up to 91 days of exposure was similar to sodium sulfate for all mixtures although lower in magnitude. Afterward, the mortar samples submersed in sodium sulfate expanded more rapidly than those in magnesium sulfate up to 7 months.

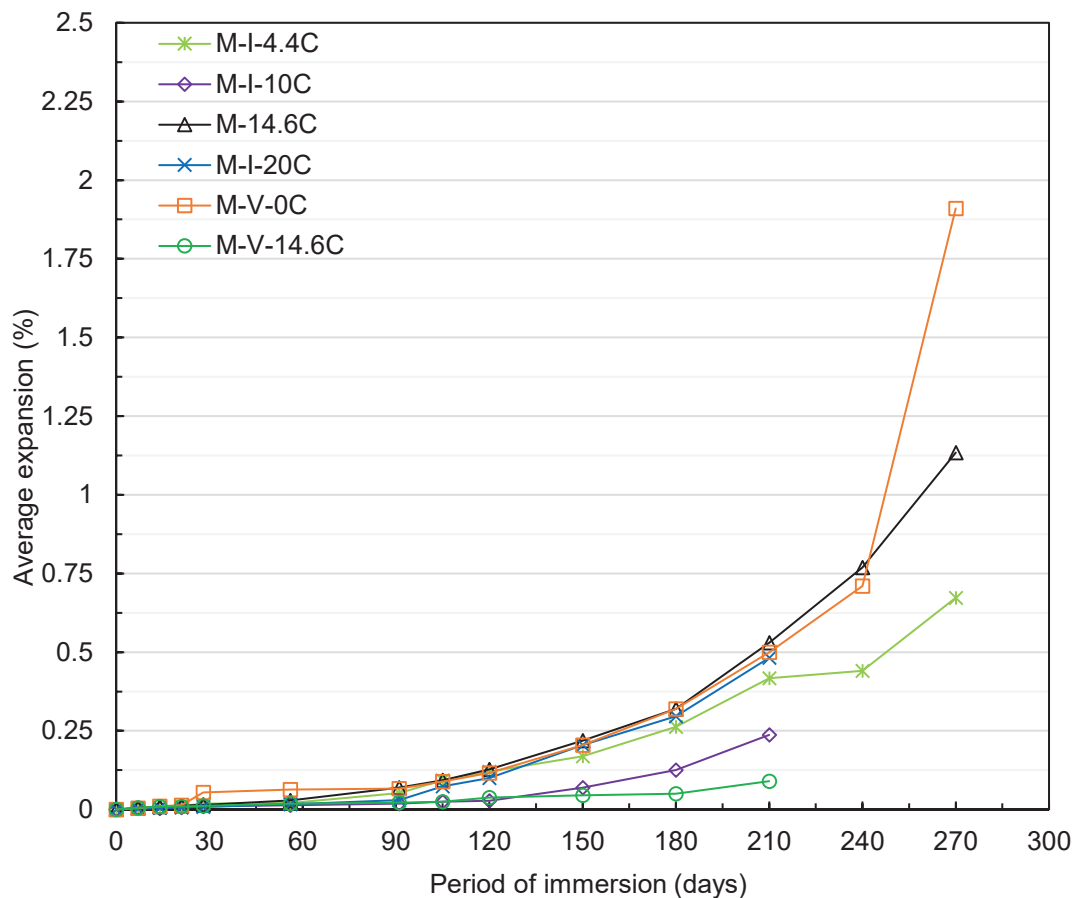


Figure 4: Expansion of different dosages of PLC mortars placed in 4.23% magnesium sulfate solution

In general, the percent expansion increased with an increasing dosage of limestone filler over the exposure time. In sodium sulfate, the percent expansion of PLCs (using Type I/II cement as a base) was proportional to the ratio of the calcitic limestone replacement up to 4 months of exposure and continued thereafter except for the M-I-20C mixture. This is in agreement with the results conducted on PLCs in other studies [78, 79]. In contrast, the expansion results of Type I/II replaced PLCs in magnesium sulfate were less affected by an increase in limestone content. Similar results on PLC mortars in magnesium sulfate are reported elsewhere [80, 81]. Interestingly, in both sulfate solutions, the M-I-14.6C and M-I-20C mixtures followed a close expansion pattern after 120 days. This might be due to the filler effect of limestone powder which reduces the C_3A content of the cement, and thus any negative affects due to a higher limestone content are negated by the lower C_3A content [82-84]. All mixtures placed in sodium sulfate were completely disintegrated after 210 days except the control cement (M-I-4.4C). On the other hand, none of the PLC mixtures were disintegrated when placed in magnesium sulfate during the same exposure period.

Overall, in sodium sulfate, the control cement (M-I-4.4C) performed better than other similar blends with the exception of the M-I-10C mixture, which performed better among Type I/II replaced PLCs in magnesium sulfate. Still, the M-I-4.4C mixture in sodium sulfate exceeded the ASTM C1157 12-month expansion limit at 120 days (Figure 3) while the M-I-10C mixture in magnesium sulfate exceeded this limit roughly at 170 days (Figure 4) [85]. The other Type I/II replaced PLC mixtures in sodium sulfate exceeded this expansion limit roughly between 65 to 95 days whereas in magnesium sulfate this occurred between 105 to 120 days.

It is evident from Figure 3 and Figure 4 that the percent expansion of M-V-0C mortar samples in both sulfate solutions was approximately the same until 8 months. In magnesium sulfate, the M-V-0C mortar showed a sudden rise in expansion with 0.05% at 28 days of exposure followed by a constant expansion until 3 months. Then, a gradual expansion was noticed until 8 months; however, a huge rise in the expansion was recorded after 9 months of exposure. This can be attributed either to the instability of brucite layer due to the expansive forces exerted by the ettringite due to the decomposition of the C-S-H matrix through the direct penetration of magnesium sulfates.

The incorporation of 14.6% calcitic limestone to the original Type V cement (M-V-14.6C) substantially improved the expansion over the exposure time. The M-V-14.6C passed the ASTM C1157 6-months expansion limit, however; it showed an expansion of 0.09% at 7 months (Figure 4), which is close to exceeding the ASTM C1157 12-month expansion limit (0.1%). The expansion of M-V-14.6C was similar to the sample with no limestone at the same immersion time when placed in sodium sulfate solution (Figure 3), which is in contrast with the behavior exhibited when adding limestone to the Type I/II cement. It is well known that the most important factor in the sulfate resistance of portland cement is the C_3A content [29, 86]. ASTM C150 [70] restricts the C_3A percentage to <5% for Type V cement to control the ettringite expansion when used in aggressive sulfate environments. In this study, the lower C_3A (4.0%) and higher fineness ($778 \text{ m}^2/\text{kg}$) of calcitic limestone powder could have contributed to its lower expansion with the added limestone. However, since both Type I/II and Type V cements have similar C_3A content, there is likely another

reason. Perhaps its higher C_2S content or lower SO_3 content also contributed to its lower expansion with added limestone especially in magnesium sulfate solution.

Overall, the Type V cement (M-V-0) showed less expansion in sodium sulfate than Type I/II cement (M-I-4.4) (Figure 3). The M-V-0C performed worst in magnesium sulfate during the entire exposure period (Figure 4), however, the addition of 14.6% calcitic limestone improved the sulfate resistance of this mixture, which outperformed all other mixtures.

4.1.2 Influence of limestone type and composition

The mortar bar expansion results of different 14.6% PLCs made with both calcitic and dolomitic limestone placed in sodium sulfate and magnesium sulfate with and without fly ash are shown in Figure 5, Figure 6, and Figure 7. Although the M-I-14.6C mixture showed the maximum expansion in both solutions, the addition of dolomitic limestone improved the sulfate resistance of this mixture both in sodium and magnesium sulfate solutions. The approximate percent expansion of the M-I-10.5C-4.1D mixture was 0.42% at 8 months exposure in both solutions (Figure 5 & 6). The Type V mortar bars (M-V-10.5C-4.1D) expanded even less (Figure 7).

When the dolomitic limestone (4.1% by mass) was incorporated into M-I-14.6C to make M-I-10.5C-4.1D, the expansion at 6 months exposure decreased by 84% and 59% in sodium and magnesium sulfate, respectively (Figure 5 & 6). Similar results on mortar bar expansion with dolomitic limestone have also been reported elsewhere [87]. Further, the

expansion of M-V-10.5C-4.1D was 54% lower than M-V-14.6C in sodium sulfate at 180 days (Figure 7). The replacement of Type V cement by 14.6% dolomitic limestone powder improved the sulfate resistance even more by 59% at 180 days in sodium sulfate (refer to Figure 3 and Figure 7).

Although some consider limestone to be an inert material, investigations have reported reactions between limestone and other components when added as a filler material in portland cement [88, 89]. These reactions are likely influencing the sulfate attack results here. Dolomite contains calcium, magnesium, and two carbonate ions with the formula $\text{CaMg}(\text{CO}_3)_2$. Compared to calcite (CaCO_3), dolomite provides an additional source of magnesium and slightly more carbonates. Because of this additional carbonate released from the dolomite, more stable AFm (alumina, ferric oxide, mono-sulfate) phases, like hemicarbonate ($\text{Ca}_4\text{Al}_2(\text{CO}_3)_{0.5}(\text{OH})_{13} \cdot 5.5\text{H}_2\text{O}$) and monocarbonate ($\text{Ca}_4\text{Al}_2(\text{CO}_3)(\text{OH})_{12} \cdot 5\text{H}_2\text{O}$) are formed during the reaction between limestone and aluminate in portland cement [90-93]. These AFm phases are more stable than monosulfate ($\text{Ca}_4\text{Al}_2(\text{SO}_4)(\text{OH})_{12} \cdot 6\text{H}_2\text{O}$) [94]. This phase change does not allow ettringite ($\text{Ca}_6\text{Al}_2(\text{SO}_4)_3(\text{OH})_{12} \cdot 26\text{H}_2\text{O}$) to transform into monosulfate even when the sulfate sources are consumed (e.g., $\text{CaSO}_4 \cdot 2\text{H}_2\text{O}$).

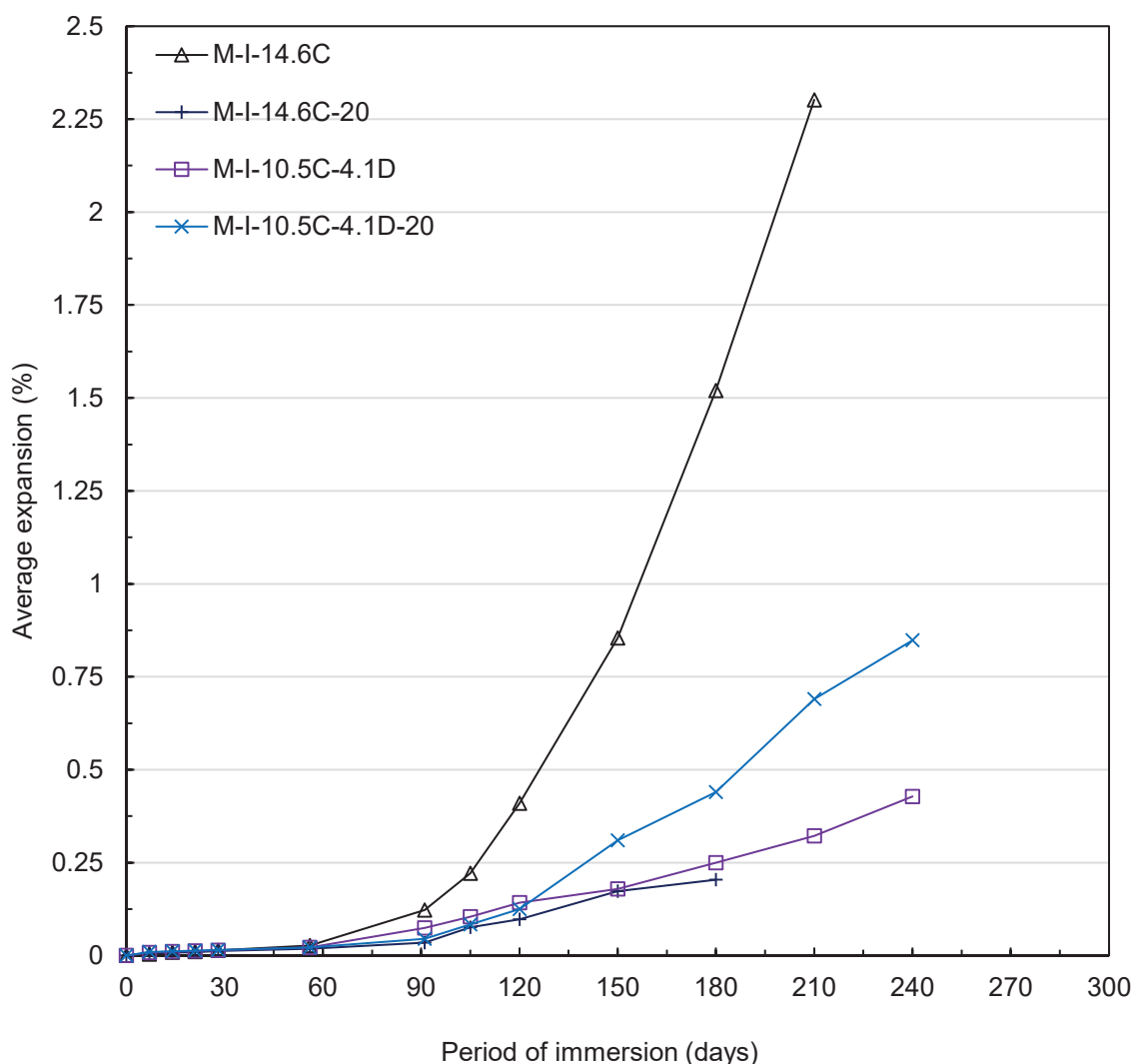


Figure 5: Expansion of different dosages of PLC mortars placed in 5% sodium sulfate solution

This phase alternation phenomenon, called ettringite stabilization, can increase the volume of hydrates and consequently reduce the porosity [88, 89, 95]. This, in addition to less monosulfate available for conversion to ettringite in the matrix, could be a potential reason for the improving sulfate resistance of all mixtures where dolomitic limestone was used to replace calcitic limestone. Another potential reason that could allow dolomitic limestone to improve sulfate resistance could be the chemical interaction that accelerates the

hydration of tricalcium silicate when calcium carbonate is added to the cements. This phenomenon was reported in another study [96] but an opposite finding has also been found [97]. It appears the differences in fineness between the two limestones had less effect than the differences in their chemistry. That is because a higher limestone fineness would typically perform better, but the higher calcitic limestone fineness compared to the dolomitic limestone did not result in better sulfate resistance.

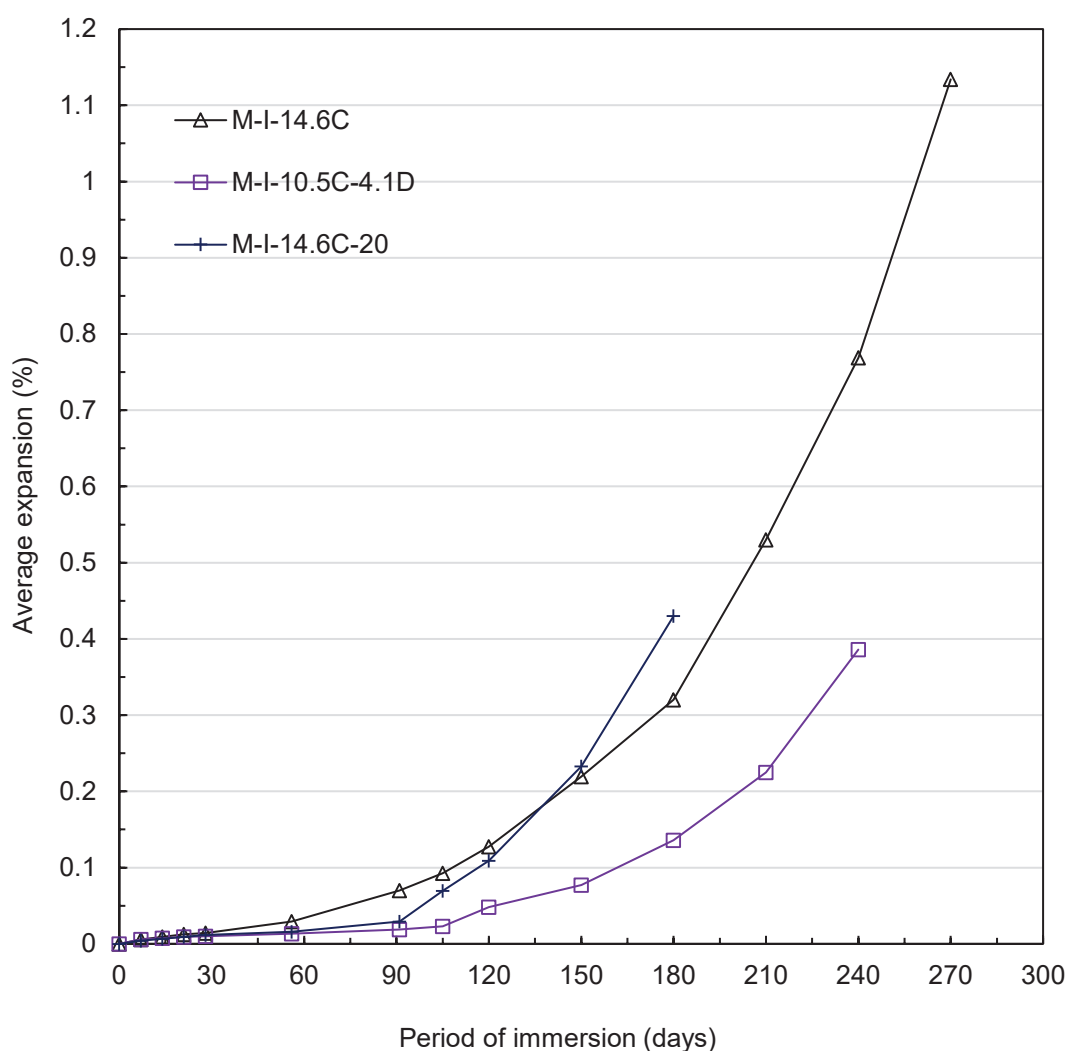


Figure 6: Expansion of different dosages of PLC mortars placed in 4.23% magnesium sulfate solution

Nevertheless, M-V-10.5C-4.1D and M-V-14.6D mixtures still exceeded the ASTM C1157 12-month expansion limit between 135 to 145 days in sodium sulfate, but at a later age than the same cement with only calcitic limestone. Similarly, while the M-I-14.6C mixture exceeded this expansion limit roughly at 80 days and 105 days in sodium and magnesium sulfate solution, respectively, the time required for M-I-10.5C-4.1D mixture to cross this limit was 100 days and 165 days for the corresponding sulfate solutions.

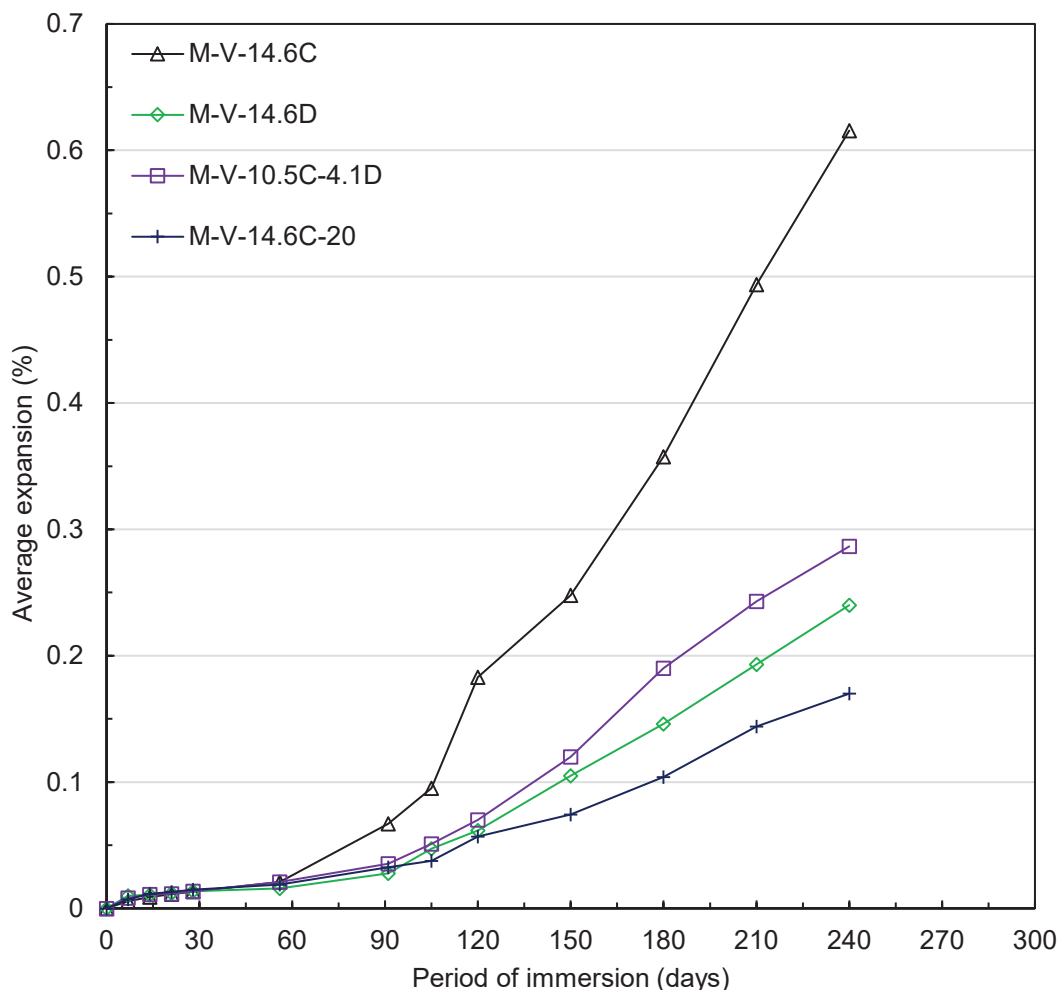


Figure 7: Expansion of different dosages of PLC mortars placed in 5% sodium sulfate solution

4.1.3 Influence of fly ash

The effect of fly ash on the sulfate attack expansion of different 14.6% PLCs (calcitic and dolomitic) in both sulfate solutions are presented in Figure 5, Figure 6, and Figure 7. The replacement of M-I-14.6C with 20% fly ash reduced the expansion approximately 645% at 180 days in sodium sulfate (Figure 5). The probable reason for this is the pozzolonic activity of fly ash that reacts with the calcium hydroxide (Ca(OH)_2) released in the hydration process of portland cement, thus reducing the availability of Ca(OH)_2 which can react with external sulfate compounds. The addition of fly ash also helps to reduce the amount of tricalcium aluminate (C_3A), which mostly influences the expansion of cementitious materials. This effect is similar to other research that has found that adding Class F fly ash (4.0% of CaO) with PLCs results in moderate sulfate resistance with 40% fly ash replacement [98].

Still, both the M-I-14.6C and M-I-14.6C-20 mixtures in sodium sulfate exceeded the ASTM C 1157 6-months expansion limit roughly at 83 days and 120 days, respectively. Generally, the percentage of CaO is the governing factor for a fly ash's resistance to sulfate attack. PLCs with 20% fly ash ($\text{CaO} < 8\%$) perform better in sulfate environments compared to fly ashes with higher calcium contents [99] in part due to the higher C_3A contents of high CaO ashes. In this study, the fly ash used contains 13.03% of CaO (which lies closer to the range of Class C fly ash), which could be a potential reason for not vastly improving the sulfate resistance of these PLCs.

Adding dolomite to the mix (M-I-10.5C-4.1D-20) resulted in a better expansion performance up to 90 days with the addition of fly ash, but had higher expansion thereafter, with 76% higher expansion with the fly ash than M-I-10.5C-4.1D at 180 days (Figure 4). The pH of the sodium sulfate solution measured in this study varied in between 12.2-13.5 which is highly alkaline in nature. Studies have shown that dolomite can undergo a dedolomitization reaction in alkaline sulfate environments where dolomite forms brucite and calcite by reacting with portlandite [100-102]. The combined effect of this brucite formation and the high CaO content of the added fly ash may be the reason for the higher expansion of the M-I-10.5C-4.1D-20 mixture.

In contrast, the fly ash addition increased the expansion of M-I-14.6C mortar specimens when placed in magnesium sulfate (Figure 6). The mortar bars expanded rapidly starting at 90 days and by 6 months had an increased expansion of about 34% compared to the M-I-14.6C mixture at the same exposure time. The expansion of M-I-14.6C-20 at 180 days was even 65% higher than the control cement (M-I-4.4C) in magnesium sulfate (Figure 4 & 6). On the other hand, the expansion of M-I-14.6C-20 reduced expansion by 37% in sodium sulfate at the same immersion time (Figure 3 & 5). To summarize, the addition of calcitic limestone and fly ash increased the expansion of mortar samples in magnesium sulfate and reduced expansion in sodium sulfate for the same mixture (M-I-14.6C-20) at the same exposure time.

For Type V cement, although the percent expansion of M-V-0C and M-V-14.6C was the same (0.36%) at 180 days in sodium sulfate exposure the addition of fly ash reduced expansion by 71% (Figure 6). Still, both samples exceeded the ASTM C1157 12-month

expansion limit by 6 months. Moreover, M-V-14.6C-20 showed overall better performance at any given age among all other PLC mortars placed in sodium sulfate exposure. The reason that the M-V-14.6C-20 mixture showed better sulfate resistance could be due to its lower SO_3 (2.2%) content. Similar results were reported on Type V cement replaced by fly ash in other studies [103-105]. Also, the lower C_3A (4.0%) and higher fineness ($778 \text{ m}^2/\text{kg}$) of the calcitic limestone powder along with the addition of fly ash could have reduced the expansion of the mortar specimens.

Overall, the addition of fly ash and limestone helped to reduce the expansion of Type V replaced PLCs more than Type I/II replaced PLCs. C_3S releases more $\text{Ca}(\text{OH})_2$ than C_2S during the hydration of portland cement. The proportion of $\text{C}_2\text{S}/\text{C}_3\text{S}$ in Type V cement is higher than the Type I/II cement which could be a reason for the lower amount of $\text{Ca}(\text{OH})_2$ and subsequently reduced expansion of these mortars in sulfate environments.

4.2 Mg and Na expansion trend

In this study, the mortar bar expansion results showed a lower expansion trend in magnesium sulfate than in sodium sulfate for the same mixtures at the same exposure period (refer to Figure 3 - 7). The calcitic limestone addition helped to reduce the expansion in magnesium sulfate, but it increased the expansion of mortar samples in sodium sulfate at 180 days of the exposure period. Overall, the calcitic limestone replaced PLCs showed reduced expansion in magnesium sulfate compared to sodium sulfate, but the reduction was higher at a higher addition of limestone (Figure 8).

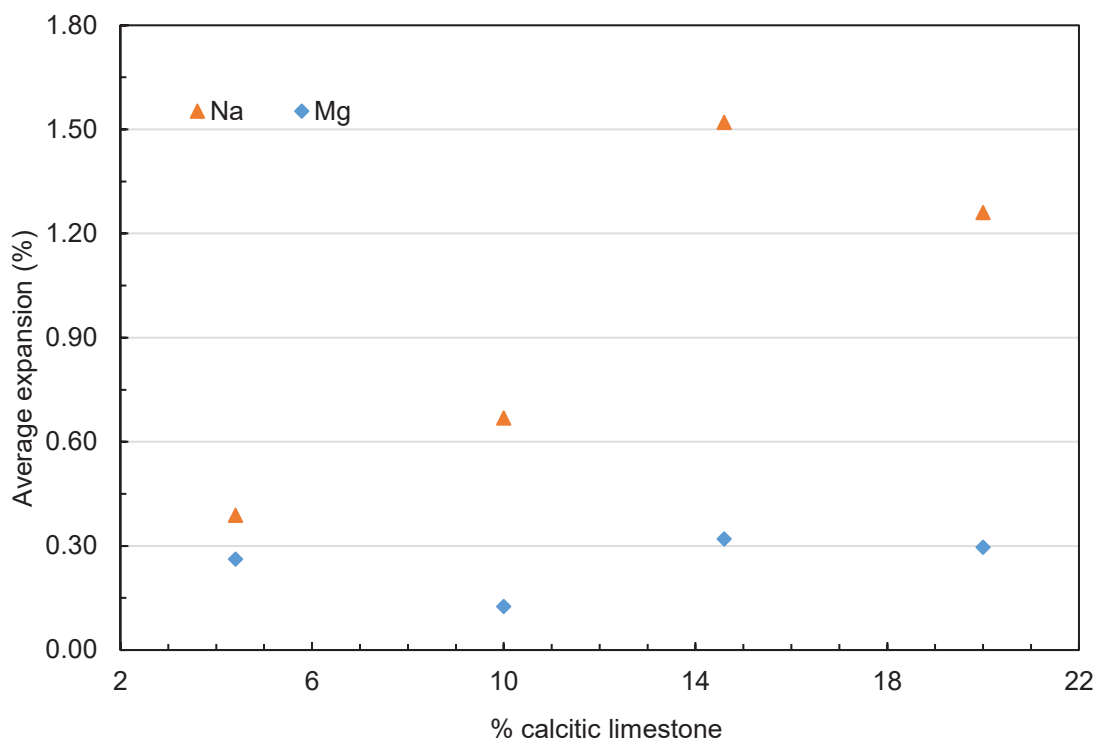


Figure 8: Expansion trend of different PLCs (calcitic limestone) in sulfate solutions at 180 days

Moreover, the overall expansion of all other cements made by replacing M-V-0C and M-I-4.4C cements with calcitic/dolomitic limestone, and fly ash was higher in sodium sulfate than magnesium sulfate over the entire study period (refer to Figure 3 – 7). Several studies have revealed the higher expansion of PLC mortars in sodium sulfate compared to magnesium sulfate using the same experimental setup [31, 78, 79, 106].

Another difference observed between Na and Mg expansion data is the rate of expansion over time. The expansion of mortar samples from all of the mixtures placed in sodium sulfate solution occurred in two-stages (Figure 3, 5, 7). In the initial stage (until 2 months),

the expansion was very low but was followed by a sudden increase in expansion due to excessive ettringite and gypsum formation in the final stage and continued in some cases until the mortar bars were completely disintegrated. This two-stage expansion trend for sodium sulfate is also reported in other studies [51, 107, 108].

On the other hand, the mortar specimens stored in magnesium sulfate solution followed a steady expansion (Figure 4, 6). This is due to the formation of a brucite layer at the exposed surface of the specimens. The low solubility of this brucite layer restricts the magnesium ion penetration into the interior matrix of mortar samples. However, the brucite layer consumes a high amount of CH and depletes the pH of the pore solution. The C-S-H provides the necessary CH to maintain the solution pH which eventually leads to decalcification of C-S-H. In a later stage of sulfate attack, the calcium ion can be completely replaced by magnesium ion, converting the C-S-H to M-S-H, which has been reported to be a non-cohesive phase. This mechanism of sulfate attack in magnesium sulfate solution has also been reported elsewhere [109, 110].

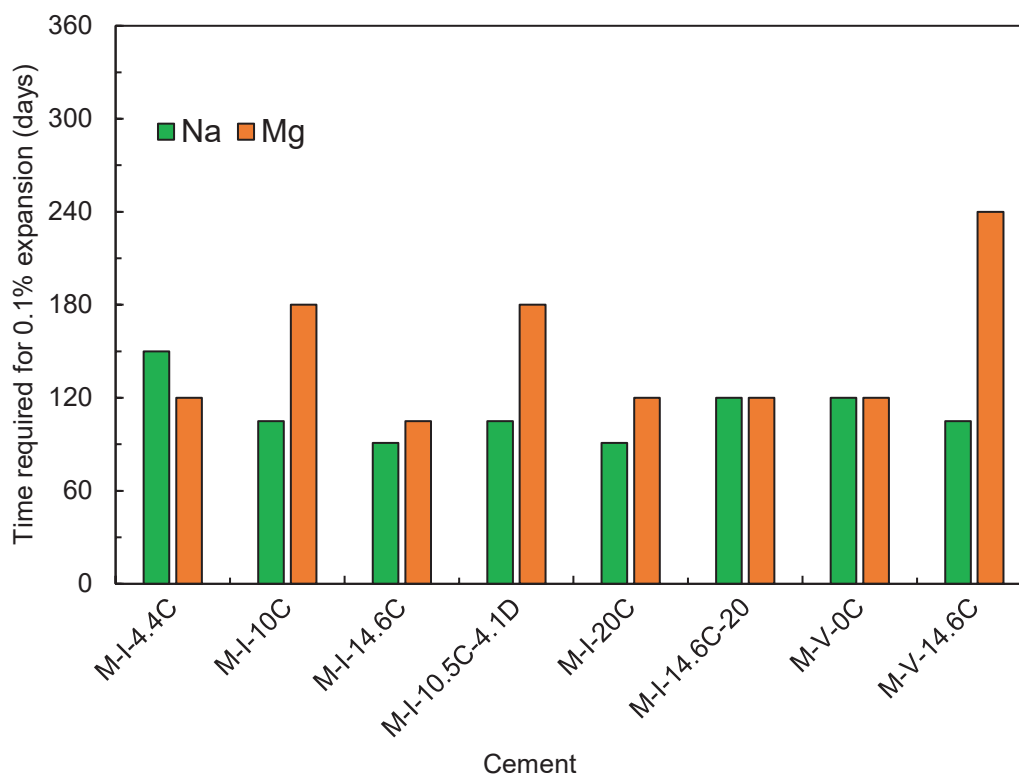


Figure 9: Time required for different PLCs to exceed the average expansion of 0.1% in sulfate solutions

The time required for some of the PLC mixtures (common in both solutions) to exceed the ASTM C1157 12-month expansion limit (0.1%) is shown in Figure 9. Eight common mixtures which were tested in both sulfate solutions are presented here. This indicates that all of the mixtures have exceeded the allowable expansion limit well prior to 12 months regardless of the sulfate solution type. The majority of the mixtures exceeded the 12-month expansion limit quicker in sodium sulfate compared to magnesium sulfate.

4.3 Visual appearance of mortar specimens

Sulfate ion penetration from external sources can lead to different degrees of deterioration in cement-based materials including changes in porosity, microcracking, expansion, flexural and compressive strength loss, spalling, mass loss and even complete disintegration. It is common for studies to include a description of the visual appearance of specimens to evaluate the sulfate performance of cementitious systems [6, 111]. The photos of mortar specimens (one from each mixture) placed in sodium and magnesium sulfates are shown in Figure 10. At the beginning of observed expansion, the pores are filled with products due to sulfate attack and thus no visible deterioration was detected. Following this, the first sign of attack starts with the deterioration of corners followed by extensive cracking along the edges. Overall, the mortar samples with higher calcitic limestone powder amounts in both solutions showed more damage in both solutions. Mortar bars with 10%; 14.6%, and 20% limestone completely disintegrated after 7 months when placed in sodium sulfate solution (Figure 10-a). The mixtures M-I-10.5C-4.1D, M-I-14.6C-20, and M-I-10.5C-4.1D-20 showed some damage at corners, warping and cracking along the edges (Figure 10-b). Although M-V-0C mortar bars showed extensive cracking and some spalling at the corners (Figure 9-b), the addition of limestone and fly ash helped to reduce the surface deterioration (Figure 10-b). The mortar bar expansion results of all mixtures placed in sodium sulfate correspond with their surface deterioration (Figure 3, 5, and 7).

In magnesium sulfate solution, a white powdery coating (probably brucite layer) was detected, and spalling was observed along the edges in almost all specimens except M-V-14.6C. The calcitic limestone replaced PLCs showed noticeable damage at the corners

along with spalling along the edges and some extensive cracking in mortars made from M-I-4.4C and M-I-10C (Figure 10-c). The addition of fly ash increased the surface degradation of M-I-14.C-20 (Figure 10-d) but the addition of dolomitic limestone reduced surface damage (Figure 10-d). However, the addition of fly ash in M-I-14.6C-20 mixture showed less surface damage and expansion in sodium sulfate probably due to the absence of the weak brucite layer. In magnesium sulfate, the worst level of degradation including spalling, cracking, and expansion was observed in M-V-0C mortar whereas M-V-14.6C showed some minor damage at the corners (Figure 10-d). The damaging phases in magnesium sulfate also were correlated with the expansion results.

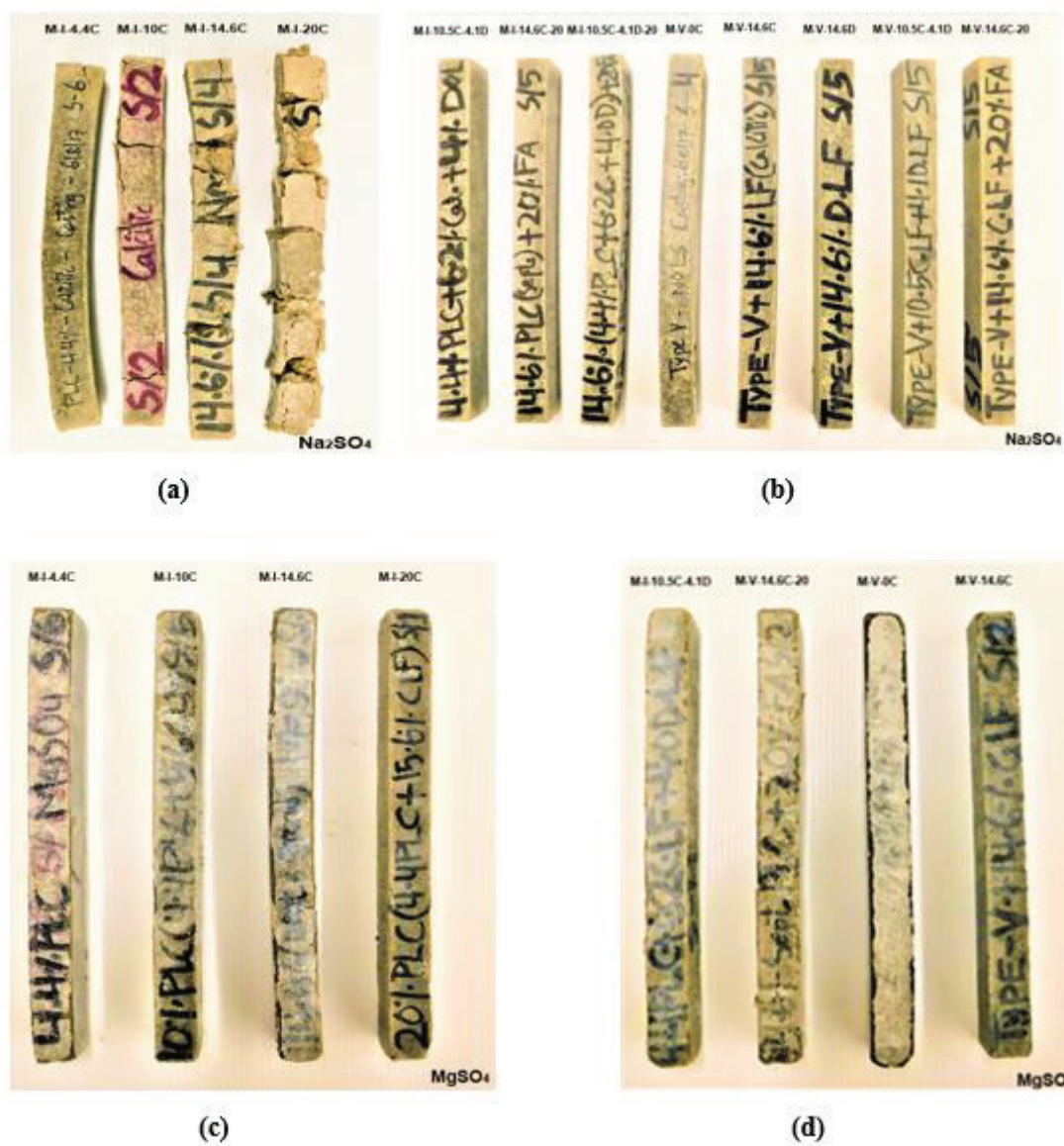


Figure 10: Images of mortar samples exposed to Na_2SO_4 (a and b) and MgSO_4 (c and d) for 7 months

4.4 Change in compressive strength of paste specimens

4.4.1 Influence of limestone percentage

The results of the compressive strength testing of paste specimens incorporating different percentages of calcitic limestone powder exposed to sodium and magnesium sulfate solutions at 23°C and 5°C are presented in Figure 11 (a-d). Additionally, the percent reduction at each exposure age in compressive strength of these paste specimens compared to 7-day strength is shown in Figure 12. It should be noted that the compressive strength values at 7 days (before submersion in the sulfate solutions) were slightly higher in general for mixtures placed in sodium sulfate compared to those placed in magnesium sulfate. This can be attributed to the variability of casting conditions, as cubes for sodium and magnesium sulfate were prepared at different times. In this study, trends are analyzed instead of absolute strength values to account for this variability.

Over the 120 day exposure period the samples undergo one of three primary strength change trends: (1) decrease, increase, decrease, (2) increase, decrease, or (3) increase, decrease, increase (less common). These strength increases can be potentially explained by two phenomenon: (1) the continued hydration of unhydrated cement particles (mostly C_3S and C_2S) which produced more hydration products, primarily C-S-H, leading to higher compressive strength and (2) gypsum and ettringite formation due to the reaction between sulfate ions and hydrated cement components [112]. These phenomena may have improved sulfate resistance of these mixtures by making a denser microstructure through filling the void spaces with the hydration products prior to any subsequent damage.

The reduction of strength is caused by continued sulfate attack, which increases cracking, opening up the microstructure and allowing more sulfate ingress, eventually resulting in greater strength loss at later ages. These subsequent reactions between sulfate ions and calcium hydroxide lead to the higher amounts of ettringite formation, which exert pressure in capillary pores resulting in significant surface deterioration and strength loss [113].

It appears that the limestone addition to the cement did not affect strength loss in the same manner it affected expansion for sodium sulfate exposure. That is, higher limestone percentages did not significantly increase strength loss as would have been predicted by their much higher expansion. In 5°C at 120 days, the P-I-10C, P-I-14.6C, and P-I-20 mixtures exhibited a slightly higher strength loss compared to the 4.4% limestone filler cement; however, the strength loss difference was relatively small³. This is in accordance with other studies that have shown higher compressive strength reduction with increased limestone replacement in cold sulfate solutions [78, 114]. This effect is less pronounced in the magnesium solution, where the 20% limestone actually shows less expansion at 120-day exposure time compared to the lower limestone cement.

At 23°C, the higher limestone cements (14.6% and 20% in sodium and 20% in magnesium) actually had lower strength loss by 120 days compared to the lower limestone cements. This is an opposite trend to that observed in expansion data in sodium sulfate solution. All PLC mixtures produced from Type I/II cement showed higher loss of strength at later ages

³ It should be noted that the strength values of these samples (and others analyzed in this study) are within one standard deviation of each other at certain ages. This is in part due to the high variability of the compressive strength results observed with the testing of these small samples. Therefore, small differences in strength loss may not be statistically significant with some of these samples.

at 5°C and 23°C compared to the P-V-0C and P-V-14.6C mixtures, which showed a significant strength increase at 120 days in both sulfate solutions at 23°C (11-a, 11-c). This can be attributed to the lower C₃S and C₃A contents in the control Type V cement which can improve the sulfate resistance compared to the Type I/II blended PLCs [79, 115-117]. Although it should be noted that C₃A does not participate in the gypsum formation reaction. This improvement in strength can also be explained as a combined result of better particle packing [118], higher cement hydration rate [116] and production of calcium carboaluminate [119]. Type V mixes performed worse at 5°C compared to 23°C in both sulfate solutions throughout the exposure period yet still better than Type I/II mixes.

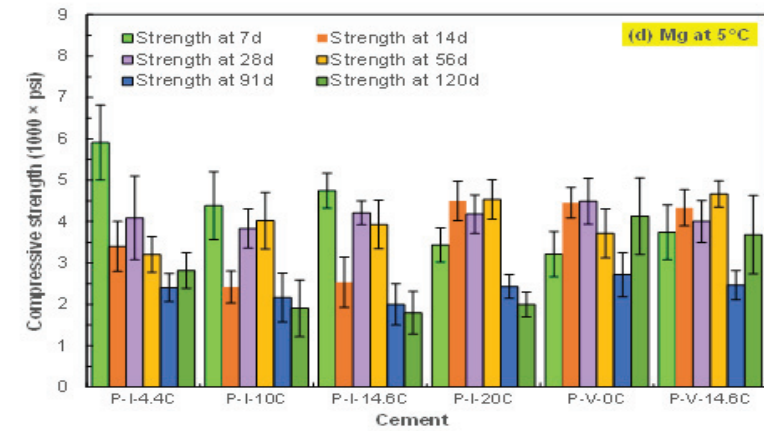
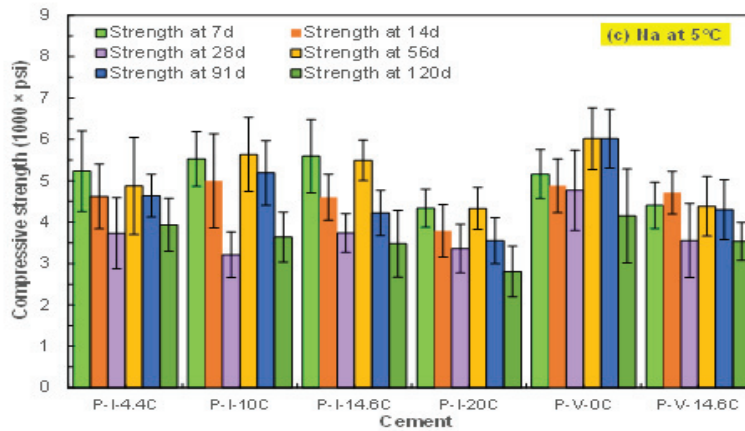
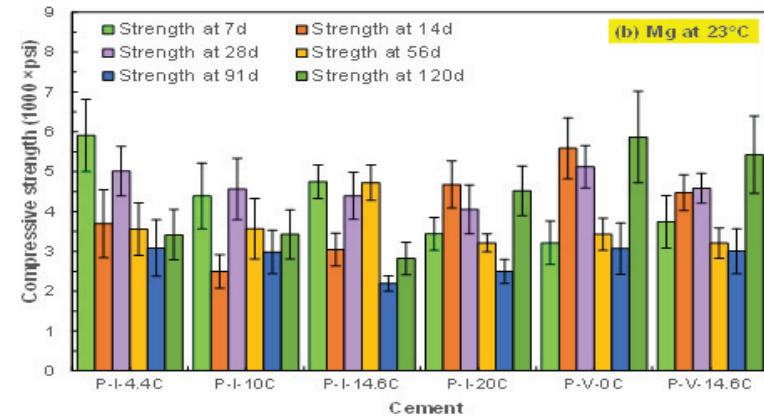
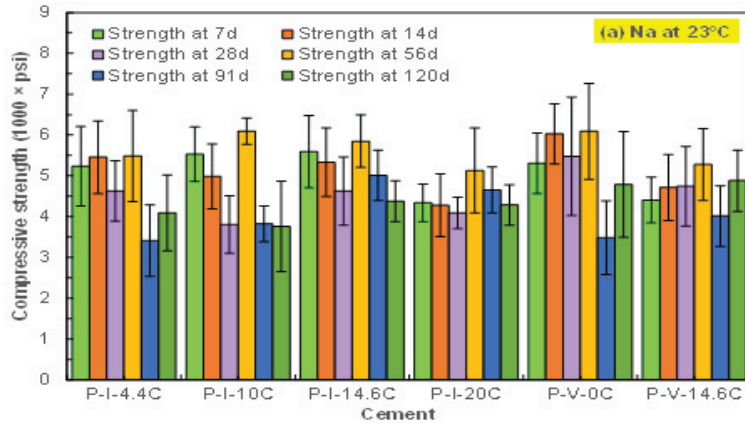


Figure 11: Compressive strength of paste cubes (calcitic limestone only) placed in sulfate solutions, 11(a) Na at 23°C, 11(b) Mg at 23°C, 11(c) Na at 5°C, and 11(d) Mg (bars show 1 standard deviation) at 5°C

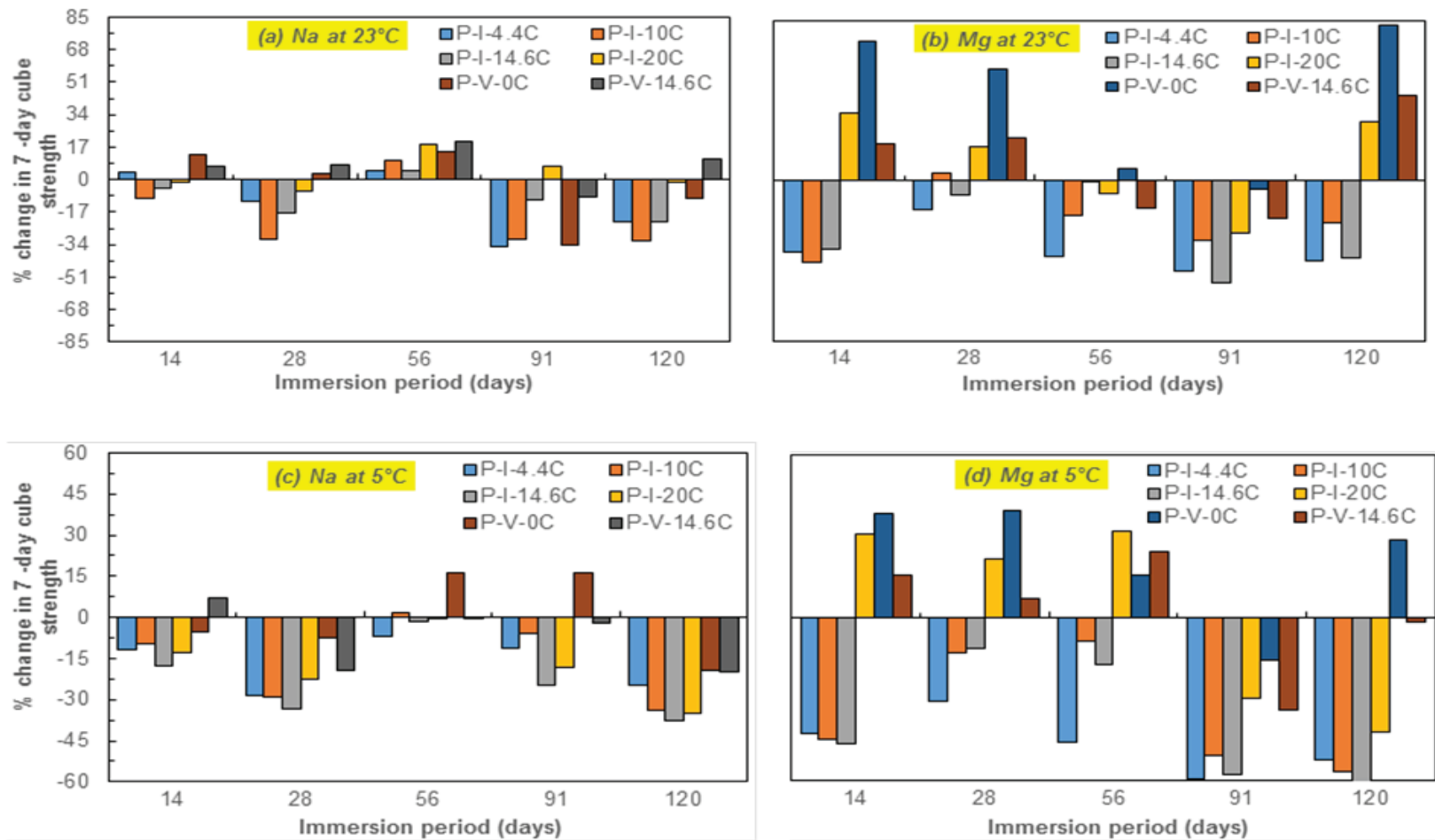


Figure 12: Percent reduction of compressive strength of paste (calcitic limestone only) cubes placed in sulfate solutions Na at 23°C, 12(b) Mg at 23°C, 12(c) Na at 5°C, and 12(d) Mg at 5°C

Figure 11 and 12 clearly reveal that the compressive strength reduction was higher at 5°C than 23°C at later ages in both solutions, but especially in magnesium sulfate. At 5°C, the maximum strength loss in all Type I/II replaced PLCs was recorded at 120 days of magnesium sulfate exposure (12-d). Generally, the kinetics and solubilities of expansive products formed during sulfate attack depend on temperature. At higher temperatures, the solubility of gypsum [120] and ettringite [121] increase as elevated temperatures make the pore solution supersaturated, which results in more precipitation of these expansive products. However, this study showed opposite results in terms of higher strength reduction at low temperatures. The principal cause of the higher strength reduction at low temperatures is due to the dissolved calcium and carbonate ions [86, 122]. The additional dissolved calcium in the pore solution results in more ettringite and gypsum formation, and the dissolved carbonates are a source for more thaumasite formation [122].

The cation type of sulfate solution affects the compressive strength and expansion results in a different manner. While the increase in the expansion was higher for specimens exposed to sodium sulfate solution, compressive strength decreased more in magnesium sulfate solution exposure. This was supported by another study [123]. Furthermore, the compressive strength results in this study showed a clear dependency on the solution cation type, temperature, and cement properties.

4.4.2 Influence of limestone type and composition

The compressive strength results of different 14.6% PLCs placed in sulfate environments with and without fly ash are shown in Figure 13 – 16. Similar strength patterns were observed for P-I-14.6C and P-I-10.5C-4.1D mixtures at both temperatures when paste samples were immersed in sodium sulfate solution (13-a, 13-c). However, the strength changing pattern was different for these mixtures in magnesium sulfate. The addition of dolomitic limestone led to less strength reduction (and strength increases in some cases) of the P-I-10.5C-4.1D mixture compared to the calcitic-only mixture at both temperatures when placed in magnesium sulfate solution (14-b, 14-d).

For the magnesium sulfate mixes, the addition of dolomite could have increased the compressive strength through ettringite stabilization [88, 89]. Further, the improved performance of the P-I-10.5C-4.1D mixture at 120 days in magnesium sulfate could be attributed to the formation of hydrotalcite ($Mg_6Al_2(OH)_{18} \cdot 3(H_2O)$) [95]. Hydrotalcite is a magnesium-containing hydrate which forms upon the dissolution of dolomite due to an increased curing temperature (25°C to 60°C) [100-102]. In this study, the elevated curing of paste specimens (50°C) could have increased the compressive strength. Research has shown that hydrotalcite is associated with portlandite consumption, which could have improved its sulfate resistance [124].

In sodium sulfate, the addition of dolomite resulted in greater strength reduction over time (14-a, 14-c). The samples placed in sodium sulfate the addition of dolomite resulted in a higher reduction in expansion compared to those placed in magnesium sulfate. There

appears to be a negative interaction with regard to strength not observed in magnesium. More research is needed to fully understand this behavior.

The compressive strength results of different 14.6% PLCs (calcitic and dolomitic) replaced by Type V cement placed in sodium sulfate solution with and without fly ash are shown in Figure 15-16. The compressive strength of P-V-14.6D and P-V-10.5C-4.1D mixtures followed a similar pattern at 23°C over the entire exposure period (15-a). The effect of the dolomitic limestone addition on strength is less pronounced for Type V cement compared to Type I/II. At 23°C, the addition of dolomite results in less strength loss at later ages echoing the results from mortar bar expansion which were lower for dolomitic mixes. The reason behind this strength improvement is likely the same for those discussed for the observed expansion reduction [87, 95, 125]. For 5°C, differences in trends between strength loss and dolomitic addition are more difficult to identify.

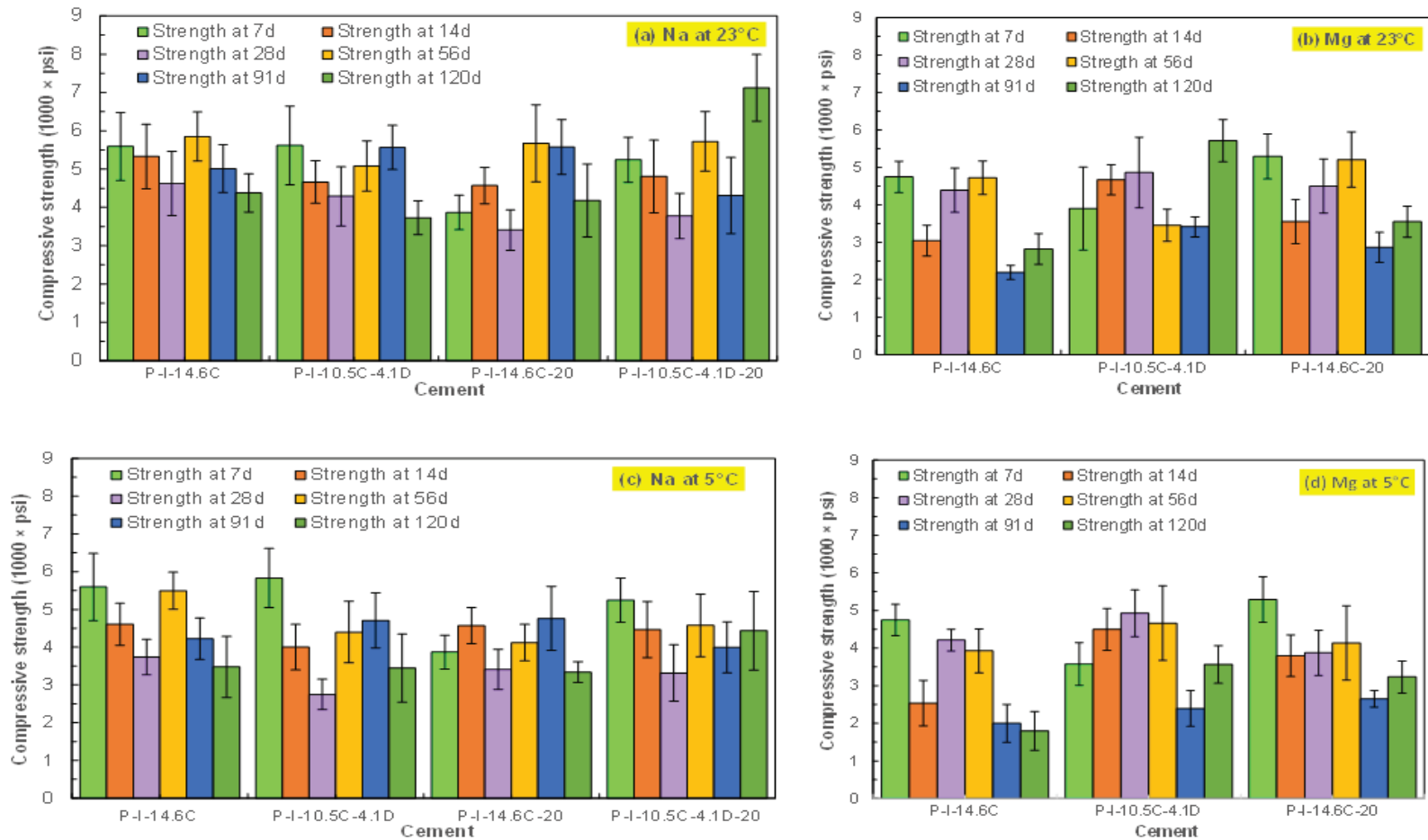


Figure 13: Compressive strength of paste (calcitic and dolomitic limestone) cubes placed in sulfate solutions, 13(a) Na 23°C, 13(b) Mg at 23°C, 13(c) Na at 5°C, and 13(d) Mg (bars show 1 standard deviation) at 5°C

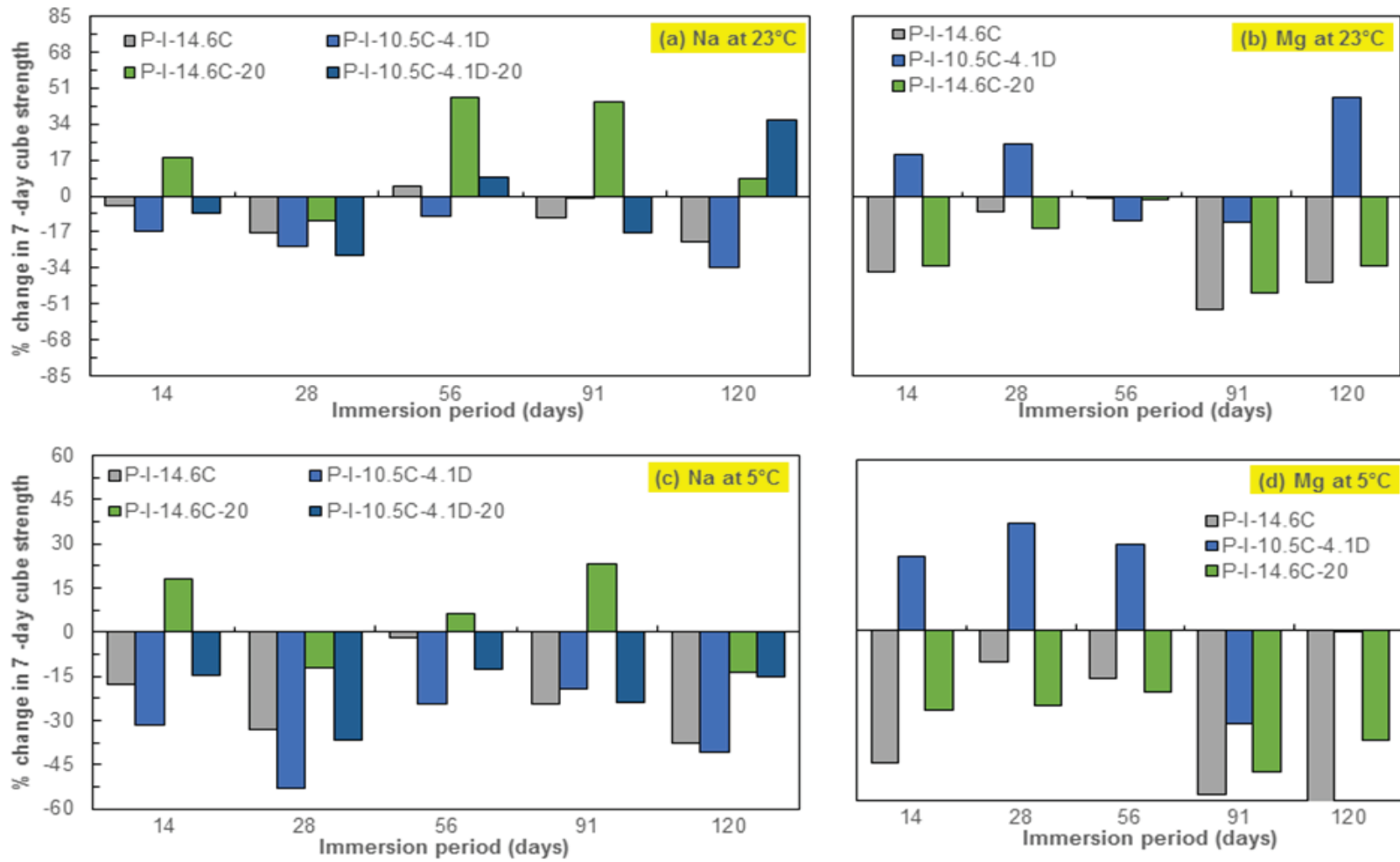


Figure 14: Percent reduction of compressive strength of paste (calcitic limestone only) cubes placed in sulfate solutions, 14(a) Na at 23°C, 14(b) Mg at 23°C, 14(c) Na at 5°C, and 14(d) Mg at 5°C

4.4.3 Influence of fly ash

The effect of fly ash addition on the compressive strength of different 14.6% PLCs (calcitic and dolomitic) in both sulfate solutions are presented in Figure 13-16. For the Type I/II cement, the addition of the fly ash resulted in decreased strength loss over time at both temperatures and in both solutions. This was true when added to calcitic-only and blended calcitic/dolomitic PLCs. Strength loss for the fly ash mixes was greater in Mg and at 5°C, similar to the mixes without fly ash.

Fly ash is known to have a considerable impact on compressive strength in normal mixtures not undergoing sulfate attack (i.e., reducing it at early ages and increasing it at later ages). Typically, Class F fly ash does not undergo pozzolanic reaction until after 3 months [126]. In this experiment, the elevated curing temperature may have initiated this reaction much earlier, resulting in the enhanced performance of the fly ash mixes seen here. Fly ash and limestone also can have a synergistic effect that results in the formation of calcium carboaluminate hydrate. The lower reactivity of the fly ash mixes in 5°C could be a result of reduced continued hydration of the fly ash often seen at lower temperatures [127, 128].

When comparing these results to the expansion data, fly ash decreased the expansion of the calcitic Type I/II-replaced PLCs, but increased expansion for dolomitic PLCs in sodium sulfate. In magnesium sulfate, expansion was also increased for calcitic PLCs. Perhaps the lower temperature curing of these mortars resulted in less pozzolanic reactivity of the fly ash prior to sulfate attack damage initiation, which could account for the differences between the strength and expansion results.

For the Type V cement, the addition of fly ash resulted in increased strength loss over time at both temperatures in sodium sulfate. Interestingly, the Type V-replaced PLCs with fly ash had lower expansion (an opposite trend). It's unclear from this data why this phenomenon occurred, but may be related to the differences in maturity between the samples due to the differing curing regimes as well as the impact of the fly ash on sulfate attack with Type V regarding ettringite formation (expansion) vs. gypsum formation (strength loss).

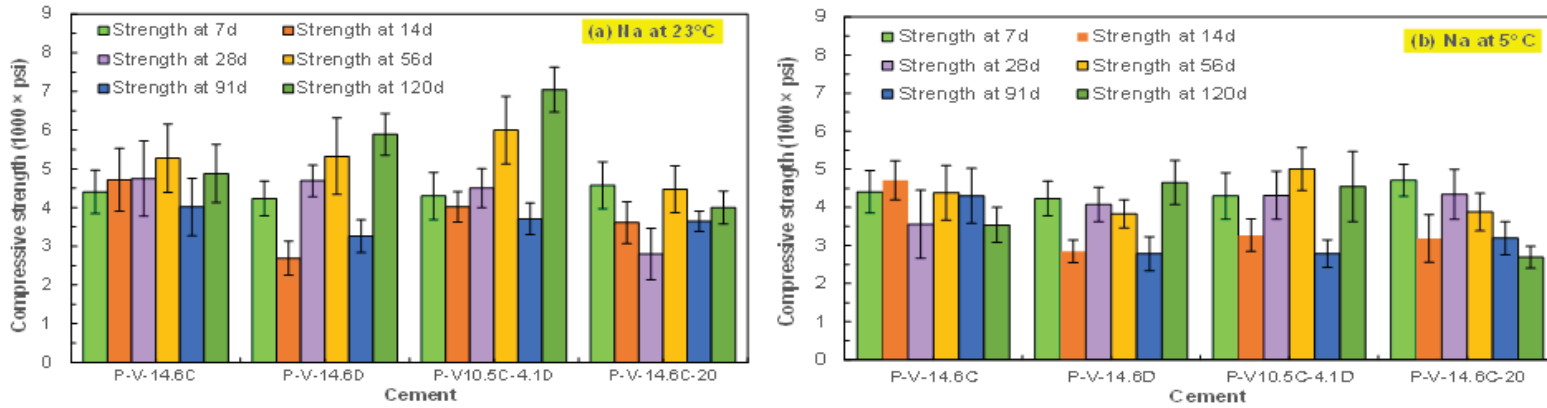


Figure 15: Compressive strength of Type V cement replaced PLC paste cubes placed in sodium sulfate solutions, 15(a) Na at 23°C and 15(b) Na at 5°C

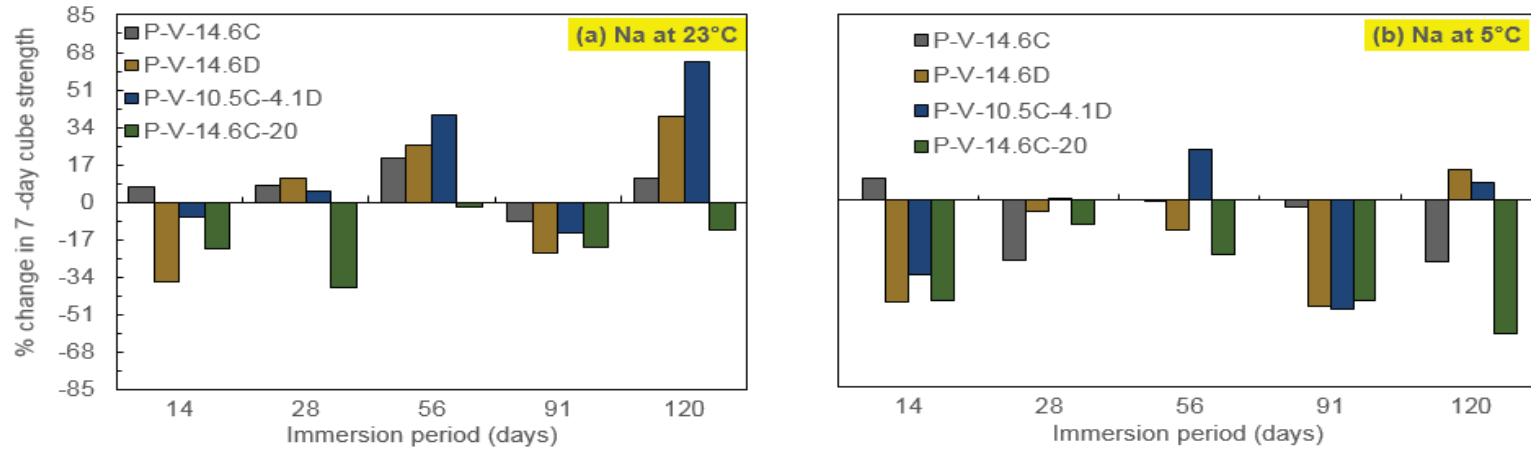


Figure 16: Percent reduction of compressive strength of Type V cement replaced PLC paste cubes placed in sodium sulfate solutions, 16(a) Na at 23°C and 16(b) Na at 5°C

4.4.4 Influence of pH

The compressive strength of different PLCs placed in sodium sulfate exposure at 5°C in a controlled pH of 7.2 is presented in Figure 17. The results from this test revealed that most of the mixtures showed higher strength loss in the controlled pH environment compared to the non-controlled pH sodium sulfate exposure especially at later ages except for the P-I-4.4C, P-V-0C, and P-V-14.6C-20 mixtures (Figure 11-17). The maximum (79%) and minimum (8%) strength reduction were observed in P-V-14.6C and P-V-0C mixtures, respectively, in pH-controlled sodium sulfate exposure (Figure 17). This indicates that the addition of limestone in Type V cement accelerates the strength reduction under acidic (pH=7.2) sodium sulfate exposure, which was not observed in the alkaline solution.

There was not any significant change in strength for P-I-4.4C and P-V-0C mixtures in both sulfate environments. However, the solution pH considerably reduced the strength of the P-I-14.6C, P-I-14.6C-20, P-I-10.5C-4.1D, and P-I-10.5C-4.1D-20 mixtures compared to the normal pH condition at 120 days of sodium sulfate exposure. The addition of dolomitic limestone did not show any significant improvement in strength here as it did with the expansion results. Fly ash addition improved Type V PLC strength, but not Type I/II PLC strength at later ages—an opposite trend to the non-pH controlled data. The pH of the concrete and the environment has a significant impact in the aggressiveness of the sulfate attack [7]. Conventional sulfate attack (ettringite and gypsum formation) is more aggressive at a lower pH because it can decalcify the concrete and the C-S-H. However, the lower pH has not been shown to promote thaumasite formation [62].

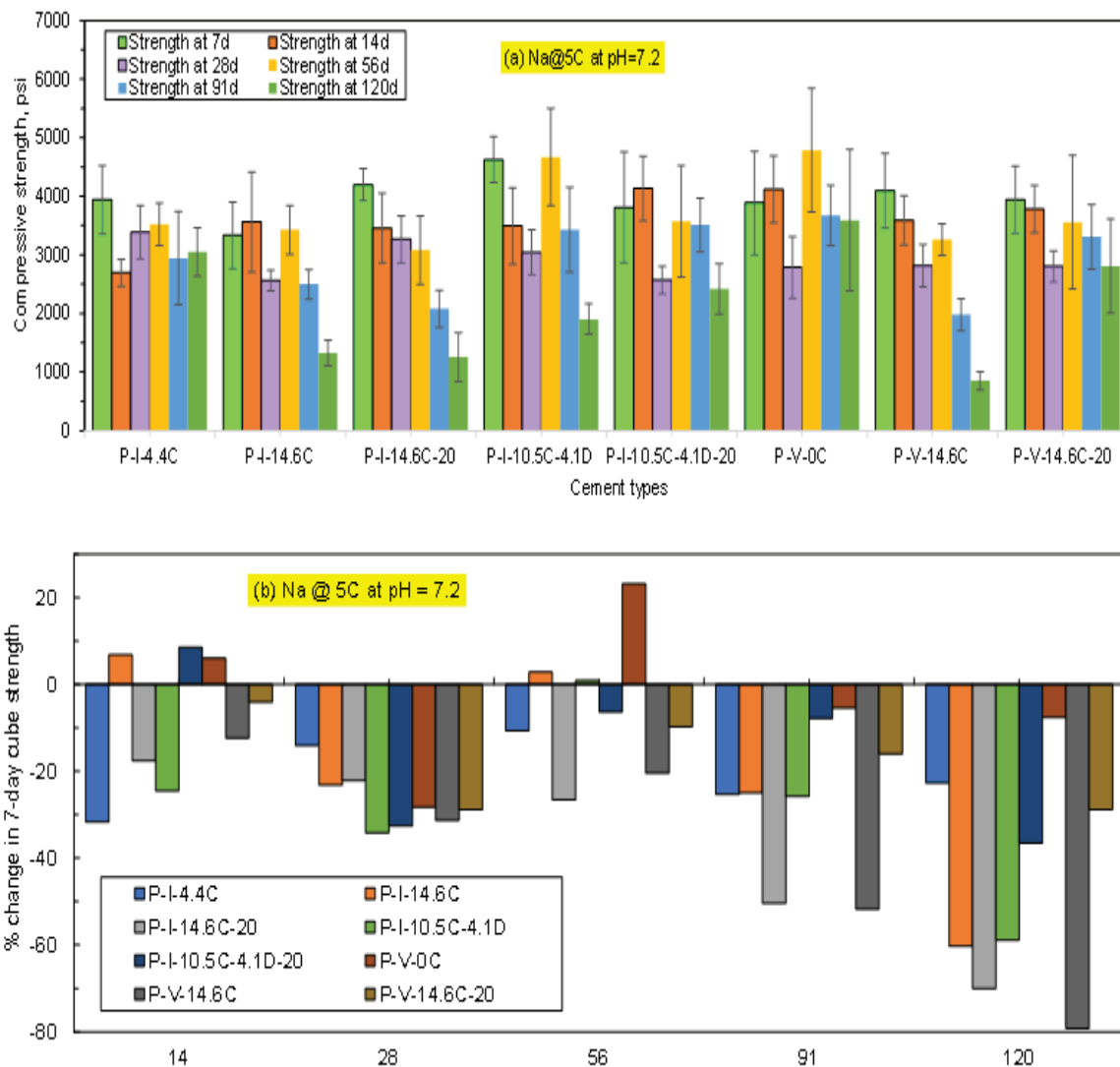


Figure 17: Compressive strength (a) and percent reduction of strength (b) of different PLCs placed in sodium sulfate solution at 5°C at pH= 7.2

4.5 Visual inspection of paste specimens

Visual inspection of the paste specimens was performed to identify the visible signs of surface damage including cracking, spalling, and softening at 120 days due to sulfate exposure. Photos of specimens immersed in sodium and magnesium sulfate solutions at both temperatures are presented in Figure 18. Between the start of testing until 56 days,

some minor corner cracks were observed in all mixtures especially for those placed at 23°C in both sulfate solutions. Generally, the first sign of attack started with the deterioration of corners followed by extensive cracking along the edges and, finally, spalling and disintegration on the specimen surfaces regardless of sulfate solution types. The visual rating system used to classify surface deterioration in this study is shown in Table 8. This visual rating system is widely used to represent the surface deterioration due to sulfate attack. The observations based on this visual rating are presented in Table 9.

Table 8: Visual rating used to classify surface damage

Rating	Description
0	No visible deterioration
1	Deterioration at corners
2	Deterioration at corners and some cracking along the edges
3	Severe cracking along the edges
4	Cracking and expansion
5	Bulge of surfaces
6	Extensive cracking and expansion
7	Extensive spalling
8	Complete disintegration



(a) Na @ 23°C

(c) Mg @ 23°C



(b) Na @ 5°C

(d) Mg @ 5°C

Figure 18: Visual appearance of paste specimens after 120 days of sodium and magnesium sulfate exposure at 23°C and 5°C

Table 9: Visual inspection of paste specimens placed in sulfate solutions at 120 days

Specimens designation	at 120 days			
	Na ₂ SO ₄ exposure		MgSO ₄ exposure	
	23°C	5°C	23°C	5°C
P-I-4.4C	1	5, 6	2	5,6
P-I-10C	2	5,6	1	6
P-I-14.6C	2	7	1	6,7
P-I-20C	3	7	1	4
P-I-10.5C-4.1D	3	5, 6	1	2
P-I-14.6C-20	2	4,5	1	3
P-I-10.5C-4.1D-20	1	4	N/A	N/A
P-V-0C	2	2	1	1
P-V-14.6C	2	2	2	4
P-V-14.6D	2	2	N/A	N/A
P-V-10.5C-4.1D	1	4	N/A	N/A
P-V-10.5C-20	2	3	N/A	N/A

Overall, the paste samples with a higher percentage of calcitic limestone powder showed more damage in both solutions, especially at 5°C (Figure 18-b, 18-d). At 5°C, the paste samples from the P-I-14.6C mixture showed extensive cracking and surface spalling. Additionally, a clear bulging on the surfaces was observed at 120 days of exposure. In contrast, the P-V-0C and P-V-14.6C mixtures showed less surface damage at both temperatures in both solutions which was also observed in expansion results. At 23°C, none of the paste samples showed significant damage in either solution (ranged from 0 - 3) (Figure 18-a, 18-c). The addition of fly ash with different PLC mixtures considerably

reduced the surface damage at both temperatures in both sulfate solutions. This indicates the surface damage accelerates with higher limestone content and at low temperature.

4.6 Mass loss of paste specimens

The mass of each of the mixture did not change significantly especially for the paste samples placed at 23°C in both solutions. The decrease in mass at this temperature lies between 0.20 – 1.1% in both solutions. However, a considerable mass decrease was observed when samples are stored at 5°C. Overall, the decrease in mass was more significant for the mixtures immersed in magnesium sulfate solution. The percent change in mass (mass loss) for some calcitic limestone replaced PLCs placed in both solutions at 5°C is shown in Figure 19-20. The calcitic limestone replaced PLCs showed a noticeable mass loss compared to all other mixtures. The rate of mass decrease was similar for all samples shown in Na. However, in Mg some of the samples didn't lose mass at later ages. The increase in mass at 120 days was higher for all mixtures placed in magnesium sulfate than in sodium sulfate. In general, the mass change is higher for higher limestone contents in both solutions. Adding limestone to Type V cement has a similar effect to mass loss as it did for Type I/II.

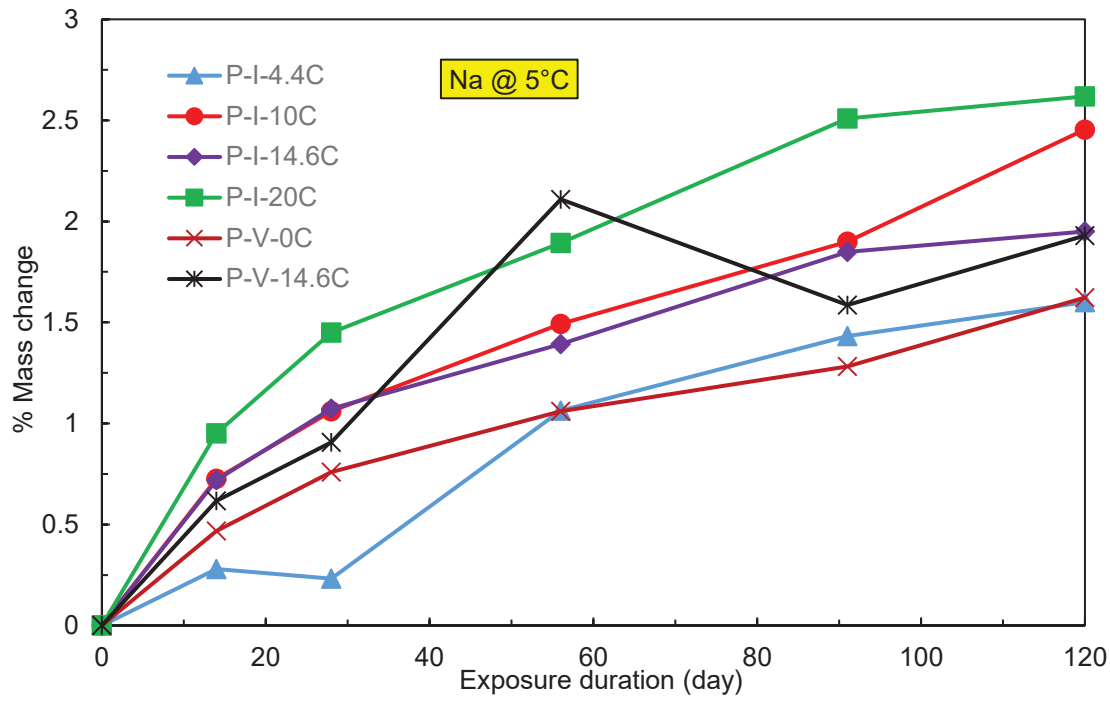


Figure 19: Mass loss of paste specimens placed in sodium sulfate solution at 5°C

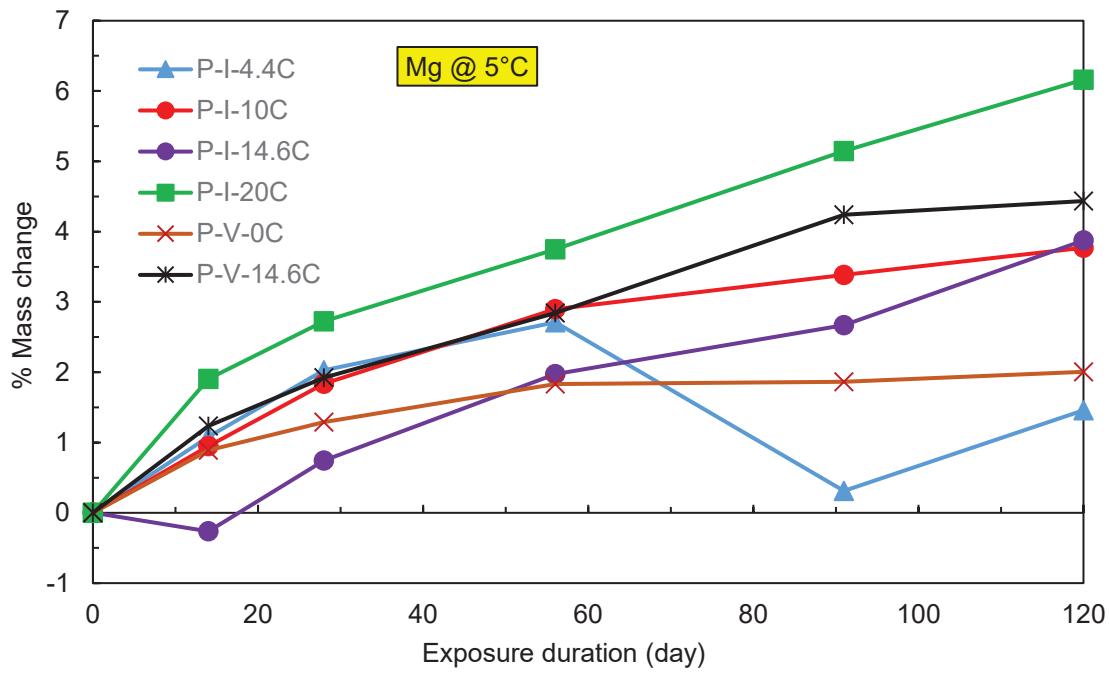


Figure 20: Mass loss of paste specimens placed in magnesium sulfate solution at 5°C

Some paste specimens showed a mass gain over the exposure duration. The mass increase can be attributed to the swelling due to the gypsum or ettringite formation in the damaged paste specimens [129]. Moreover, it could even be due to the filling of pores by expansion reaction products which made the paste denser and thereby increase the weight [130] or the water absorption during the hydration of cement [131]. Therefore, the changes in mass to predict the sulfate resistance of paste specimens is not as accurate as other methods shown in this study.

4.7 Mineralogical changes measured by X-ray diffraction

4.7.1 X-ray diffraction results in Na₂SO₄ solution

The results of the XRD analysis on paste specimens exposed to sodium sulfate solution at 28 days and 120 days at 5°C are presented in Figure 21-24. The XRD traces show that the main products associated with sulfate attack are gypsum, ettringite, and thaumasite. Other mineral components detected include calcite, calcium silicate, and portlandite (a hydration product). The peak intensities of gypsum and portlandite observed in all mixtures at both testing ages did not show any correlation to the percentage of limestone used to replace the control cements. The main sulfate reaction products found in calcitic limestone replaced PLCs were ettringite and thaumasite at 28 days (Figure 21) and 120 days (Figure 22) of sodium sulfate exposure. There was also some gypsum available at both testing ages.

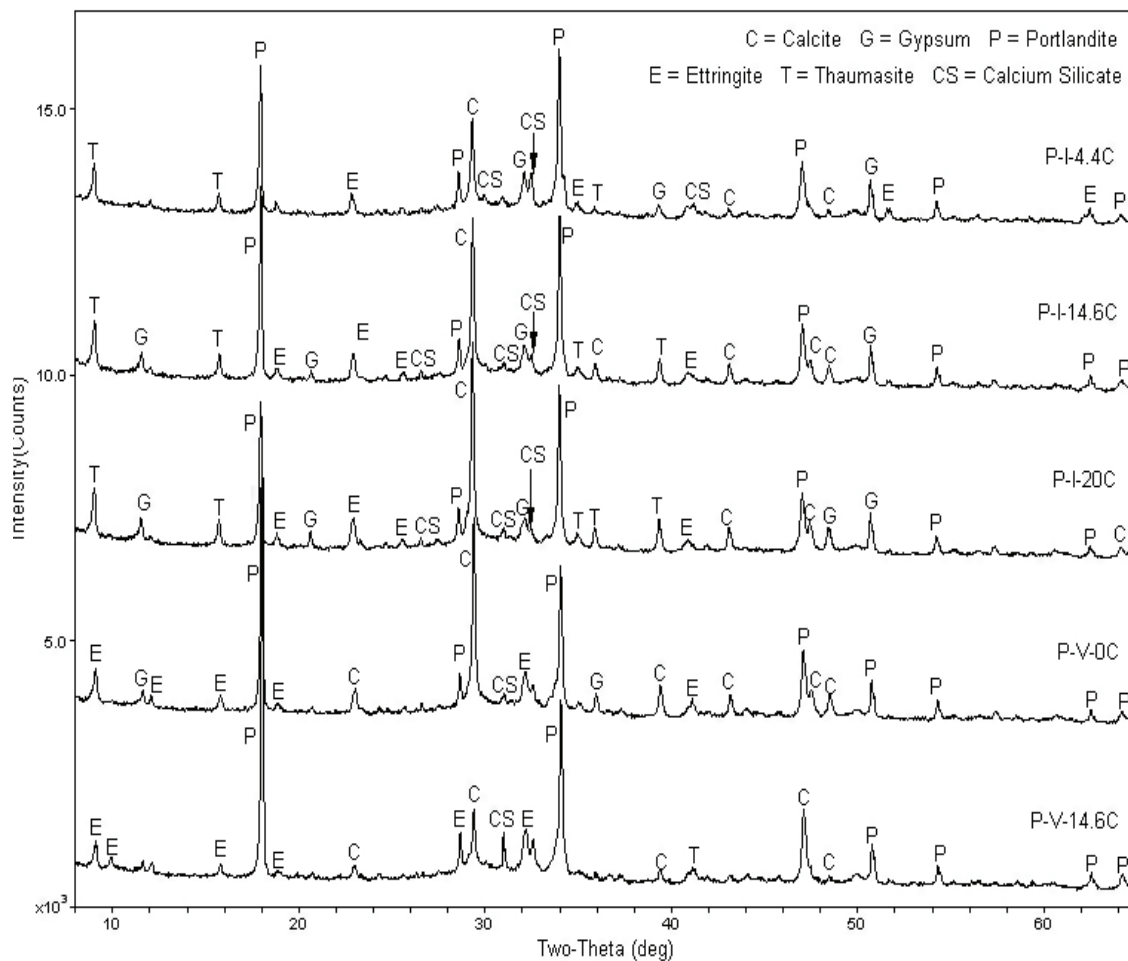


Figure 21: XRD patterns of paste samples exposed to sodium sulfate solution at 5°C for 28 days

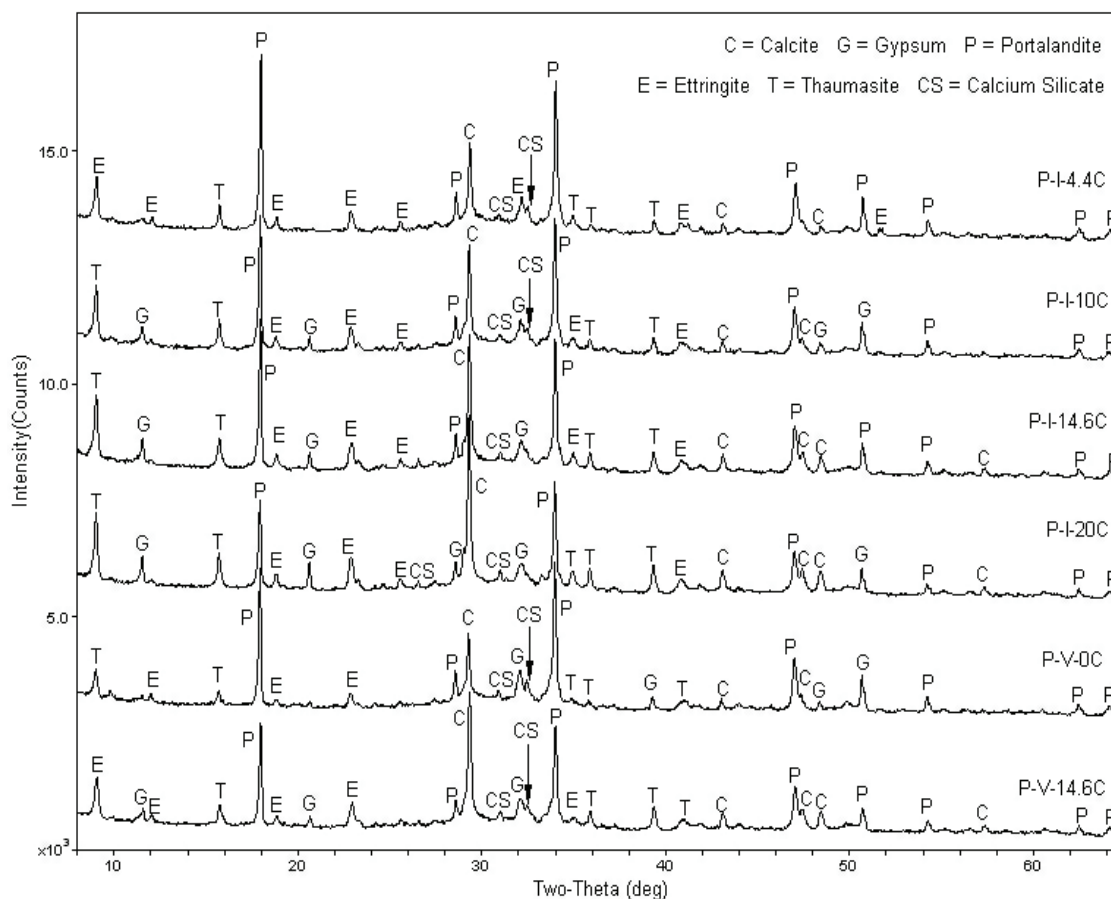


Figure 22: XRD patterns of paste samples exposed to sodium sulfate solution at 5°C for 120 days

At 28 days, thaumasite was observed in all mixtures except P-V-0C. The intensity of ettringite and thaumasite in all mixtures was higher at 120 days compared to 28 days in addition to more peaks associated with these reaction products (Figure 22). As expected, relatively strong calcite peaks were identified in P-I-4.4C, P-I-10.5C, P-I-14.6C, and P-I-20C paste specimens due to the replacement of the control Type I/II cement by calcitic limestone powder. The increase in calcite peaks with increased limestone (calcitic) content at 28 days and 120 days sodium sulfate exposure was observed at $2\theta = 29.4^\circ$ as shown in Figure 21 and Figure 22, respectively.

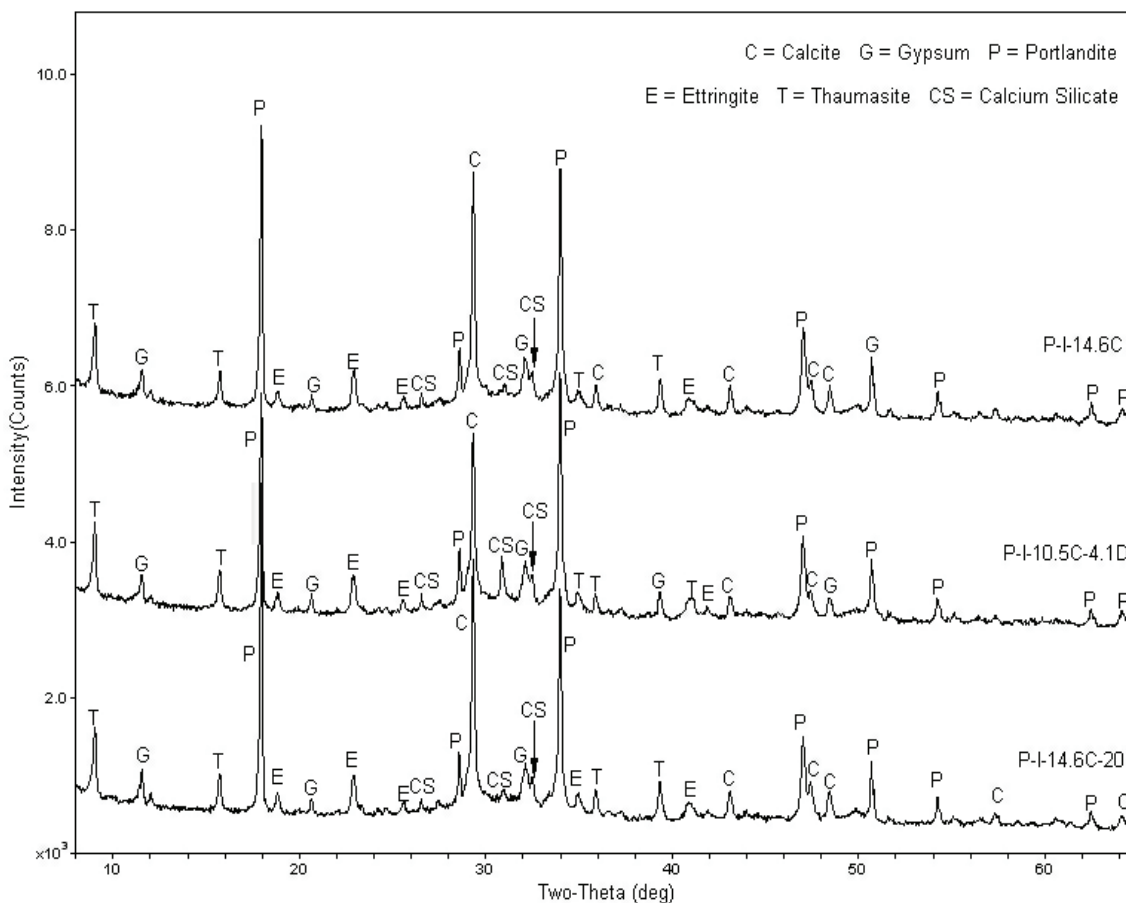


Figure 23: XRD patterns of paste samples exposed to sodium sulfate solution at 5°C for 28 days

At 28 days, P-V-14.6C showed smaller calcite peaks than P-V-0C (Figure 21). The P-V-0C mixture does not contain any added limestone and the presence of calcite could potentially come from the atmospheric CO₂ during sample preparation.

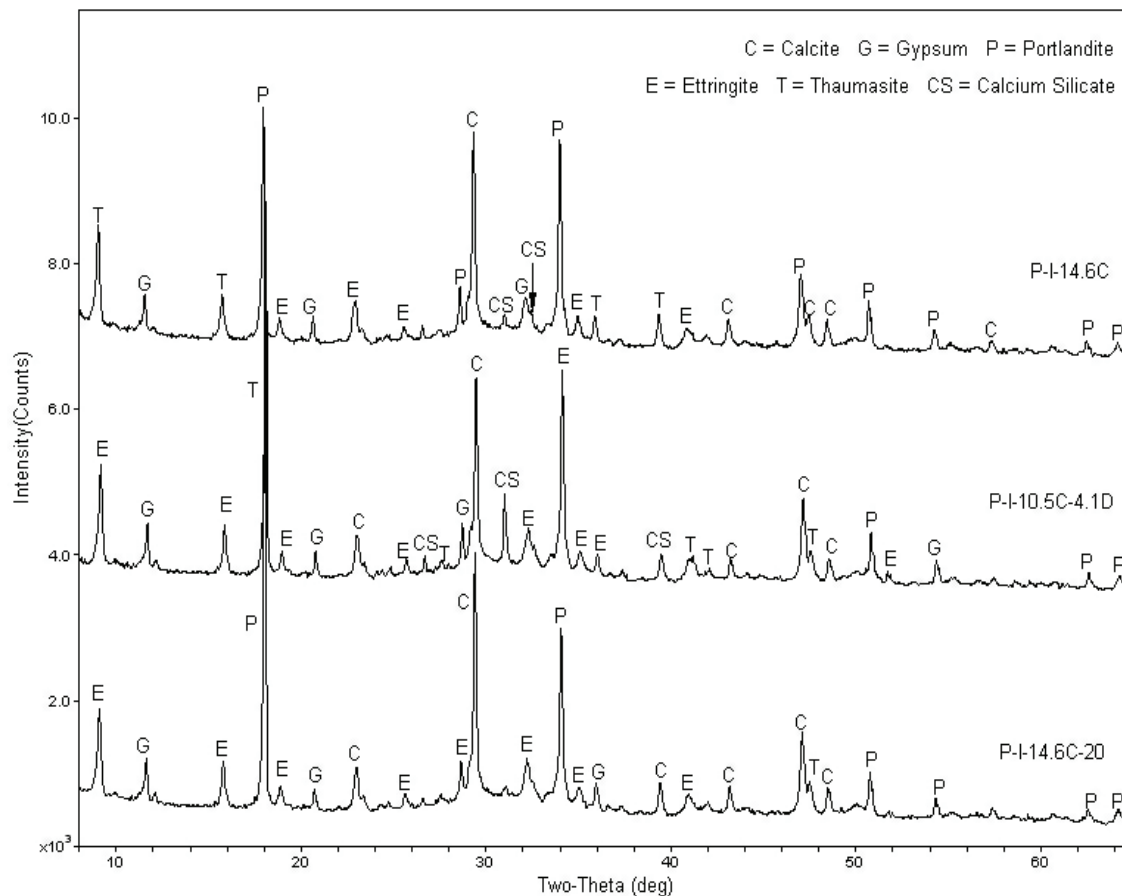


Figure 24: XRD patterns of paste samples exposed to sodium sulfate solution at 5°C for 120 days

The conversion of ettringite to thaumasite was detected at $2\theta = 9.1^\circ$, $2\theta = 15.8^\circ$, and $2\theta = 41.1^\circ$ in P-V-0C sample between 28-120 days (Figure 22). For P-V-14.6C at 120 days, the conversion of other minerals to thaumasite was not observed, but more thaumasite was formed and a reduction in calcite and portlandite peaks was observed compared to 28-day data. To note, there was not any noticeable difference in mortar bar expansion (up to 180 days) and cubes strength (up to 120 days) between P-V-0C and P-V-14.6C mixtures as discussed earlier.

The XRD patterns of P-I-14.6C, P-I-10.5C-4.1D, and P-I-14.C-20 mixtures exposed to sodium sulfate are shown in Figure 23-24. There are anomalies between the ettringite and thaumasite products at 28 days and 120 days in P-I-10.5C-4.1D. Specifically, some ettringite was observed at 28 days that converted into thaumasite at 120 days. Literature has revealed that due to structural similarities between ettringite and thaumasite it can be difficult to distinguish between these minerals or it can even be due to the ettringite stabilization [132].

Interestingly, at 120 days, the P-I-10.5C-4.1D mixture showed the highest peak for thaumasite and ettringite at $2\theta = 19.1^\circ$ and $2\theta = 34.2$, respectively, which was converted from portlandite found at 28 days (Figure 23-24). Although the P-I-10.5C-4.1D mixture showed higher expansion reduction than P-I-14.6C, more strength loss was observed due to the thaumasite formation at later ages.

The P-I-14.6C-20 mixture showed stronger calcite and portlandite peaks at 120 days than P-I-14.6C (Figure 24). At 28 days, the P-I-14.6C-20 mixture showed a combination of thaumasite and ettringite and many of these thaumasite peaks appeared as ettringite at 120 days. There were not any considerable changes in peak intensities at later ages for this mixture. In general, the compressive strength reduction due to sulfate attack is greatest for thaumasite formation. The P-I-14.6C-20 mixture showed less strength reduction than P-I-14.6C at 120 days. The higher strength reduction of P-I-14.6C mixture can be attributed to the progressed thaumasite and ettringite phases at a later age (compared to 28 days) and relatively higher peak intensities at 120 days (Figure 24).

Generally, higher amounts of limestone (a carbonate source) in PLCs and low temperature, which increases the solubility of CO_2 in water, increase the likelihood of thaumasite formation. In this study, the XRD showed that ettringite and thaumasite are responsible for the deterioration of PLC paste specimens at 5°C . Based on the thaumasite formation hypothesis, thaumasite can be formed due to the topochemical conversion of ettringite in the presence of sufficient silicate and carbonate sources [133, 134]. The effect of solution pH is very important. In Na_2SO_4 exposure, another sulfate reaction product, NaOH , is formed which increases the pH (because of higher solubility) of the solution. In our study, the pH of sodium sulfate solution was in the range of 12.2-13.5 over the entire testing period, which may have stabilized the ettringite phases. Thus the conversion of ettringite to thaumasite did not take place. However, it is evident that the sodium sulfate attack is attributed to ettringite and thaumasite formation more so than due to gypsum formation.

4.7.2 X-ray diffraction results in MgSO_4 solution

The results of XRD analysis of paste specimens exposed to magnesium sulfate solutions at 5°C are presented in Figure 25–28. The same minerals were observed here as with sodium sulfate in addition to brucite. The dominating sulfate reaction products found in calcitic limestone replaced PLCs were gypsum, ettringite, and thaumasite at 28 days while gypsum and thaumasite were most prevalent at 120 days of magnesium sulfate exposure (Figure 25-28).

Figure 25 shows weak peaks of gypsum and strong peaks of portlandite for all calcitic limestone replaced PLCs. At 120 days, the gypsum peaks became much stronger and portlandite peaks became weaker (Figure 26) due to the sulfate attack.

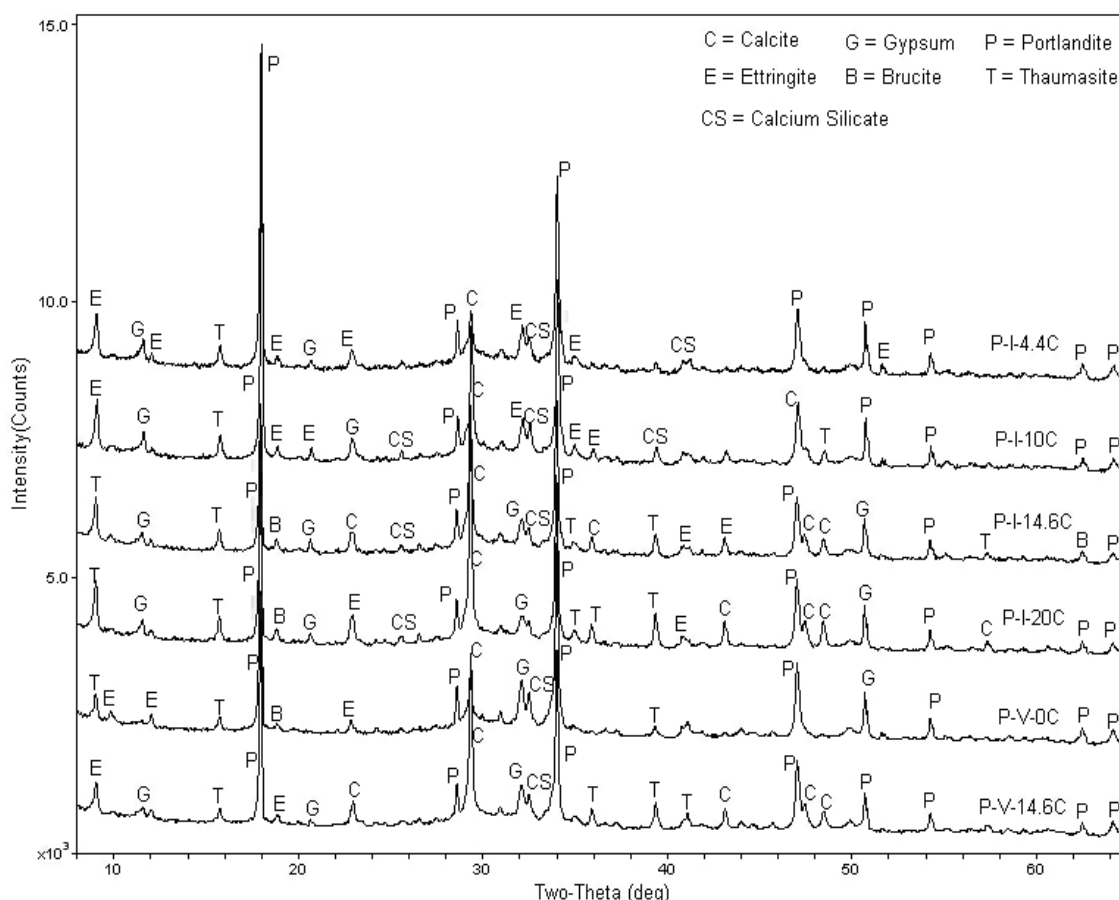


Figure 25: XRD patterns of paste samples exposed to magnesium sulfate solution at 5°C for 28 days

For example, at $2\theta = 11.6^\circ$ and 20.7° at 28 days, there was no considerable change in gypsum peaks with increased limestone content in all mixtures, whereas significantly higher gypsum peaks were identified at this 2θ position at 120 days of magnesium sulfate exposure for cements with higher limestone contents (Figure 25-28). Interestingly, at 120

days, a strong gypsum peak was found at $2\theta = 29.1^\circ$ between portlandite ($2\theta = 28.7^\circ$) and calcite ($2\theta = 29.4^\circ$) peaks for P-I-10C, P-I-14.6C, P-I-20C, and P-V-14.6C paste mixtures (Figure 26). Similarly, some new gypsum peaks are also observed between $2\theta = 30^\circ$ to 36° at 120 days of sulfate immersion (Figure 26).

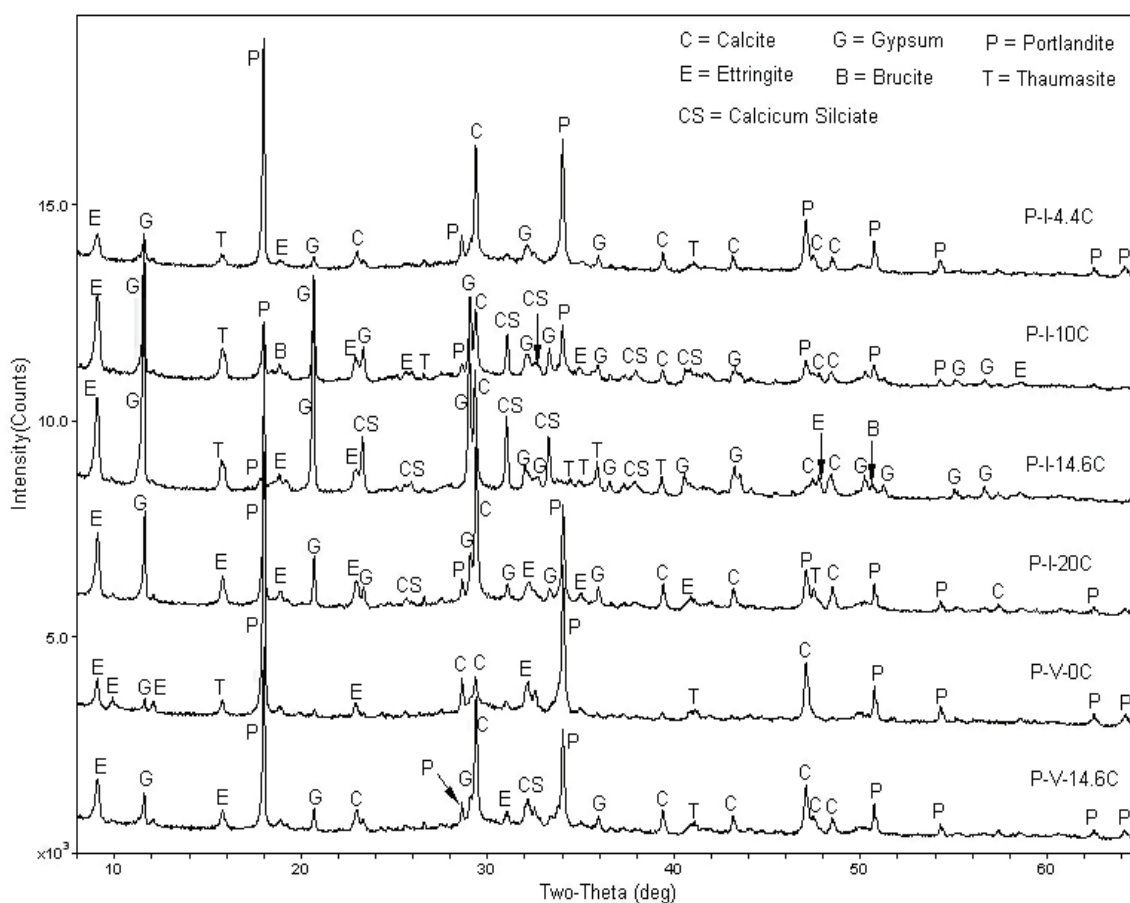


Figure 26: XRD patterns of paste samples exposed to magnesium sulfate solution at 5°C for 120 days

On the other hand, a substantial reduction of portlandite peaks was observed at $2\theta = 18.1^\circ$ and 34.1° at 120 days compared to 28 days (Figure 26). For the P-I-14.6C mixture, at $2\theta = 34.1^\circ$, portlandite was completely consumed and more thaumasite was formed at 120 days. It is clear that the conversion of portlandite to thaumasite is mainly responsible for a

significant strength reduction (65% at 120 days) of this mixture (discussed in the compressive strength section). However, there was not any significant change in strength reduction for higher limestone contents in magnesium sulfate exposure (Figure 12).

One difference for the samples in magnesium sulfate compared to sodium sulfate is the change of thaumasite to ettringite at later ages. For example, at $2\theta = 9.1^\circ$, P-I-14.6C, P-I-20C, and P-V-0C showed thaumasite at 28 days when it showed stronger ettringite peaks at 120 days. As discussed earlier (section 4.7.1), this can be the structural similarity or co-existence of these minerals at an early age which is difficult to identify through XRD. The mineralogical phases of P-V-0C and P-V-14.6C mixtures remained unchanged at 120 days. There was not any noticeable strength reduction in these mixtures at 120 days compared to 28 days, which corresponds well to this finding. However, there was 84% expansion reduction in M-V-14.6C compared to M-V-0C at 180 days.

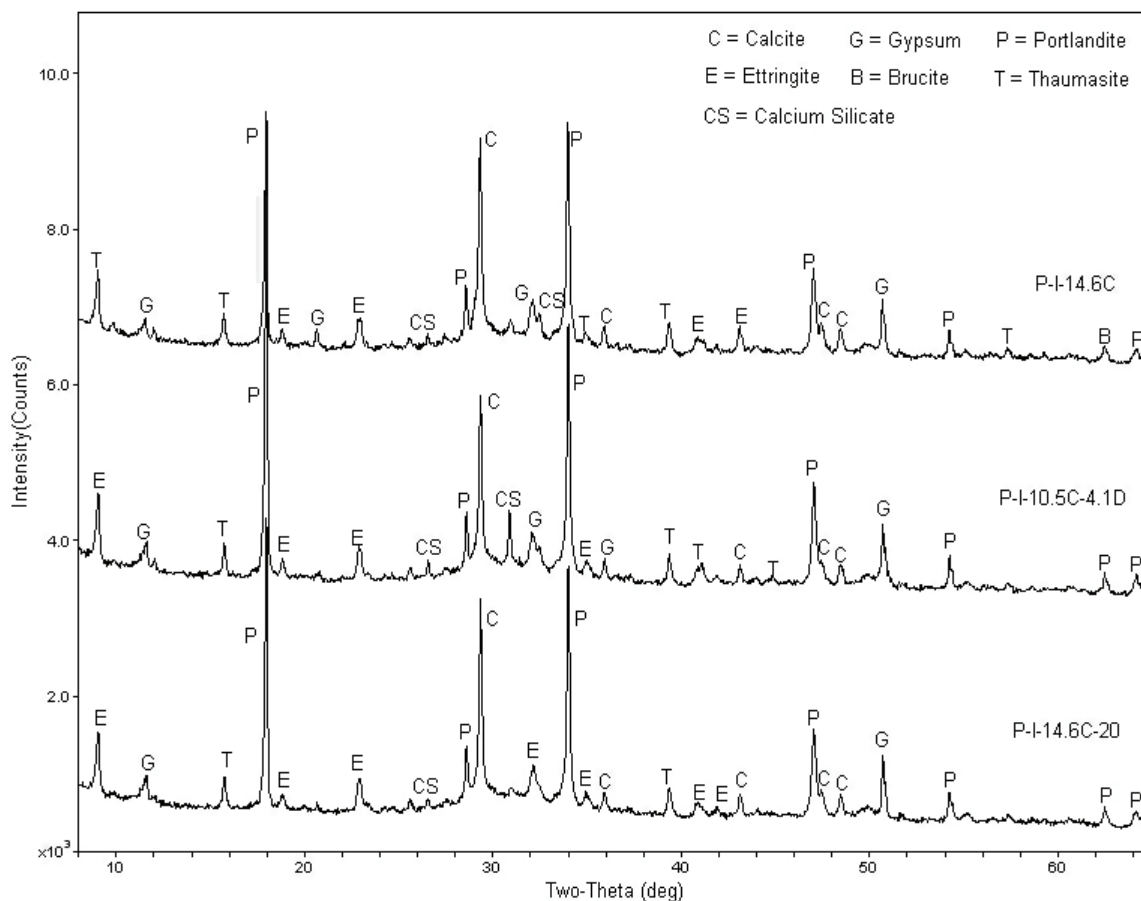


Figure 27: XRD patterns of paste samples exposed to magnesium sulfate solution at 5°C for 28 days

The changes in sulfate attack reaction products at later ages in the P-I-14.6C mixture was quite different than those found in P-I-10.5-4.1D. Fewer gypsum compounds, less thaumasite, and no brucite were found in P-I-10.5C-4.1D sample when compared to P-I-14.6C. The improved performance of P-I-10.5C-4.1D mixture measured by the mortar bar expansion and compressive strength results (discussed earlier) is likely due to these differences.

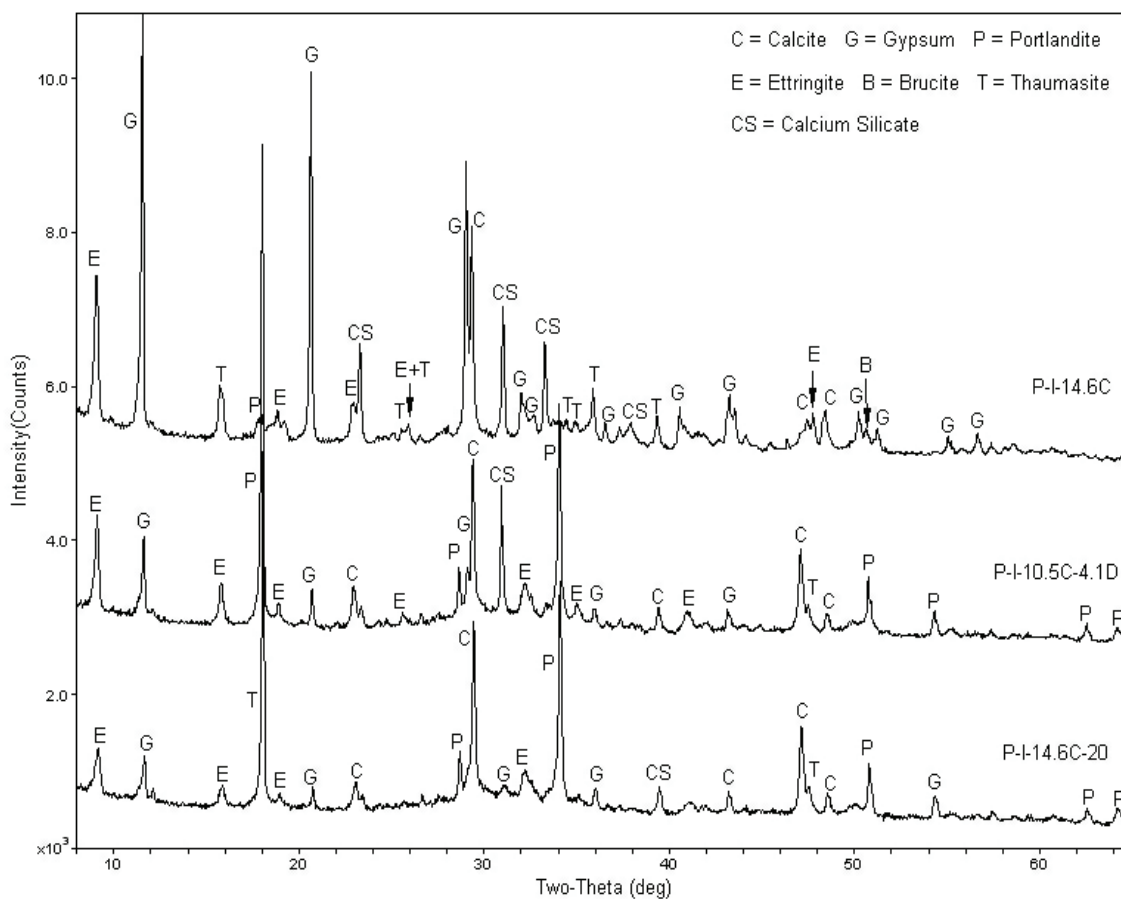


Figure 28: XRD patterns of paste samples exposed to magnesium sulfate solution at 5°C for 120 days

In general, in MgSO_4 exposure the pH of the solution does not change significantly due to the limited leaching of $\text{Mg}(\text{OH})_2$ formed as a sulfate reaction product. This is because of the low solubility of brucite compared to the portlandite available in the pore solution [79]. In this study, the pH of the magnesium sulfate was in the range of 6.5-10 which indicates that more gypsum was formed over the exposure duration. This can be attributed to C-S-H destabilization due to the lower pH values. Overall, it can be predicted that the damage due to magnesium sulfate attack is primarily from gypsum and thaumasite formation.

5. Conclusion

External sulfate attack is one of the durability issues for cement-based materials at room and low temperature. The results from this study showed a wide variability in mortar bar expansion results and paste cube strength loss in different sulfate exposures and temperatures. Based on the results the following conclusions can be drawn.

The expansion of Type I/II replaced PLCs increases with increased dosages of calcitic limestone in both sulfate solutions. However, the addition of calcitic limestone reduces the expansion of Type V replaced PLCs especially when placed in magnesium sulfate exposure

The combination of dolomitic and calcitic limestone reduces sulfate expansion significantly compared to calcitic limestone alone. This can be attributed to the ettringite stabilization due to the carbonates released from the dolomite.

The addition of fly ash with limestone improved the sulfate resistance of PLCs by reducing expansion, especially in sodium sulfate exposure.

Higher strength loss was observed for the paste specimens placed at a low temperature (5°C) and in magnesium sulfate. Type V cement showed comparatively lower strength loss even at 5°C in both solutions. The strength gain and loss at 23°C is due to the changes in hydration and differences in the deposition of hydration products over the entire exposure period. Moreover, the strength loss was not directly related to the percentage of limestone added to the control Type I/II and Type V cements.

Higher surface deterioration was observed with increased limestone addition especially in sodium sulfate where many samples were disintegrated after 240 days of immersion. In contrast, there was no mortar bar disintegration in magnesium sulfate. More cracking, bulging, and spalling on pastes was observed when placed at 5°C than 23°C at later ages.

All paste specimens showed some cracking at the corner and along the edges even at 23°C. Extensive cracking and spalling were observed on paste specimens placed at 5°C in both sulfate solutions. Higher limestone replacement showed more damage.

The sulfate attack in sodium sulfate was dominated by ettringite and thaumasite whereas gypsum and thaumasite were the main phases that triggered magnesium sulfate attack as shown in the XRD analysis.

Overall, higher expansion was observed in mortar bars placed in sodium sulfate and higher strength reduction was recorded for paste samples placed in magnesium sulfate solution. The compressive strength results in this study showed a clear dependency on the solution cation type, temperature, and cement properties.

Type I/II and Type V cements with or without added limestone have been shown to be prone to sulfate-attack to varying degrees. The composition of the cement, limestone, and added SCMs such as fly ash significantly impacts sulfate resistance as measured by expansion and strength loss, which is often neglected. Understanding these effects in addition to testing PLCs in the sulfate environments that they will encounter in the field is paramount in formulating a properly sulfate-resistant PLC concrete.

Bibliography

1. Palm, S., et al., Cements with a high limestone content—Mechanical properties, durability and ecological characteristics of the concrete. *Construction and building materials*, 2016. 119: p. 308-318.
2. Bonavetti, V., et al., High-strength concrete with limestone filler cements. *Special Publication*, 1999. 186: p. 567-580.
3. ASTM, C., 150, Standard specification for portland cement. *Annual book of ASTM standards*, 2002. 4.
4. ASTM, C., 595. Standard Specification for Blended Hydraulic Cements. *Annual book of ASTM standards*, 2000. 4.
5. Monteiro, P.J. and K.E. Kurtis, Time to failure for concrete exposed to severe sulfate attack. *Cement and Concrete Research*, 2003. 33(7): p. 987-993.
6. Irassar, E., Sulfate attack on cementitious materials containing limestone filler—A review. *Cement and Concrete Research*, 2009. 39(3): p. 241-254.
7. Gonzalez, M. and E. Irassar, Effect of limestone filler on the sulfate resistance of low C3A Portland cement. *Cement and Concrete Research*, 1998. 28(11): p. 1655-1667.
8. Irassar, E., et al., Sulfate attack on sulfate-resistant Portland cement containing limestone filler. *IBRACON Materials Journal (Brazil)*, 2005. 1(1): p. 17-32.
9. ASTM, Standard Test Method for Length Change of Hydraulic-Cement Mortars Exposed to a Sulfate Solution, in C1012M-18a. 2018, ASTM International

10. C109, A., Standard Test Method for Compressive Strength of Hydraulic Cement Mortars (Using 2-in. or [50-mm] Cube Specimens), in ASTM International 2016.
11. Kurtis, K., et al., Accelerated test for measuring sulfate resistance of calcium sulfoaluminate, calcium aluminate, and Portland cements. *Journal of materials in civil engineering*, 2001. 13(3): p. 216-221.
12. Monteiro, P., *Concrete: microstructure, properties, and materials*. 2006: McGraw-Hill Publishing.
13. Neville, A.M., *Properties of concrete*. Vol. 4. 1995: Longman London.
14. Cohen, M., Theories of expansion in sulfoaluminate-type expansive cements: schools of thought. *Cement and Concrete Research*, 1983. 13(6): p. 809-818.
15. Santhanam, M., M.D. Cohen, and J. Olek, Effects of gypsum formation on the performance of cement mortars during external sulfate attack. *Cement and Concrete Research*, 2003. 33(3): p. 325-332.
16. Diamond, S. and R. Lee, Microstructural alterations associated with sulfate attack in permeable concretes. American Ceramic Society, Inc, *Materials Science of Concrete: Sulfate Attack Mechanisms(USA)*, 1999: p. 123-173.
17. Hansen, W. Crystal growth as a source of expansion in Portland cement concrete. in *Proc. ASTM*. 1963.
18. Hansen, W., *Attack on Portland Cement Concrete by Alkali Soils and Waters-A Critical Review*. *Highway Research Record*, 1966(113).
19. Mather, B., Discussion of "The Process of Sulfate Attack on Cement Mortars" by Shen Yang, Xu Zhongzi, and Tang Mingshu. *Advanced Cement Based Materials*, 1997. 5(3-4): p. 109-110.

20. Mehta, P., Sulfate attack on concrete--a critical review. *Mater. Sci. Concr.*, III pp., 1992. 105.
21. ASTM, C., 1012-95a," Standard Test Method for Length Change of Hydraulic Cement Mortars Exposed to a Sulfate Solution". American Society for Testing and Materials, Committee C-1, Subcommittee C, 1995. 1: p. 29.
22. Hurlbut Jr, C., Ettringite from Franklin, New Jersey. *American Mineralogist*, 1960. 45: p. 1137-1143.
23. Bensted, J., Thaumasite—background and nature in deterioration of cements, mortars and concretes. *Cement and Concrete Composites*, 1999. 21(2): p. 117-121.
24. Erlin, B. and D.C. Stark, Identification and occurrence of thaumasite in concrete a discussion for the 1965 HRB symposium on aggressive fluids. *Highway Research Record*, 1966(113).
25. Hobbs, D., Thaumasite sulfate attack in field and laboratory concretes: implications for specifications. *Cement and Concrete Composites*, 2003. 25(8): p. 1195-1202.
26. Crammond, N., The thaumasite form of sulfate attack in the UK. *Cement and Concrete Composites*, 2003. 25(8): p. 809-818.
27. Bassuoni, M. and M. Nehdi, Durability of self-consolidating concrete to different exposure regimes of sodium sulfate attack. *Materials and Structures*, 2009. 42(8): p. 1039-1057.
28. Rahman, M. and M. Bassuoni, Thaumasite sulfate attack on concrete: Mechanisms, influential factors and mitigation. *Construction and Building Materials*, 2014. 73: p. 652-662.

29. Marchand, J., I. Odler, and J.P. Skalny, Sulfate attack on concrete. 2003: CRC Press.
30. Hartshorn, S., J. Sharp, and R. Swamy, Thaumasite formation in Portland-limestone cement pastes. Cement and Concrete Research, 1999. 29(8): p. 1331-1340.
31. Bensted, J., Thaumasite—direct, woodfordite and other possible formation routes. Cement and Concrete Composites, 2003. 25(8): p. 873-877.
32. Clark, L., Thaumasite Expert Group Report: review after three years experience. A report prepared in consultation with the Thaumasite Expert Group and British Research Establishment, Watford, 2002.
33. Slater, D., M. Floyd, and D. Wimpenny, A summary of the Highways Agency Thaumasite Investigation in Gloucestershire: the scope of work and main findings. Cement and Concrete Composites, 2003. 25(8): p. 1067-1076.
34. Freyburg, E. and A. Berninger, Field experiences in concrete deterioration by thaumasite formation: possibilities and problems in thaumasite analysis. Cement and Concrete Composites, 2003. 25(8): p. 1105-1110.
35. Romer, M., L. Holzer, and M. Pfiffner, Swiss tunnel structures: concrete damage by formation of thaumasite. Cement and Concrete Composites, 2003. 25(8): p. 1111-1117.
36. Ma, B., et al., Thaumasite formation in a tunnel of Bapanxia Dam in Western China. Cement and Concrete Research, 2006. 36(4): p. 716-722.

37. Lee, S.-T., et al., Occurrence of thaumasite in lining concrete of old-tunnel structure, in Geotechnical Engineering for Disaster Mitigation and Rehabilitation. 2008, Springer. p. 860-865.
38. Long, G.-c., et al., Deterioration of concrete in railway tunnel suffering from sulfate attack. Journal of Central South University of Technology, 2011. 18(3): p. 881.
39. Bickley, J.A., The repair of Arctic structures damaged by thaumasite. Cement and Concrete Composites, 1999. 21(2): p. 155-158.
40. Rogers, C., M. Thomas, and H. Lohse. Thaumasite from Manitoba and Ontario, Canada. in proceedings of the international conference on Cement Microscopy. 1997. International Cement Microscopy Association.
41. Soroka, I. and N. Setter, Effect of mineral fillers on sulfate resistance of Portland cement mortars, in Durability of Building Materials and Components. 1980, ASTM International.
42. Hooton, R.D., Effects of carbonate additions on heat of hydration and sulfate resistance of Portland cements, in Carbonate additions to cement. 1990, ASTM International.
43. Zelić, J., et al., Durability of the hydrated limestone-silica fume Portland cement mortars under sulphate attack. Cement and concrete research, 1999. 29(6): p. 819-826.
44. Bellmann, F. and J. Stark, Prevention of thaumasite formation in concrete exposed to sulphate attack. Cement and Concrete Research, 2007. 37(8): p. 1215-1222.
45. Matthews, J., Performance of limestone filler cement concrete. Impact of ENV, 1994. 197: p. 113-147.

46. Tsivilis, S., K. Sotiriadis, and A. Skaropoulou, Thaumasite form of sulfate attack (TSA) in limestone cement pastes. *Journal of the European Ceramic Society*, 2007. 27(2-3): p. 1711-1714.
47. Skaropoulou, A., G. Kakali, and S. Tsivilis, A study on thaumasite form of sulfate attack (TSA) using XRD, TG and SEM. *Journal of thermal analysis and calorimetry*, 2006. 84(1): p. 135-139.
48. Borsoi, A., et al., Sulfate attack on blended Portland cements. *ACI Special Publications*, 2000. 192: p. 417-432 %@ 0065-7891.
49. Colleparidi, M., et al. Resistance to sulfate attack of mixtures with limestone-Portland blended cements. 2003.
50. GAO, X.-j., B.-g. MA, and H.-w. DENG, Influence of binder composition on the thaumasite form of sulfate attack of concrete [J]. *Journal of Harbin Institute of Technology*, 2007. 10: p. 011.
51. Clifton, J.R., G. Frohnsdorff, and C. Ferraris, Standards for evaluating the susceptibility of cement-based materials to external sulfate attack. *Materials Science of Concrete: Sulfate Attack Mechanisms*, J. Marchand and JP Skalny, eds., The American Ceramic Society, 1999: p. 73-98.
52. Al-Dulaijan, S.U., Sulfate resistance of plain and blended cements exposed to magnesium sulfate solutions. *Construction and Building Materials*, 2007. 21(8): p. 1792-1802.
53. Cao, H., et al., The effect of cement composition and pH of environment on sulfate resistance of Portland cements and blended cements. *Cement and Concrete Composites*, 1997. 19(2): p. 161-171.

54. Skaropoulou, A., G. Kakali, and S. Tsivilis, Thaumasite form of sulfate attack in limestone cement concrete: The effect of cement composition, sand type and exposure temperature. *Construction and Building Materials*, 2012. 36: p. 527-533.
55. Ramezani-pour, A.M. and R.D. Hooton, Thaumasite sulfate attack in Portland and Portland-limestone cement mortars exposed to sulfate solution. *Construction and Building Materials*, 2013. 40: p. 162-173.
56. Schmidt, T., Sulfate attack and the role of internal carbonate on the formation of thaumasite. 2007.
57. Justnes, H., Thaumasite formed by sulfate attack on mortar with limestone filler. *Cement and Concrete Composites*, 2003. 25(8): p. 955-959.
58. Crammond, N. and M. Halliwell, The Thaumasite Form of Sulfate Attack in Concretes Containing a Source of Carbonate Ions-a Microstructural Overview. *Special Publication*, 1995. 154: p. 357-380.
59. Thomas, M., C. Rogers, and R. Bleszynski, Occurrences of thaumasite in laboratory and field concrete. *Cement and Concrete Composites*, 2003. 25(8): p. 1045-1050.
60. Jawed, I., S. Goto, and R. Kondo, Hydration of tetracalcium aluminoferrite in presence of lime and sulfates. *Cement and Concrete Research*, 1976. 6(4): p. 441-453.
61. Höglund, L., Some notes of ettringite formation in cementitious materials; influence of hydration and thermodynamic constraints for durability. *Cement and Concrete Research*, 1992. 22(2-3): p. 217-228.
62. Zhou, Q., et al., The role of pH in thaumasite sulfate attack. *Cement and Concrete Research*, 2006. 36(1): p. 160-170.

63. Gaze, M. and N. Crammond, The formation of thaumasite in a cement: lime: sand mortar exposed to cold magnesium and potassium sulfate solutions. *Cement and Concrete Composites*, 2000. 22(3): p. 209-222.
64. Nixon, P. and I. Longworth, Concrete in aggressive ground: an introduction to BRE Special Digest 1. *Concrete*, 2001. 35(8): p. 62-66.
65. Sims, I. and S.A. Huntley, The thaumasite form of sulfate attack-breaking the rules. *Cement and Concrete Composites*, 2004. 26(7): p. 837-844.
66. Aguilera, J., et al., Formation of thaumasite in carbonated mortars. *Cement and Concrete Composites*, 2003. 25(8): p. 991-996.
67. Klieger, P., Significance of tests and properties of concrete and concrete-making materials. Vol. 169. 1994: ASTM International.
68. Glasser, F.P., J. Marchand, and E. Samson, Durability of concrete—degradation phenomena involving detrimental chemical reactions. *Cement and Concrete Research*, 2008. 38(2): p. 226-246.
69. Mirvalad, S. and M. Nokken, Minimum SCM requirements in mixtures containing limestone cement to control thaumasite sulfate attack. *Construction and Building Materials*, 2015. 84: p. 19-29.
70. C150, A., Standard specification for Portland cement. 2012, West Conshohocken, PA.
71. ASTM, Standard specification for standard sand. C778-13, 2013.
72. ASTM, A., Standard Specification for Blended Hydraulic Cements. 2016, USA: ASTM International.

73. ASTM, Standard Practice for Mechanical Mixing of Hydraulic Cement Pastes and Mortars of Plastic Consistency, in ASTM International 2014.
74. ASTM, Standard Practice for Use of Apparatus for the Determination of Length Change of Hardened Cement Paste, Mortar, and Concrete. 2017.
75. 201, A.C., ACI 201.2R - 16 Guide to Durable Concrete. 2016. p. 34-34.
76. Mehta, P.K., Evaluation of Sulfate Resisting Cements by a New Test Method. 1974, California University Berkeley Structural Engineering Lab.
77. Santhanam, M., M.D. Cohen, and J. Olek, Mechanism of sulfate attack: a fresh look: Part 2. Proposed mechanisms. Cement and Concrete Research, 2003. 33(3): p. 341-346.
78. Lee, S. and R. Hooton, Influence of limestone addition on the performance of cement mortars and pastes exposed to a cold sodium sulfate solution. Journal of Testing and Evaluation, 2015. 44(1): p. 414-423.
79. Tosun, K., et al., Effects of limestone replacement ratio on the sulfate resistance of Portland limestone cement mortars exposed to extraordinary high sulfate concentrations. Construction and Building Materials, 2009. 23(7): p. 2534-2544.
80. Skaropoulou, A., et al., Long term behavior of Portland limestone cement mortars exposed to magnesium sulfate attack. Cement and Concrete Composites, 2009. 31(9): p. 628-636.
81. Torres, S., et al., Long term durability of Portland-limestone cement mortars exposed to magnesium sulfate attack. Cement and Concrete Composites, 2003. 25(8): p. 947-954.

82. Malhotra, V.M. High-performance concrete and performance and quality of concrete structures: proceedings, second CANMET/ACI international conference, Gramado, RS, Brazil, 1999. 1999. American Concrete Institute.
83. Bonavetti, V., et al., Limestone filler cement in low w/c concrete: a rational use of energy. *Cement and Concrete Research*, 2003. 33(6): p. 865-871.
84. Cyr, M., P. Lawrence, and E. Ringot, Efficiency of mineral admixtures in mortars: quantification of the physical and chemical effects of fine admixtures in relation with compressive strength. *Cement and Concrete Research*, 2006. 36(2): p. 264-277.
85. C1157M, A., Standard Performance Specification for Hydraulic Cement. 2017.
86. Baradan, B., et al., Determination of optimum limestone content in Portland limestone cement production from the viewpoint of mechanical performance and sulfate originated durability problems. TÜBİTAK research project (MAG 104I083), 4th interim report (in Turkish), 2007. 45.
87. Tsvivilis, S., et al., A study on the parameters affecting the properties of Portland limestone cements. *Cement and Concrete Composites*, 1999. 21(2): p. 107-116.
88. Matschei, T., B. Lothenbach, and F.P. Glasser, The role of calcium carbonate in cement hydration. *Cement and Concrete Research*, 2007. 37(4): p. 551-558.
89. Lothenbach, B., et al., Influence of limestone on the hydration of Portland cements. *Cement and Concrete Research*, 2008. 38(6): p. 848-860.
90. Bonavetti, V., V. Rahhal, and E. Irassar, Studies on the carboaluminate formation in limestone filler-blended cements. *Cement and Concrete Research*, 2001. 31(6): p. 853-859.

91. Feldman, R., V.S. Ramachandran, and P.J. Sereda, Influence of CaCO_3 on the hydration of $3\text{CaO} \cdot \text{Al}_2\text{O}_3$. *Journal of the American Ceramic Society*, 1965. 48(1): p. 25-30.
92. Bensted, J., Some hydration investigations involving portland cement-Effect of calcium carbonate substitution of gypsum. *World Cement Technology*, 1980. 11(8).
93. Barker, A. and H.P. Cory. The early hydration of limestone-filled cements. in *Blended Cements in Construction. Papers Presented at the International Conference, University of Sheffield, UK, 9-12 September 1991*. 1991.
94. Matschei, T., B. Lothenbach, and F. Glasser, The AFm phase in Portland cement. *Cement and Concrete Research*, 2007. 37(2): p. 118-130.
95. Zajac, M., W. Dienemann, and G. Bolte. Comparative experimental and virtual investigations of the influence of calcium and magnesium carbonate on reacting cement. in *Proceedings of the 13th international congress on the chemistry of cements, Madrid*. 2011.
96. Pera, J., S. Husson, and B. Guilhot, Influence of finely ground limestone on cement hydration. *Cement and Concrete Composites*, 1999. 21(2): p. 99-105.
97. Ye, G., et al., Influence of limestone powder used as filler in SCC on hydration and microstructure of cement pastes. *Cement and Concrete Composites*, 2007. 29(2): p. 94-102.
98. Mulenga, D., J. Stark, and P. Nobst, Thaumasite formation in concrete and mortars containing fly ash. *Cement and Concrete Composites*, 2003. 25(8): p. 907-912.

99. Hossack, A.M. and M.D. Thomas, Evaluation of the effect of tricalcium aluminate content on the severity of sulfate attack in Portland cement and Portland limestone cement mortars. *Cement and Concrete Composites*, 2015. 56: p. 115-120.
100. Galı, S., et al., Kinetics of dolomite–portlandite reaction: Application to Portland cement concrete. *Cement and Concrete Research*, 2001. 31(6): p. 933-939.
101. García, E., et al., Dedolomitization in different alkaline media: Application to Portland cement paste. *Cement and Concrete Research*, 2003. 33(9): p. 1443-1448.
102. Zhang, X., F. Glasser, and K. Scrivener, Reaction kinetics of dolomite and portlandite. *Cement and Concrete Research*, 2014. 66: p. 11-18.
103. Al-Dulaijan, S.U., et al., Sulfate resistance of plain and blended cements exposed to varying concentrations of sodium sulfate. *Cement and Concrete Composites*, 2003. 25(4-5): p. 429-437.
104. Dikeou, J.T., Fly ash increases resistance of concrete to sulfate attack. 1975: United States Government.
105. Ghafoori, N., et al., Effects of class F fly ash on sulfate resistance of Type V Portland cement concretes under continuous and interrupted sulfate exposures. *Construction and Building Materials*, 2015. 78: p. 85-91.
106. Tosun-Felekoğlu, K., The effect of C3A content on sulfate durability of Portland limestone cement mortars. *Construction and Building Materials*, 2012. 36: p. 437-447.
107. Tian, B. and M.D. Cohen, Does gypsum formation during sulfate attack on concrete lead to expansion? *Cement and Concrete Research*, 2000. 30(1): p. 117-123.

108. Kurtis, K.E., P.J. Monteiro, and S.M. Madanat, Empirical models to predict concrete expansion caused by sulfate attack. *Materials Journal*, 2000. 97(2): p. 156-161.
109. Bonen, D. and M.D. Cohen, Magnesium sulfate attack on portland cement paste-I. Microstructural analysis. *Cement and Concrete Research*, 1992. 22(1): p. 169-180.
110. Santhanam, M., *Studies on sulfate attack: mechanisms, test methods, and modeling*. 2001.
111. Skaropoulou, A., et al., Long term behavior of Portland limestone cement mortars exposed to magnesium sulfate attack. *Cement and Concrete Composites*, 2009. 31(9): p. 628-636.
112. Hekal, E.E., E. Kishar, and H. Mostafa, Magnesium sulfate attack on hardened blended cement pastes under different circumstances. *Cement and Concrete Research*, 2002. 32(9): p. 1421-1427.
113. Naik, N., et al., Sulfate attack monitored by microCT and EDXRD: influence of cement type, water-to-cement ratio, and aggregate. *Cement and Concrete Research*, 2006. 36(1): p. 144-159.
114. Ramezani pour, A.A., et al., Influence of various amounts of limestone powder on performance of Portland limestone cement concretes. *Cement and Concrete Composites*, 2009. 31(10): p. 715-720.
115. Irassar, E., M. Gonzalez, and V. Rahhal, Sulphate resistance of type V cements with limestone filler and natural pozzolana. *Cement and Concrete Composites*, 2000. 22(5): p. 361-368.

116. Vuk, T., R. Gabrovšek, and V. Kaučič, The influence of mineral admixtures on sulfate resistance of limestone cement pastes aged in cold MgSO₄ solution. *Cement and Concrete Research*, 2002. 32(6): p. 943-948.
117. Purnell, P., O. Francis, and C. Page, Formation of thaumasite in synthetic cement mineral slurries. *Cement and Concrete Composites*, 2003. 25(8): p. 857-860.
118. Sprung, S. and E. Siebel, Assessment of the suitability of limestone for producing Portland limestone cement. *ZKG International*, Edition B, 1991. 44(1): p. 1-11.
119. Voglis, N., et al., Portland-limestone cements. Their properties and hydration compared to those of other composite cements. *Cement and Concrete Composites*, 2005. 27(2): p. 191-196.
120. Azimi, G., V. Papangelakis, and J. Dutrizac, Modelling of calcium sulphate solubility in concentrated multi-component sulphate solutions. *Fluid Phase Equilibria*, 2007. 260(2): p. 300-315.
121. Perkins, R.B. and C.D. Palmer, Solubility of ettringite (Ca₆ [Al (OH) 6] 2 (SO₄) 3 · 26H₂O) at 5–75 C. *Geochimica et Cosmochimica Acta*, 1999. 63(13-14): p. 1969-1980.
122. Blanco-Varela, M., J. Aguilera, and S. Martinez-Ramirez, Effect of cement C3A content, temperature and storage medium on thaumasite formation in carbonated mortars. *Cement and Concrete Research*, 2006. 36(4): p. 707-715.
123. Verbeck, G., Field and laboratory studies of the sulphate resistance of concrete. 1967.

124. Machner, A., et al., Limitations of the hydrotalcite formation in Portland composite cement pastes containing dolomite and metakaolin. *Cement and Concrete Research*, 2018.
125. Dhir, R., et al., Evaluation of Portland limestone cements for use in concrete construction. *Materials and Structures*, 2007. 40(5): p. 459.
126. Berry, E. and V.M. Malhotra. Fly ash for use in concrete-a critical review. in *Journal Proceedings*. 1980.
127. De Weerd, K., et al., The effect of temperature on the hydration of composite cements containing limestone powder and fly ash. *Materials and Structures*, 2012. 45(7): p. 1101-1114.
128. Escalante, J., et al., Reactivity of blast-furnace slag in Portland cement blends hydrated under different conditions. *Cement and Concrete Research*, 2001. 31(10): p. 1403-1409.
129. Rozière, E., et al., Durability of concrete exposed to leaching and external sulphate attacks. *Cement and Concrete Research*, 2009. 39(12): p. 1188-1198.
130. Lee, S.-T., Influence of recycled fine aggregates on the resistance of mortars to magnesium sulfate attack. *Waste Management*, 2009. 29(8): p. 2385-2391.
131. Persson, B., Sulphate resistance of self-compacting concrete. *Cement and Concrete Research*, 2003. 33(12): p. 1933-1938.
132. Edge, R.A. and H. Taylor, Crystal structure of thaumasite, $[Ca_3Si(OH)_6 \cdot 12H_2O](SO_4)(CO_3)$. *Acta Crystallographica Section B: Structural Crystallography and Crystal Chemistry*, 1971. 27(3): p. 594-601.

133. Pajares, I., S. Martínez-Ramírez, and M. Blanco-Varela, Evolution of ettringite in presence of carbonate, and silicate ions. *Cement and Concrete Composites*, 2003. 25(8): p. 861-865.
134. Hartshorn, S., J. Sharp, and R. Swamy, The thaumasite form of sulfate attack in Portland-limestone cement mortars stored in magnesium sulfate solution. *Cement and Concrete Composites*, 2002. 24(3-4): p. 351-359.

Appendix: A

Limestone Dosage and Magnesium Sulfate Concentration Calculation

Limestone dosage calculation

Based on the QXRD test results, the percent the amount of CaCO_3 in control Type I/II cement, calcitic limestone, and dolomitic limestone were 91, 95, and 9, respectively. According to ASTM C595 any blended cement must have to contain a minimum of 70% of CaCO_3 . To meet this requirement in some blended mixes the amount of calcitic and dolomitic filler have been adjusted with the control Type I/II cement.

The mixes where only calcitic limestone has been used to make the blended cements already meet the ASTM C595 requirement as both contain over 70% of CaCO_3 . Besides this, some adjustments have been performed in mixtures where both dolomitic and calcitic limestone are being used. The final proportions taken from each filler are presented in Table 1 and Table 2.

Table 1: Weight % CaCO_3 based on QXRD test results

Ingredients	Control Type I/II cement	Calcitic limestone	Dolomitic limestone
Wt. % CaCO_3	91	95	9

Table 2: Fraction of limestone filler in different blended mixtures

Name of the blends	Original cement	Calcitic limestone	Dolomitic limestone	Overall % CaCO_3
M-I-10.5C-4.1D	Type I/II	6.1	4.1	70.22
M-V-10.5C-4.1D	Type V	10.5	4.1	70.83

Sample Calculation:

$$((4.4 \times 91)/14.6) + ((6.1 \times 95)/14.6) + ((4.1 \times 9)/14.6)$$

$$= 27.42\% \text{ (control Type I/II)} + 40.34\% \text{ (calcitic limestone)} + 2.46\% \text{ (dolomitic limestone)}$$

$$= 70.22 \% \text{ of CaCO}_3$$

Magnesium sulfate concentration calculation

According to ASTM C1012, 50 gm of sodium sulfate powder needs to be added in 1000 ml of water to make 5% sodium sulfate solution. The percentage of SO_4 in NaSO_4 is calculated as 67.62 % which has a concentration of 33808 mg/L (based on the molar mass calculation for example, NaSO_4 has a molar mass of 142 g where SO_4 contains 96.02 g and Na contains the rest of the amount). Similarly, the total molar mass of MgSO_4 is 120.32 g, where, SO_4 contains 79.8% of total mass. To make the sulfate concentration exactly same as Na (50 g used in 1000 mL of water to make 33808 mg/L) 42.36 g of total MgSO_4 has been calculated.

The detailed calculations are shown below:

$$\text{Mg} \times 1 = 24.30 \text{ g}$$

$$\text{SO}_4 \times 1 = 96.02 \text{ g, where S} = 32.06 \text{ g and O} = 15.99 \text{ g}$$

$$\text{Thus, SO}_4 = (32.06 \times 1) + (15.99 \times 4) = 96.02 \text{ g}$$

$$\text{Total molar mass of MgSO}_4 = 24.30 \text{ g} + 96.02 \text{ g} = 120.32 \text{ g}$$

$$\% \text{ SO}_4 = (96.02/120.32) = 79.8\%$$

By iteration 42.36 g has been selected to make SO₄ concentration of 33808 mg/L in Mg SO₄ solution.

$$\text{SO}_4 \text{ concentraion} = (79.8/100) \times 42.36 \text{ g} = 33808 \text{ mg/L}$$

Appendix: B

Sulfate Concentration in South Dakota Soil

The sulfate in South Dakota soil is prevalent and widely distributed. The different ionic concentration was analyzed based on the saturated paste, which was conducted by Natural Resources Conservation Service (NRCS) under United States Department of Agriculture (USDA). The saturated paste extraction is done on a water extract of the soil at saturation. Therefore, it could be a realistic data point for concentrations of these ions under natural conditions. The saturated paste extract is normally only done on soils with electrical conductivity of more than 0.25 dS/m in 1:2 soil: water. The soil sample analyzed in the study is not completely representative for South Dakota as it was collected from a single point. There can be substantial variability in soil properties within relatively short lateral distances and vertically within a soil profile at a single site. The cations like sodium and magnesium associated with sulfate ion were separated for all test samples. Soil samples were extracted from a certain depth range in each county which is called horizons. Horizons are the naturally occurring layers formed by the interaction of soil forming factors (climate, organisms, relief, and parent material) over time. Soil characteristics within a horizon are relatively uniform and all sites in the database are sampled by horizon.

The depth of horizons varies widely within a county which was measured in centimeters and sulfate, sodium, and magnesium concentration were quantified in millimole/liter (for this study it has been converted to mg/L). There is no uniform relationship between the concentrations of ions with its depth. Some counties showed higher magnesium concentration others are dominated by sodium ions (Figure 1 and Figure 2). However, some counties showed almost similar magnesium and sodium concentration instead of its variability in horizons depth. Similar associated sodium and magnesium cations sulfate concentration also followed a fluctuating trend over 39 counties. Davison county was found

to be the only one to exceed the very severe (S3 where sulfate concentration is > 10000 mg/L) exposure class as per ACI 201 (Guide to Durable Concrete) (Figure 3). More than 50 % of total counties in South Dakota possessed a sulfate concentration above 1500 mg/L which indicates severe exposure class (S2). The sodium, magnesium, and sulfate ions data presented in Figure 1 and 2 is the average of each county (average of available sample data of NRCS study). The graphical presentation also shows the maximum and minimum ion concentration found in each county.

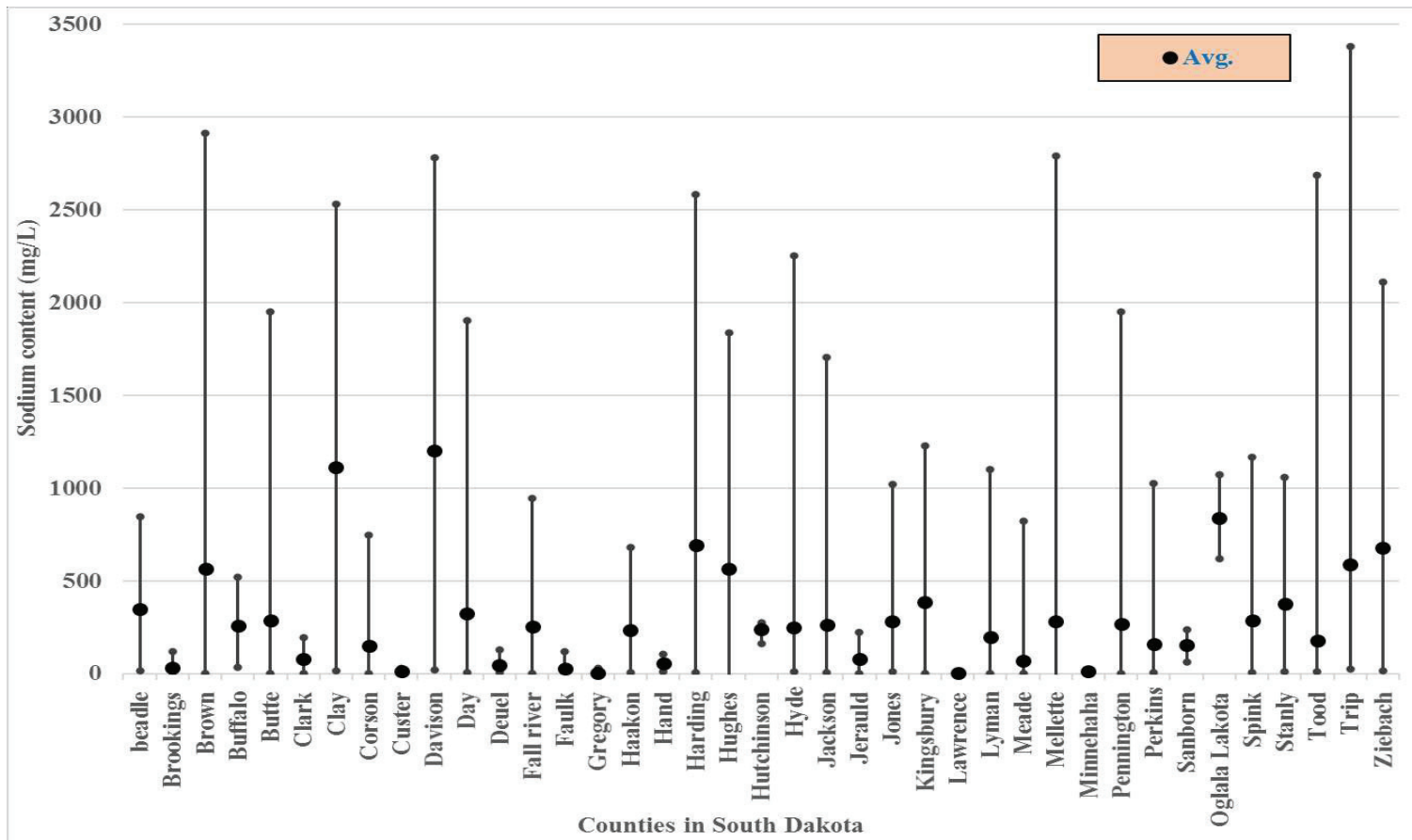


Figure 1: Countywide average Na ions concentration in South Dakota soil (Source: NRCS)

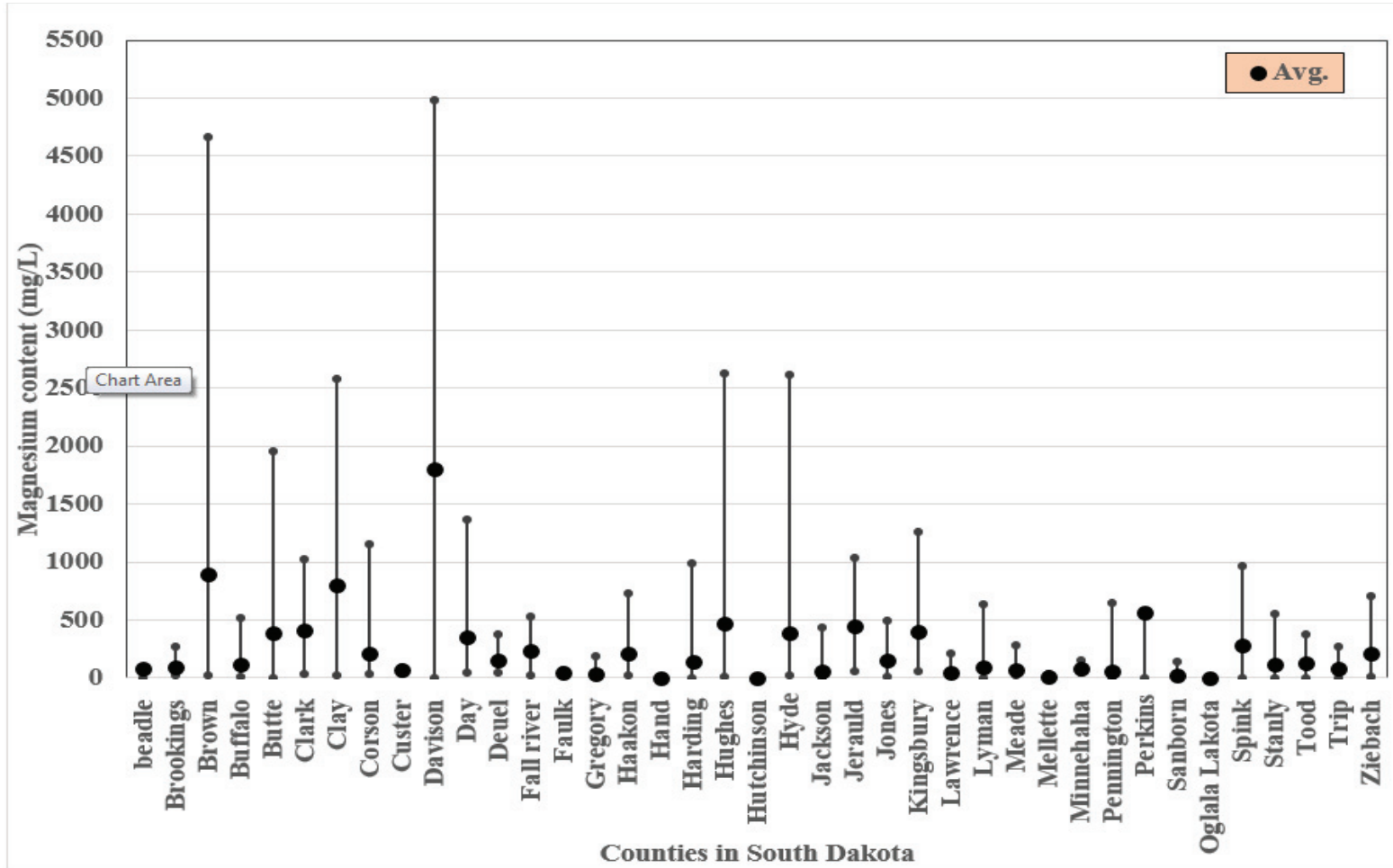


Figure 2: Countywide average Mg ions concentration in South Dakota soil (Source: NRCS)

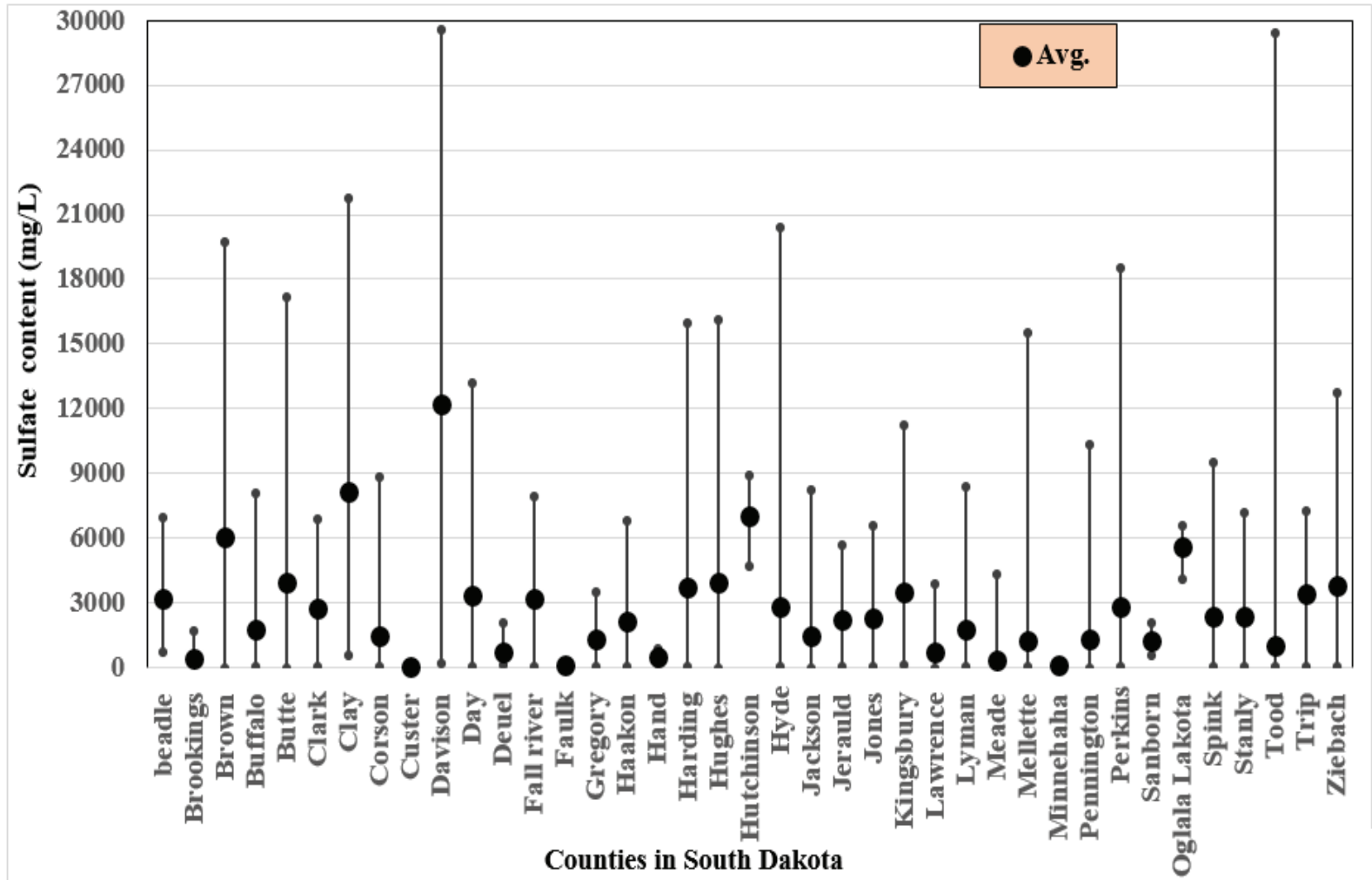


Figure 3: Countywide average sulfate ions concentration in South Dakota soil (Source: NRCS)

Vita

Md Manjur A Elahi was born in Barisal district, Bangladesh on September 1st, 1989. He finished his high school degree from Govt. Syed Hatem Ali College, Barisal, Bangladesh. He received his Bachelor degree in Civil Engineering in August, 2011 from Khulna University of Engineering & Technology, Khulna Bangladesh. Manjur started his career as a project engineer in a real estate company in Dhaka city, Bangladesh. He was directly involved in construction execution and supervision of three multistoried residential buildings. After working four years, he moved to the United States and attended at South Dakota School of Mines as a Graduate Research Assistant. He has been studying in the Master in Civil Engineering (thesis option) program under Dr. Christopher Shearer and has been researching the sulfate attack in portland-limestone cement, a project funded by the South Dakota Department of Transportation.